Inter-American Development Bank

Coastal Disaster Risk Profile and Adaptation Recommendations Considering Climate Change Scenarios for Belize

Environment, Rural Development and Risk Management Division

Martínez, Jara
Medina, Raúl
Aguirre-Ayerbe, Ignacio
Pellón, Erica
Ramírez, Marta,
Menéndez, Pelayo
Casal, Cristina
Cánovas, Verónica
Delgado, Diego
Jiménez, Julián
Suárez, Ginés

TECHNICAL NOTE Nº
IDB-TN-2419

January, 2022

Coastal Disaster Risk Profile and Adaptation Recommendations Considering Climate Change Scenarios for Belize

Martínez, Jara
Medina, Raúl
Aguirre-Ayerbe, Ignacio
Pellón, Erica
Ramírez, Marta,
Menéndez, Pelayo
Casal, Cristina
Cánovas, Verónica
Delgado, Diego
Jiménez, Julián
Suárez, Ginés

January, 2022

IDB
Inter-American Development Bank

Cataloging-in-Publication data provided by the
Inter-American Development Bank
Felipe Herrera Library
Coastal Disaster Risk Profile and Adaptation Recommendations Considering Climate Change Scenarios for Belize / Jara Martínez, Raúl Medina, Ignacio Aguirre-Ayerbe, Erica Pellón, Marta Ramírez, Pelayo Menéndez, Cristina Casal, Verónica Cánovas, Diego Delgado, Julián Jiménez, Ginés Suárez.
p. cm. — (IDB Technical Note ; 2419)

Includes bibliographic references.
1. Coastal zone management-Economic aspects-Belize. 2. Shore protection-Economic aspects-Belize. 3. Coastal ecology-Conservation-Belize. 4. Wetland restoration-Economic aspects-Belize. I. Martínez, Jara. II. Medina, Raúl. III. Aguirre-Ayerbe, Ignacio. IV. Pellón, Erica. V. Ramírez, Marta. VI. Menéndez, Pelayo. VII. Casal, Cristina. VIII. Cánovas, Verónica. IX. Delgado, Diego. X. Jiménez, Julián. XI. Suárez, Ginés. XII. Inter-American Development Bank. Environment, Rural Development and Risk Management Division. XIII. Series.
IDB-TN-2419

Jel Code: Q540 Climate; Natural Disasters and Their Management; Global Warming

Key words: Disaster Risk Management. Climate Risk Assessment. Integrate Coastal Zone Management.

This document was prepared by:

Inter - American Development Bank: Gines Suarez - Senior Disaster Risk Management Specialist; Jiménez Julián - IDB Environment Consultant.

IH Cantabria: Jara Martínez - Deputy Project Manager and Coastal Specialist; Ignacio Aguirre-Ayerbe - Disaster Risk Management Specialist; Erica Pellón - Coastal Erosion Numerical Modeling Specialist; Marta Ramírez - Coastal Numerical Modeler; Pelayo Menéndez -Natural Capital Assessment Specialist; Raúl Medina - Project Manager; Casal Cristina - Coastal Management Supporting Staff; Cánovas Verónica - Coastal Engineering Supporting Staff; Delgado Diego - GIS Supporting Staff.

Valuable contributions were also received from the Government of Belize through the Coastal Zone Management Authority and Institute (CMAI) and the Ministry of Infrastructure Development and Housing (MIDH). The design and preparation of this document was financed through the Technical Cooperation BL-T1098 Capacity building for Climate Vulnerability Reduction in Belize.

INDEX

LIST OF FIGURES

LIST OF TABLES

APPENDIX

1. INTRODUCTION

Belize is a low-lying Caribbean coastal country and its location makes the country prone to be struck by hurricanes. The most recent example of a catastrophic event in Belize is Hurricane Earl which made landfall in the country in August 2016 and destroyed or damaged at least 2,000 homes (Stewart, 2017); over US$100 million in losses to the agriculture sector only (IFRC, 2016). Some of the most important storms which have affected Belize in the past are Hurricane Hattie-Simone (1961), Hurricane Fifi (1974), Hermine (1980), Hurricane Keith (2000) or Hurricane Iris (2001) (IDB, 2011). Additionally, Belize is highly vulnerable to the effects of climate change (CC) and its associated risks, in particular, sea-level rise very likely to affect Belize (IPCC, 2007), which will exacerbate hurricane impacts in the near future.

In addition, the United Nations Framework Convention on Climate Change identifies Belize as one of the most vulnerable countries to climate change, since Belize's population and economic activity are largely concentrated in low-lying coastal zones. Sea level rise is expected to worsen damages derived from tropical cyclones in Belize.

This report aims to assess the risk of coastal flooding and coastal erosion derived from tropical cyclones at the level of the Coastal Units (see Table 5) for the current situation and for the horizon year 2050 under climate change scenario (see section 0).

This report is structured into six chapters, plus the foreword (background of the project):

1. Introduction, which describes project objectives and the organization of the report
2. Hazard Assessment
3. Coastal protection service by ecosystems
4. Risk Assessmen
5. References

2. HAZARD ASSESSMENT

2.1. Introduction

Tropical cyclones can produce extreme wind, rainfall, waves and surges in coastal areas. In this study, the target hazards are i) coastal flooding and ii) coastal erosion driven by tropical cyclones (TC). Therefore, TC-generated rainfall and wind have not been considered in this study as specific hazards, although extreme winds and rainfall contribute to potential property damage and loss of life.

In this assignment, it is understood that coastal flooding occurs when normally dry land is flooded by seawater, so the contribution of local rainfall or run-off has not been taken into account. Thus, both target hazards, coastal flooding and erosion, are driven by storm surge and waves. In its turn, storm surge is governed by the wind setup, the inverse barometer effect caused by the TC low pressure system and by the wave action in terms of wave run-up (wave set-up, surf beat and swash). On the other hand, incident waves are generated by the wind blowing on the sea surface and consequently, the analysis of extreme winds generated by TCs has been included in this study (as a driver of both storm surge and waves but not as a hazard by itself).

The estimation of the hazards induced by a particular TC is meaningful and useful only when it is related to a likelihood/probabilistic statement, e.g. the probability of exceeding a certain coastal retreat in 100 years. Thus, a stochastic approach is proposed for the probabilistic characterization of the target hazards. Consequently, astronomical tides have not been included in the hazard assessment as they induce symmetrical oscillations around the mean sea level that are negligible when averaged in the long term and, furthermore, Belize presents a tidal range of 15-30 cm (microtidal) according to Kjerfve et al. (1982).

In this chapter the methodology and results of the hazard assessment are detailed. Following this introduction, section 2.2 describes the modelling train for the atmospheric and marine dynamics (atmospheric pressure, winds, surges and waves) related to TCs, section 2.3 and 2.4 focus on the methodology for the modelling of coastal flooding and coastal erosion, respectively, and section 2.5 shows the obtained results.

The target hazards have been characterized in the present situation and under climate change in the horizon year 2050, the selected climate changes scenarios and projections are detailed next.

2.1.1 Climate change scenarios and projections

Climate change shall induce changes in coastal flooding and erosion in Belize mainly due to climate change-derived mean sea-level rise and changes in weather patterns, possibly resulting in increased intensity, size and duration of storms and, particularly, of tropical cyclones.

In this section, climate changes scenarios and projections for the dynamics of tropical cyclones and the mean sea level rise are detailed.

2.1.1.1. Changes in tropical cyclone dynamics

A global increase in storm duration and intensity has been observed since the mid-1970s, with the consequent increase in the potential destruction driven by these extreme events (Stephenson and Jones, 2017). Specifically, the number of category 4 and 5 hurricanes (on the Saffir-Simpson scale) increased by about 75% between 1970 and 2012 (IPCC, 2013). In the particular case of North Atlantic tropical cyclones, several studies have observed more activity since 1995 (Goldenberg et al., 2001) and higher frequency of very intense tropical cyclones since the 1990s (e.g., Bender et .al., 2010). These trends show a correlation with long term changes in tropical Atlantic oceanic and atmospheric conditions, such as increased mean surface temperature, increased tropospheric water vapor and fluctuations in vertical wind shear (IPCC, 2013).

Regarding the future changes in tropical cyclone activity in the North Atlantic, Bender et al (2010) suggested that the overall frequency of Atlantic storms may decrease by 28% but the frequency of the most intense storms may increase by 80% until 2100 under the SRES A1B scenario (medium emissions, AR4, 2007). Furthermore, increased precipitation rates and higher wind speeds are also likely for future Atlantic tropical cyclones (IPCC 2013). Similar results were obtained by Knutson et al. (2015) on a global scale. However, they indicated that these changes may not take place in each individual basin. These authors simulated tropical cyclones globally in a warmer late-twenty-first-century climate, obtained from a CMIP5 RCP4.5 multimodel ensemble.

Recent publications (IPCC 2019) state that there is an emerging evidence of an increase in the proportion of Cat. 4 or 5 TC with low confidence but an increase in extreme sea-level events with high confidence.

In summary, previous studies on climate change-derived changes in future tropical cyclones dynamics are not conclusive and their findings related to trends in hurricane frequencies and intensities should be treated with caution as significant uncertainty still exists. Therefore, this

study considers no changes in hurricane dynamics in the future; the study is based on historical tropical cyclones in order to characterize tropical cyclones dynamics in the current situation and in the horizon year.

2.1.1.2. Sea level rise

Regardless of the uncertainty on changes in tropical cyclones dynamics, tropical cyclone-derived impacts will worsen (specifically coastal flooding) as a result of accelerated sea-level rise (Woodruff et al. 2013). In fact, according to the National Adaptation Plan (NAP) for Belize, sea-level rise (SLR) will lead to: i) increased erosion and inundation; ii) loss of beaches, agricultural lands and crops, coastal wetlands and mangroves; iii) saline intrusion into freshwater lenses; iv) damage to infrastructure and v) displaced coastal communities.

The future rate of sea-level rise in Belize may vary under different climate change projections and SLR scenarios:

- According to the National Adaptation Plan (NAP) for Belize, sea level is projected to rise 10 cm, 38 cm and 120 cm by 2030, 2050 and 2100, respectively, in a high emission scenario (NAP for Agriculture and Water Sectors in Belize, 2017).
- On the other hand, results from three ensemble members of the A2 scenario (adopted in the IPCC AR4 report, 2007) indicate an increase of 40 cm in the Caribbean's sea level by 2080 (Second National Communication Report for Belize, 2011).
- More recently, Slangen et al. (2014) published regional sea-level rise projections for the scenarios used by the IPCC in the AR5 report: RCP4.5 and RCP8.5 (IPCC, 2013). These authors analyzed sea-level change resulting from changing ocean circulation, increased heat uptake and atmospheric pressure in 21 CMIP5 climate models.
- In addition, Kopp et al. (2014, 2017) provided a global set of physically-based local sea-level (LSL) projections for the same scenarios, based on a probabilistic approach to obtain full uncertainty distributions. This work was based on the combined processes modeled and on non-climatic local background effects, such as sinking or rising land.

The following table summarizes the values obtained from these authors, showing the median regional sea-level rise projection together with the 90% confidence interval (if available).

Table 1. Median Sea Level Rise Projections (cm) (±90% Confidence Intervals) by 2030, 2050 and 2100, from the NAP (2017), Slangen et. al. (2014) and Kopp et al. (2014).

	Relative Sea Level Rise (cm)		
year	**NAP (2017), high emission scenario**	**Slangen (2014), RPC8.5**	**Kopp (2014), RCP8.5**
2030	10	16± 5	15 ± 12
2050	38	27.5± 6	35 ± 20
2100	120	83 ± 19	91 ± 58

For this study, projections by Slangen et al. (2014) have been selected, due to their complete overview of regional sea-level rise. The hazard assessment in the future situation shall consider the most pessimistic climate change scenario (i.e., RCP8.5) for the horizon year 2050 and therefore, the adopted value for the sea level rise is 27.5 cm.

2.2 Modelling of atmospheric and marine dynamics related to TC

Usually, the historical TC track information is not enough to consistently estimate return periods for wind, waves and storm surge due to the very low probability of the most intense events and the limited timeframe of the available records. In this study, aligned with the probabilistic approach for the hazard assessment, a Monte Carlo method is proposed to populate the TC track database. This method consists of generating numerous synthetic simulations based on weighted TC statistics of the TC parameters, in which the mean values and statistical distribution patterns are in agreement with observations. This way, long time series (i.e. 1.000 to 10.000 years) of synthetic TCs are obtained based on the historical TC records.

TC-derived wind, waves and surges are highly complex functions of TC parameters (track, intensity and size) and coastal features (geometry and bathymetry). In this study, the wind and pressure fields related to a particular TC are reconstructed using parametric vortex models based on the historical and synthetic TC parameters. Then, wind and pressure are used as forcing of the hydrodynamic (storm surge) and wave models.

The schematic representation of this methodology is shown in Figure 1.

Figure 1. Methodological Sketch for the Probabilistic TC Dynamics

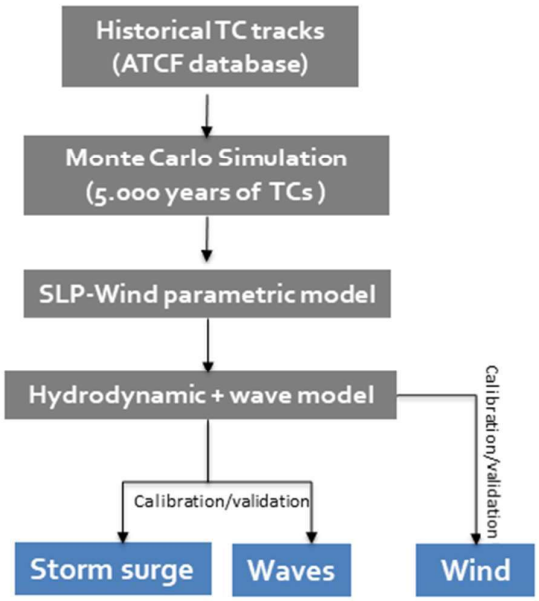

Next, the four steps (grey boxes in Figure 1) of the proposed methodology are detailed.

2.2.1 TC tracks database

The historical TC records have been obtained from the Automated Tropical Cyclone Forecast System (ATCF) database, developed by the Naval Research Laboratory for the Joint Typhoon Warning Center (JTWC). This database covers five basins and integrates a variety of data sources. For the Atlantic Ocean, data is provided by the National Hurricane Center (NHC, NOAA) in the HURricane DATabase (HURDAT2). This dataset contains 6-hourly time-series of tropical cyclone center location (latitude and longitude in tenths of degrees) and intensity (maximum 1-minute surface wind speeds in knots and minimum central pressures in millibars) for all Tropical Storms and Cyclones observed from 1851 to date.

According to the ATCF database, 69 TCs in total have affected the national territory of Belize (within a radius of 100 km) in the last 165 years (see Figure 2); 45 out of them have reached Category 1 or higher in the Saffir-Simpson hurricane scale (≥64 knots).

Figure 2. Historical Tropical Cyclones Tracks Affecting Belize from 1851 to Date (Left) and TC Climatology by Calendar Month and TC Category in the Saffir-Simpson Scale (Right).

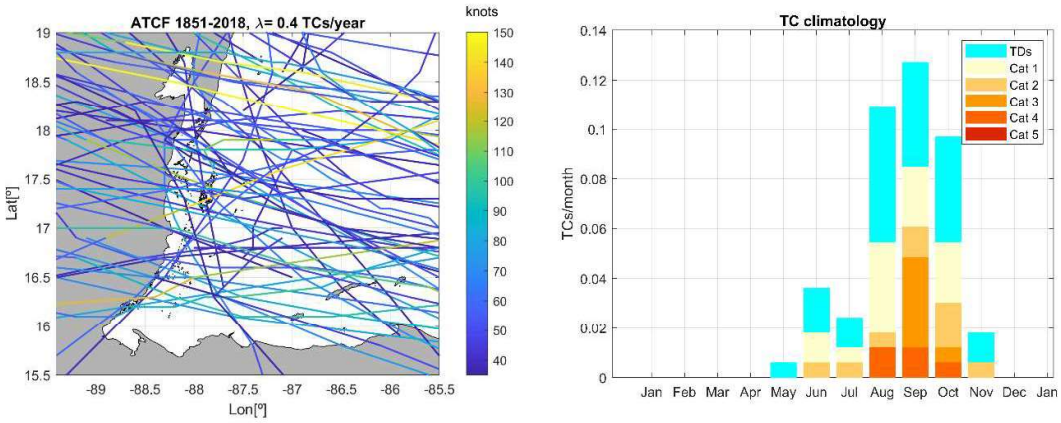

However, high uncertainty and lack of homogeneity exist in the data before the satellite era (~1970). Thus, only information from 1970 to date has been considered to estimate the current frequency of TCs: a total of 10 category 1 or higher-TCs have affected Belize in the last 50 years (see Table 2), with one of these TCs every 5 years approximately (0.21 TCs/year).

Table 2. Historical TCs with Category 1 or Higher that Have Affected Belize from 1970 to 2018.

TC name	Date	Max wind speed (knots)	Min pressure (mbar)
EDITH	Sept. 1971	140.48	942
FIFI	Sept. 1974	95.62	959
GRETA	Sept. 1978	115.48	946
DOLLY	Aug. 1996	70	989
KEITH	Sept. 2000	120	938
IRIS	Oct. 2001	126.2	947
DEAN	Aug. 2007	151.32	905
RICHARD	Oct. 2010	85.49	977
ERNESTO	Aug. 2012	85.16	972
EARL	Aug. 2016	75.34	979

2.2.2 Monte Carlo simulation of TC tracks

A stochastic model is necessary to extend the historical available TC records of 165 years to 5000 years. This model aims to complement the historical TCs database with hundreds of synthetic TCs maintaining the same statistical behavior.

The proposed model (Nakajo et al., 2014) is based on the joint probability functions of the TC parameters and temporal correlations and it has been widely used and validated in numerous applications. Within a 100 km buffer around Belizean coasts, 652 synthetic TC tracks in 5000 years have been generated based on the historical TCs tracks of 49 events in 165 years, from 1851 to 2018 (see Figure 3).

Figure 3. Historical TCs Tracks within 100 km from Belize's Coastline (Left) and Synthetic Tracks Generated for the Study (Right).

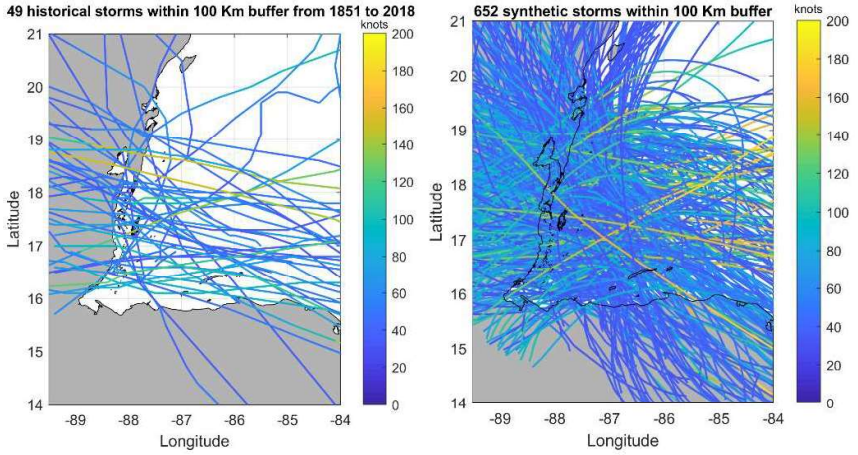

A comprehensive set of TCs of category 1 and higher (maximum sustained 1-min winds up to 64 knots) has been selected to avoid repetitions and short-lived TCs. A total number of 19 historical and 290 synthetics TCs meet these requirements.

Finally, Figure 4 shows the good agreement between the probability density functions of the TC parameters obtained from both the 165 years historical record and the 5000 years period synthetic database obtained for Belize.

Figure 4. Comparison of the Probability Density Functions of the TC Parameters (ATCF in Blue; Synthetic in Red). Left: Central Pressure; Central: Maximum Wind Speed; Right: Joint Distribution of Central Pressure and Wind Speed.

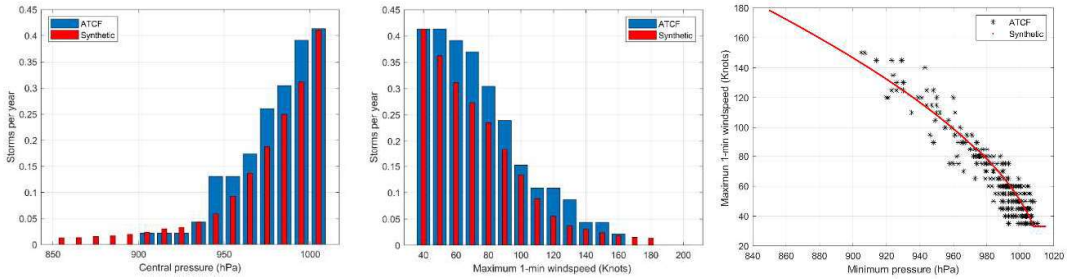

2.2.3 Wind and sea level pressure parametric model

The meteorological dynamics (wind and pressure fields) of the selected TCs (19 historical and 290 synthetic) have been modeled. To that end, state-of-the-art analytic models (i.e. parametric wind and pressure models) have been applied, since they have been proven to produce very satisfactory results with low computational cost and few input parameters.

Specifically, the surface axisymmetric wind field is estimated by means of the parametric Dynamic Holland Model (Fleming et al., 2008), which accounts for the dynamic changes in the model parameters due to the hurricane motion as an improvement of the commonly used Holland (1980). According to this model, the wind speed at the gradient level (*Vg*), which represents a static version of the TC, is determined as follows:

$$Vg(r) = \sqrt{(R/r)^B \cdot \exp\left(1 - \left(\frac{R}{r}\right)^B\right) \cdot {v_m}^2 + r^2 \cdot \frac{f^2}{4} - r \cdot \frac{f}{2}}$$

Where r is the radius, R the radius of maximum winds, f the Coriolis parameter, v_m the maximum wind speed at the top of the atmospheric boundary layer and B the Holland parameter (which varies between 1 and 2.5). This parameter is calculated as:

$$B = \frac{\rho e V^2}{(P_n - P_c)}$$

Where ρ is the density of air (ρ=1.15 kg/m^3), P_n is the ambient atmospheric pressure, P_c is the storm's central pressure and e is Euler's number.

Finally, *Vg* is multiplied by the boundary layer adjustment factor (β=0.9) to transfer the wind speed at the top of the atmospheric boundary layer to the sea surface (10-m) and a fraction of

the storm translation velocity is added, which accounts for the asymmetry of the wind field induced by the surface background wind (Lin and Chavas, 2012), to obtain the characteristic asymmetric pattern of a TC in motion.

The radius of maximum winds is not available for the synthetic TCs. In those cases, this parameter is calculated based on the relationship found by Knaff et al. (2015):

$$R_m = 218.3784 - 1.2014V_m + \left(\frac{V_m}{10.9844}\right)^2 - \left(\frac{V_m}{35.3052}\right)^3 - 145.5090\cos\varphi$$

Where R_m is expressed in nautical miles, V_m is the intensity in knots and ϕ is the latitude.

As for the surface pressure field P, it is calculated as follows:

$$P(r) = (P_n - P_c)exp\left(-\left(\frac{R}{r}\right)^B\right) + P_c$$

As an example, Figure 5 shows the 10-m and 10-min averaged wind and atmospheric pressure footprints of the hurricane Hattie, which made landfall south of Belize City in October 1961.

Figure 5. 10-m Wind Speed in m/s (left) and Surface Atmospheric Pressure Footprints in mbar (right) of Hurricane Hattie (October, 1961).

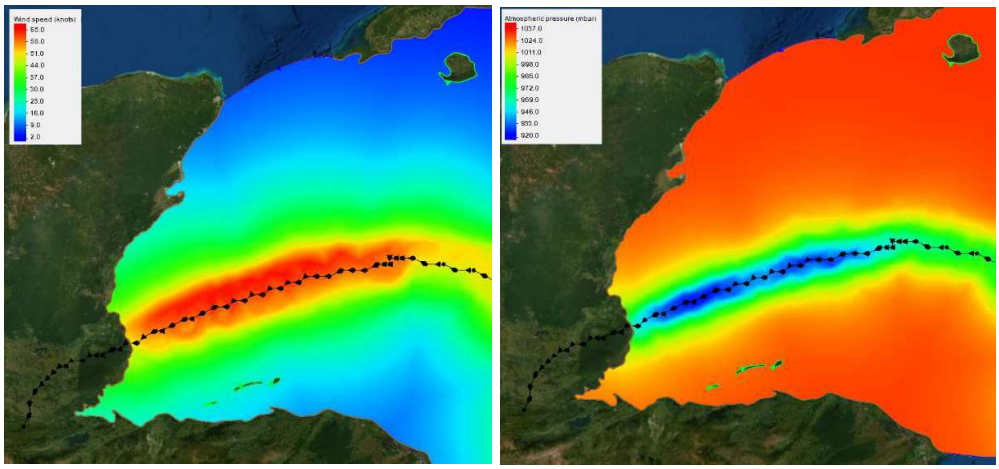

2.2.4 ADCIRC+SWAN storm surge and wave modelling

Based on the atmospheric pressure and wind fields obtained for each of the 309 selected TCs (19 historical + 290 synthetic), waves and surge levels have been modeled using the state-of-the-art numerical models ADCIRC+SWAN, which have been widely validated with measured waves and storm surges data for several historical storms (Dietrich et al., 2012).

One of the main strengths of the ADCIRC+SWAN model is the ability to use unstructured finite element meshes, with very fine resolution near the coast and much coarser resolution in open waters. Such a high resolution allows a realistic representation of the coastline and hence a better estimation of the storm surge and waves. A mesh of 56607 nodes was designed based on the Localized Truncated Error Analysis (Hagen et al., 2001), which optimized the placement of nodes to properly incorporate the physics underlying tidal flow and circulation to the mesh generation process. Mesh resolution ranges from 500 m along the coastline, cayes and shallow area to 35 km in open waters (Figure 6).

Figure 6. Computational Domain and Bathymetry Used to Perform the Storm Surge and Wave Modelling (Left) and Zoom Over the Area Around Belize City (Right).

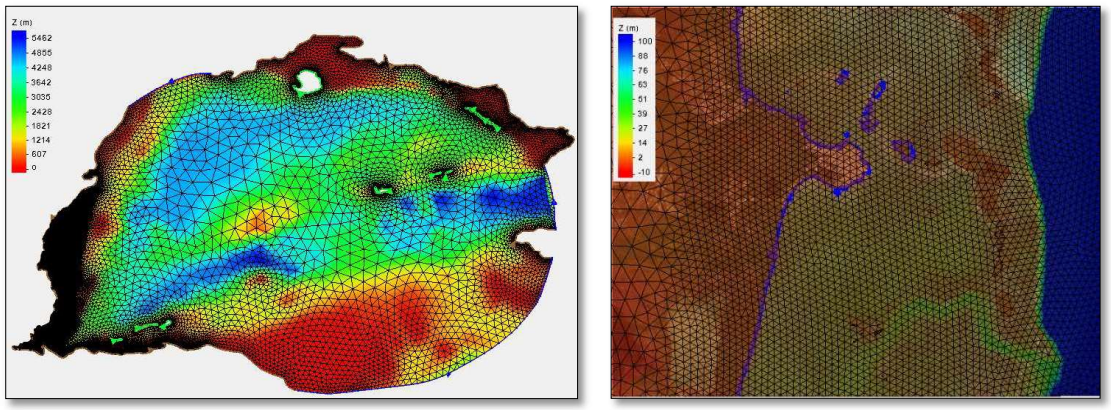

The ADCIRC (ADvanced CIRCulation model) solves the depth averaged barotropic form of the shallow water equations (Luettich and Westerink, 2004) in the modelling mesh. It computes the generalized wave continuity equation (GWCE) in order to obtain water levels, and the vertically integrated momentum equations to obtain currents. It has been run in fully non-linear, two-dimensional mode with wetting and drying feature enabled. The GWCE solution has been implemented using a spatially variable weighting parameter (τ_0), where τ_0 is specified as functions of the mesh element size and water depth. Bottom friction was parameterized using a quadratic formulation where the drag coefficient is a function of water depth via the Manning's n coefficient.

Wind velocities, water levels, currents and bottom friction calculated by ADCIRC are the inputs to the third-generation wave model SWAN (Simulating Waves Nearshore, Booij, 1999). SWAN computes the wind generated waves, the radiation stresses and their gradients in the

same unstructured mesh, which are the inputs to ADCIRC, assimilated as a forcing function. This interaction cycle takes place every 10 minutes of simulated time.

SWAN (41.20) model computes the evolution in time and space of the wave action density spectrum. Computations are performed using 36 directions and 36 frequency bins. The wind drag coefficient formulation of Zijlema et al. (2012) has been used to simulate TC waves and the bottom friction is computed in ADCIRC using the Manning's n coefficient and then converted to roughness length by SWAN. Source terms include wind input, quadruplet interactions, white-capping, triads, bottom friction and wave breaking. To account for the flow resistance and according to Passeri et al. (2011), Manning's n coefficient has been fixed to 0.02 in open waters, to 0.05 in shallow waters and 0.1 over land.

Before simulating the tropical cyclone marine dynamics, the model configuration and mesh domain have been validated. With this purpose, a 40-days simulation (with a 2-day ramp-up period) of astronomical tide has been carried out and results have been compared with measurements by the tidal gauge located in the Port of Belize (coordinates -88.2º longitude, 17.4735º latitude). The model has been forced with the amplitude and phase of the following tidal constituents: M2, S2, N2, K2, K1, O1, P1, Q1, M4, MS4, MN4, MM and MF. Tidal harmonics have been obtained from the TPX08 database (http://volkov.oce.orst.edu/tides/global.html). The comparison of both datasets (modeled and measured) shows a good agreement in both, the phase and the amplitude and the differences can be considered negligible. These results demonstrate the capability of the model to reproduce the time evolution of sea levels due to astronomical forcing and validate the used values of Manning's n coefficient (Figure 7). Unfortunately, the available instrumental record does not capture the signal of any relevant hurricane for the validation of the associated storm surge.

Figure 7. Comparison of ADCIRC-Modeled and Measured Astronomical Tide at the Port of Belize.

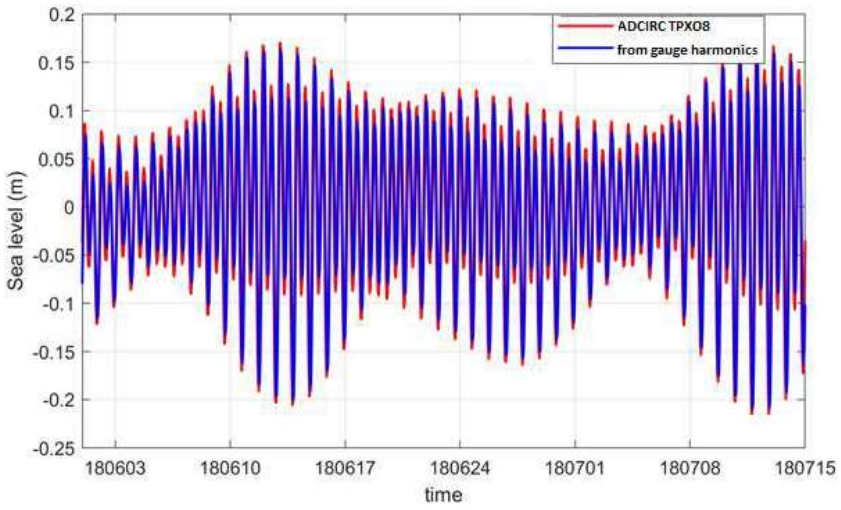

Finally, the National Data Buoy Center (NDBC) from NOAA (https://www.ndbc.noaa.gov/) has one permanent buoy located within our computational domain that has records at the target timeframe: Stations 42056 (-84.946º, 19.812 º). However, this buoy is located far from the tracks of modelled TCs and therefore model validation is limited. A certain influence of hurricane Earl (2016) can be observed in this station (see Figure 8) but the magnitudes between model results and buoy records differ significantly due to the distance between the buoy and the TC track, which implies that observations are influenced by other conditions not included in the model and not related to TC dynamics.

Figure 8. Comparison of Measured and SWAN-Modelled Significant Wave Height, Hs (m), for Hurricane Earl (August 2016).

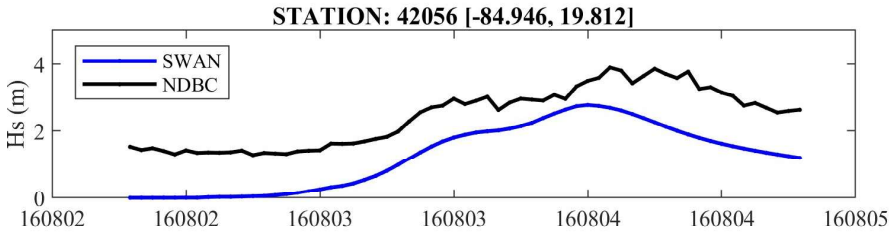

After validation, the simulation of the TCs dataset has been performed. For each modelled TC, ADCIRC+SWAN models estimate the hourly time series of wind and pressure fields, water elevation and wave parameters (significant wave height, mean wave direction and mean and peak wave period) at all nodes of the modelling mesh for both, the current situation and

considering a mean sea level rise of 27.5 cm in the horizon year 2050, according to the RCP8.5 scenario. As an example, Figure 9 and Figure 10 show the results obtained from ADCIRC+SWAN models for 4 historical TCs that have affected Belize.

Figure 9. ADCIRC-Derived Maximum Water Elevation (in meters) Obtained for 4 Historical Hurricanes in Belize.

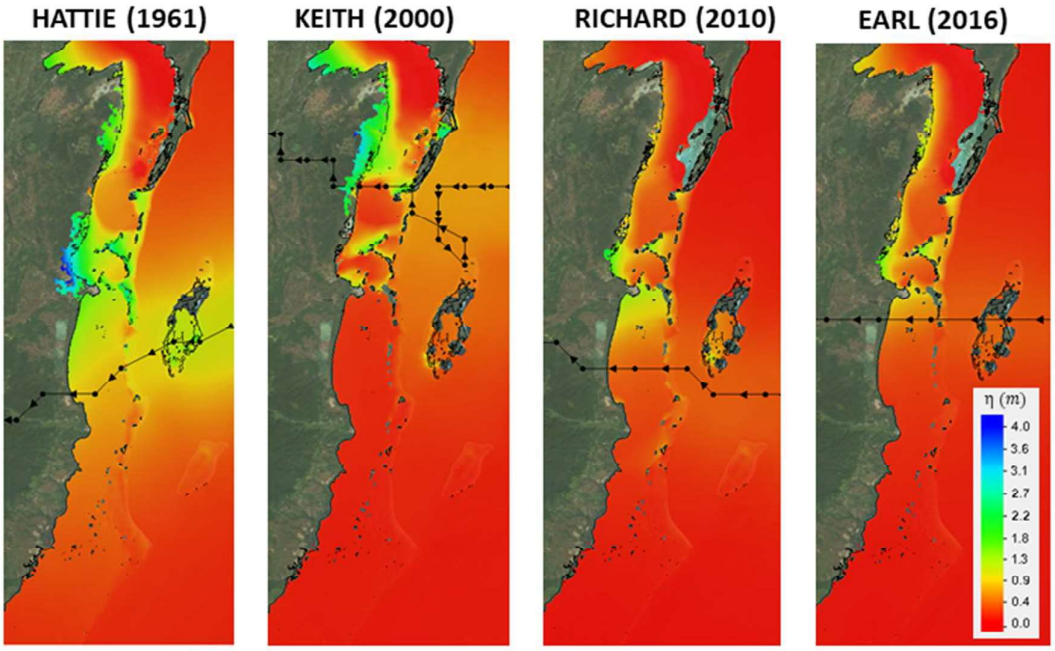

Figure 10. SWAN-Derived Maximum Significant Wave Height (in meters) Obtained for 4 Historical Hurricanes in Belize.

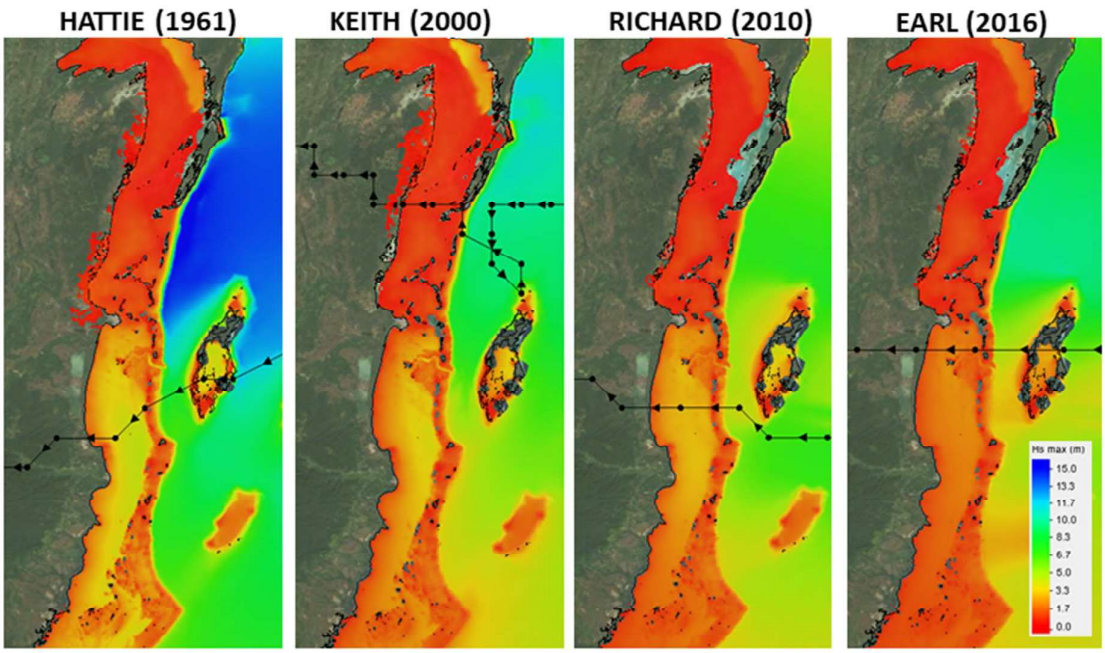

2.2.5 Statistical analysis of TC dynamics

Based on the results of the atmospheric and marine dynamics of the 309 historical and synthetic TCs, specific return periods and extreme value statistical distributions have been estimated.

Given the total number of simulated TCs (309) and the estimated frequency of category 1 or higher-TCs in Belize (0.21 TCs/year), as per in section 0, the TC database corresponds to 1471 simulated years. Therefore, the estimation of return periods up to 500 years seems reasonable. The return periods (Rp) are calculated according to the relationship proposed by Izaguirre et al. (2017):

$$Rp = (1/v) \cdot [1/(1-p)]$$

Where Rp is the return period in years, v is the frequency of TC events and p is the probability of occurrence.

It is assumed that the development of storms is a stationary Poisson process and the extreme value distribution of the variables of interest is obtained based on the peaks-over-threshold (POT) method with a Generalized Pareto Distribution (GDP). The probability density function for the GDP with shape parameter $k \neq 0$, scale parameter σ, and threshold parameter θ, is:

$$f(x|k,\sigma,\theta) = \left(\frac{1}{\sigma}\right)\left(1 + k\frac{(x-\theta)}{\sigma}\right)^{-1-\frac{1}{k}}$$

As an example, the extreme value distributions of wind speed (see Figure 12), water elevation (see Figure 14) and significant wave height (see Figure 16) have been determined at the following sites (see Figure 11) along the Belize coast:

Figure 11. Locations Along the Belize Coast Where the Extreme Value Distributions of Water Elevation, Wind Speed and Significant Wave Height Have Been Determined.

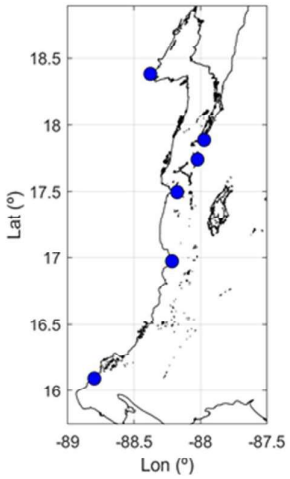

Location	Coordinates [Lon, Lat] (°)	Depth (m)
Corozal	[-88.377,18.385]	0.6
San Pedro	[-87.972,17.89]	6.5
Caye Caulker	[88.022,17.738]	0.9
Belize City	[-88.175,17.497]	2
Dangriga	[-88.214,16.972]	6.3
Punta Gorda	[88.799,16.092]	2.8

Figure 12. GDP Fits to the 10-min Averaged Surface Wind Speed in m/s at the Six Sites in Figure 11.

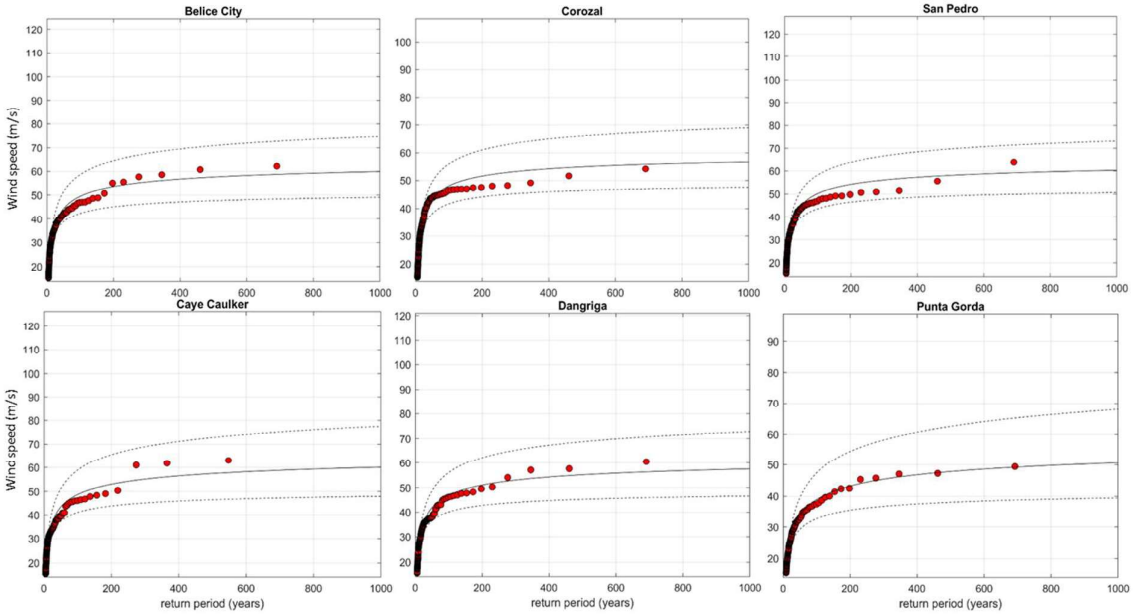

Based on this approach the return period maps for the wind speed have been obtained by computing results at each node of the modelling grid (Figure 13). In general, the spatial variation of the 10-min averaged surface (at 10 m) wind speed shows a gradient from south to north along the Belize coast, with values increasing to the north. For the return period of 500 years, the highest wind speed has been found in the central area, covering Belize City and Caye Caulker. At these locations, 10-min wind speeds higher than 60 m/s have been obtained.

Figure 13. 10, 50, 100 and 500 Years Return Periods Maps of the Surface (10 m Height) and 10-min Averaged Wind Speeds in m/s.

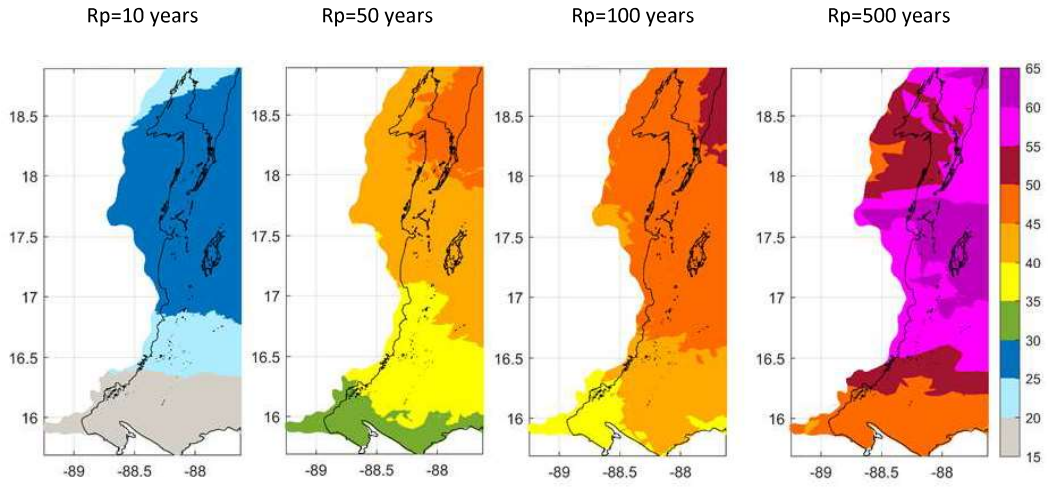

As for the maximum water elevation at the selected locations in Figure 11, Figure 14 shows the GPD for the two analyzed mean sea level scenarios (current and in the horizon year 2050 including SLR scenario). The largest storm surge values are obtained in Corozal, followed by Belize City, with 3.1 m and 1.95 m, respectively, for the 200 years return period. In general, the storm surge results show an increase of more than 20% as a result of a SLR of 0.275 m along the coast of Belize, with maximum differences in San Pedro and Punta Gorda. However, no significant differences have been observed in Corozal.

Figure 14. GDP Fits to the Water Elevation for the two Simulated Mean Sea Level Scenarios (i.e., Present Conditions and RCP8.5 Scenario by 2050) at Four of the Six Sites in Figure 11.

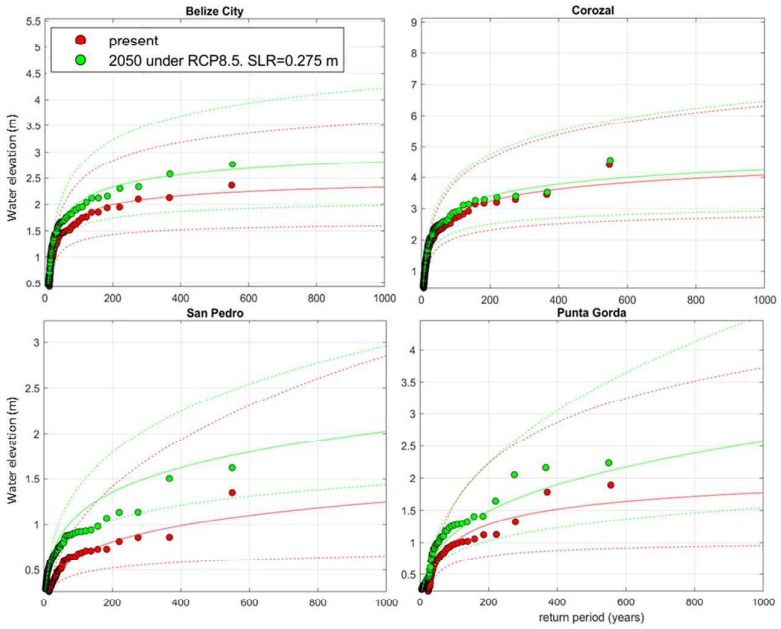

The statistical results for the storm surge have been validated using the available literature:

- the "CHaRIM Project: Belize national flood hazard mapping methodology and validation report" (2016) provides storm surge return periods at specific locations in Belize. 0 shows the comparison between results obtained from that project with those estimated in this study for two different return periods: 10 and 100 years. There is a very good agreement in the values obtained for the northern and central regions of Belize (San Pedro, Belize City and Corozal), whereas significant discrepancies have been found in the south (i.e. Punta Gorda), where results of this study are significantly lower.

Table 3. Comparison of 10 and 100 Years Return Periods Storm Surge at Different Locations Along Belize Coastline, Obtained in this Study and in the Project "CHaRIM Project Belize National Flood Hazard Mapping Methodology and Validation Report" (2016).

	Storm surge (m). Tp = 10 years		**Storm surge (m). Tp = 100 years**	
	CHaRIM Project (2016)	*This study*	*CHaRIM Project (2016)*	*This study*
San Pedro	0.3	0.5	1.2	1.17
Belize City	0.4-0.7	0.2- 0.7	1.4- 1.6	1.7
Dangriga	0.6	0.2	1.9	1.28
Punta Gorda	0.8	<0.1	2.3	1
Corozal	0.6	0.8	2.6	2.5

- The "hurricane rehabilitation and disaster preparedness project" and the historical hurricanes reports by NEMO agree on the pattern of lower storm surge towards the southern regions, which has been observed in this study (at least for return periods ≤100 years).

For the analysis of the spatial distribution of significant wave height (Hs) induced by TCs, the maximum envelope of the 309 simulated TCs waves is shown in Figure 15.

Figure 15. Spatial Distribution of Maximum Significant Wave Height in Meters.

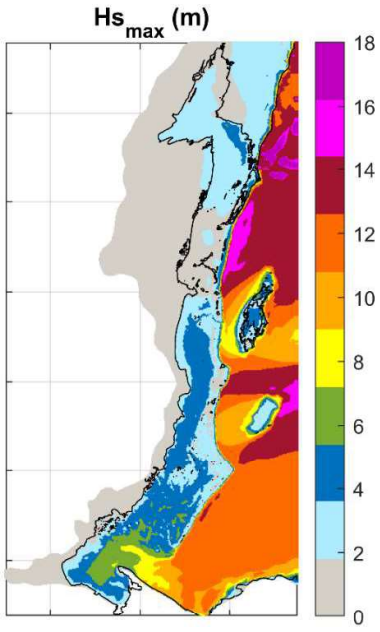

The numerous cayes, islands and reefs protect the Belize coastline from waves. Therefore, Belize City and surroundings are affected by relatively small significant wave heights, whereas this value increases southward, with its maximum value in Dangriga (i.e., 3.3 m), since Punta Gorda is partially protected against waves from the southeast by the Punta de Manabique. Seaward of this natural barrier, maximum values of Hs reach up to 18 m. The GDP of significant wave height (Hs) shows that wave height is limited by wave breaking in all cases (see Figure 16). Maximum values and minimum differences between the current situation and the future horizon year 2050 under RCP8.5 scenario (SLR=27.5 cm) at San Pedro in Ambergris Cay, where water depth is maximum, followed by Dangriga.

Figure 16. GDP Fits to the Significant Wave Height for the Two Simulated Mean Sea Level Scenarios (i.e., Present Conditions and RCP8.5 Scenario by 2050) at Four of the Six Sites in Figure 11.

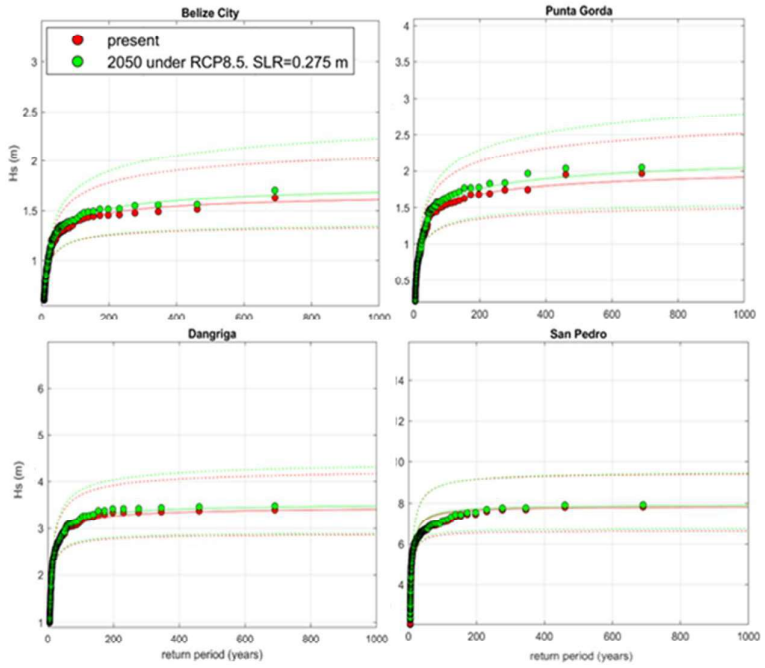

2.3 Flood modelling

There are different approaches to model coastal flooding, from 2D methods to 3D hydrodynamic models. The former are simplified approaches that require little computational effort but show some limitations in terms of the physical processes included (Bates et al., 2005). This study uses the two-dimensional depth-integrated ADCIRC hydrodynamic model, coupled with SWAN, which provides storm surge and wave set-up (see section 2.2.4) and, also, overland inundation for the current situation and in the horizon year 2050 under RCP8.5 scenario (SLR=27.5 cm). The accuracy of these results is highly dependent on the quality and resolution of the available digital terrain model (DTM). In this study, the MERIT-DEM with ~90 m resolution has been used.

Due to the lack of high water marks in Belize, a qualitative validation of the flood levels and flood extent has been performed based on the information provided by:

- The National Emergency Management Organization (NEMO) reports.
- Results from the project "Disaster risk and climate change vulnerability assessment for Belize City" (IHCantabria, 2017).

- The report for the “hurricane rehabilitation and disaster preparedness project” (2001).

According to the “hurricane rehabilitation and disaster preparedness Project“ (2001), the most recent hurricane to have caused major impacts on Belize was Hurricane Keith, which occurred in October 2000. This hurricane resulted in severe flooding in the northern half of the country, which is clearly observed in our results (Figure 17). The extensive flooded area observed on the northern coast of Belize coincides with the northern lowlands which exhibits less than 2 m of elevation. According to the hurricane report, surges of 0.3-0.61 m were experienced in the coastal areas of Belize District. We obtained values between 0.2 m to 1.4 m in the south and north coasts of Belize City, respectively. In relation to the hurricane Richard (2010), most of the impact was caused by its strong associated wind and storm surge in Belize City and surroundings (NEMO report, 2010). Our simulation shows the same affected area, with maximum values of storm surge of 2.1 m in the area located north of Belize City. Finally, the hurricane Earl caused damage to piers and marinas in Belize City, Caye Caulker and Ambergris Caye (NEMO report, 2016). These damages could be produced by the associated storm surge, which achieved values between 0.9-1.1 m in these regions (Figure 17).

Figure 17. Storm Surge and Overland Inundation (In Meters) Produced by Three Historical Hurricanes in Belize.

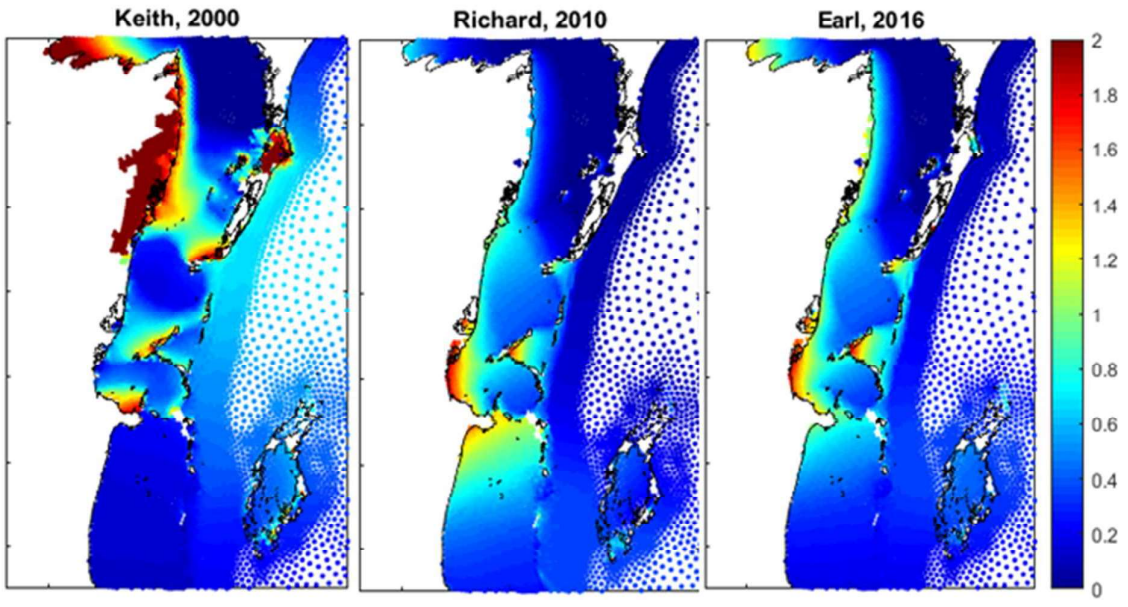

Table 4 shows quantitative results of storm surge obtained in this study and in the Baseline study for Belize City (2016). For the three analyzed historical TCs, the estimated values are in good agreement between both studies. Furthermore, according to the “hurricane rehabilitation

and disaster preparedness Project“ (2001), the maximum storm surge reported for Hattie TC was between 4.5-6 m, which also agrees with our results. This was the most destructive hurricane to have hit Belize in the last century. Its effects in terms of flooding extent can be observed in Figure 9.

Table 4. Comparison of Storm Surge Results Obtained in This Study and in the Project “Disaster Risk and Climate Change Vulnerability Assessment for Belize City. Baseline Study for Belize City” (2016), for Three Historical Hurricanes.

Historical TC	Storm surge (Baseline study for Belize City, 2016)	Storm surge (present study)
Hattie (1961)	>4.5 m north of the Belize City	4.5 m at ~10 km north of Belize City
Keith (2000)	1.3 m in Belize City	From 0.2 m (in the south) to 1.8 m (in the north) around the Belize Peninsula
Earl (2016)	1.2 -1.5 m in Ladyville	1.45 m in Ladyville

Finally, the statistical analysis of TC-derived coastal flooding is based on the approach already described in section 2.2.5 and coastal flooding maps for different return periods (10, 50, 100 and 500 years) are shown in section 2.5.1, for the current situation and in the future horizon year 2050 under RCP8.5 scenario (SLR=27.5 cm).

2.4 Erosion modelling

Coastal areas and, particularly beaches, experience morphological changes in shorter timescales than most geological features that usually show significant changes only after thousands of years. This rapid evolution of coastal areas, originated by a wide range of drivers of morphological change, including natural or man-made drivers, can take place in a wide range of spatial and time scales, which complicates the understanding of the processes involved in shoreline change. Furthermore, the dimensionality (3D) of coastal processes brings additional complexity to the study. Currently, there is no unique theory to analyze at the same time all scales (temporal and spatial) of coastal three-dimensional processes. Therefore, several simplifications regarding the dimensionality, the drivers for change or the scale of the relevant processes involved are needed to assess in a feasible way the hazard of coastal erosion as described below:

- Although several causes of coastal erosion in Belize have been reported[1] such as sand mining, dredging, land reclamation, damming of rivers, reef destruction, obstruction of longshore drift and haphazard vegetation clearance, in this study coastal erosion due to tropical cyclones only is analyzed.
- The time scale of the processes involved is therefore short-term (form hours to only a few days), in accordance with the duration of the drivers for change (storm events) and shoreline response to those drivers. The spatial scale and resolution of the analysis are related to the extent of the study area as detailed below.
- Regarding the dimensionality of the erosion process, the main impact of tropical cyclones is related to the cross-shore sediment transport due to high energy waves and high sea levels that erode the subaerial beach profile and cause deposition of the eroded sediment in the submerged beach and therefore a 2D approach (cross-shore) has been selected for this study. The impacts of longshore sediment transport are usually relevant in longer timescales and, additionally, their study requires a higher resolution since they are highly influenced by small scale coastal structures and the local morphology.

Consequently, a two-dimensional (cross-shore) model, XBEACH, aimed to simulate hydrodynamic and morphodynamic processes and impacts on sandy coasts on the time scale of storms has been selected for this work. XBEACH includes the hydrodynamic processes of short wave transformation (refraction, shoaling and breaking), long wave (infragravity wave) transformation (generation, propagation and dissipation), wave-induced setup and unsteady currents. The morphodynamic processes include bed load and suspended sediment transport, avalanching, bed update and breaching during a storm. In this study, the hydrostatic mode of XBEACH (Roelvink et al., 2009) has been used, in this mode variations in the amplitude of short waves area solved separately from the long waves (surf beat), currents and morphological change. This saves considerable computational time, with the expense that the phase of the short waves is not simulated. Given the lack of measurements of TC-derived coastal erosion in Belize, the configuration parameters of this numerical model have been set based on a previous validation of this modelling approach in the Caribbean region[2].

---

[1] Beach erosion in Belize (2001). The Coastal Zone Management Authority and Institute. https://www.coastalzonebelize.org/wp-content/uploads/2010/04/erosion_brochure.pdf

[2] Country Disaster Risk Profile for The Bahamas. IHCantabria, 2019.

This study covers hundreds of kilometers along the continental coastline and along the Belizean cayes and consequently the selected approach for the analysis is based on an averaged beach profile for each one of the 22 Coastal Units (CU, see Table 5). The beach profile at each CU has been characterized by means of a theoretical beach profile for the intertidal area with a shorefront slope of 1:20 and a horizontal berm of 1 m over the mean sea level. The bathymetry of the submerged beach profile at each CU has been extracted from the bathymetric data in shallow areas acquired from TCarta.

Table 5. Coastal Units (CU) in Belize.

Region	Coastal Planning Region	#	CU
Northern Belize	Northern Region	1	NR-North
		2	NR-Central
		3	NR-South
		4	NR-Cayes
	Ambergris Caye	5	AC-North
		6	AC-South
Central Belize	Central Region	7	CR-North
		8	CR-Central
		9	CR-South
		10	CR-Cayes
	Caye Caulker	11	CC
	Turnefe Atoll	12	TA
	Lighthouse Reef Atoll	13	LA
Southern Belize	South Northern Region	14	SN-North
		15	SN-South
		16	SN-Cayes
	South Central Region	17	SC-North
		18	SC-South
		19	SC-Cayes

	Southern Region	20	SR-North
		21	SR-South
		22	SR-Cayes

Time series of storm surge and waves for each one of the 309 TCs at each CU have been obtained from the marine dynamic modelling (see section 2.2) for the current situation and for the horizon year 2050 under RCP8.5 scenario (SLR=27.5 cm). This is the input of XBEACH model that simulates hydro-morphodynamic processes in the nearshore area and on the beach during each TC in the database and yields the corresponding morphological changes of the beach profile. Finally, the statistical analysis of TC-derived coastal erosion is based on the approach already described in section 2.2.5 and coastal erosion maps for different return periods (10, 50, 100 and 500 years) are shown in section 2.5.2.

The model XBEACH accounts for the effects of vegetation and hard structures, and therefore various beach profiles depending on the typology of the backshore of the beach have been modelled for each CU. To do so, each CU has been subdivided into segments according to 5 different littoral typologies identified in the study area:

Type 1. Hard structure.

Type 2. Sandy beach backed by vegetation.

Type 3. Mangrove.

Type 4. Coral reef.

Type 5. Waterway or wetland.

These elements have been included in the numerical model, only if they are present in the corresponding CU (see Figure 18).

Figure 18. Segmentation in 5 Coastal Typologies and Delimitation of the 22 CUs.

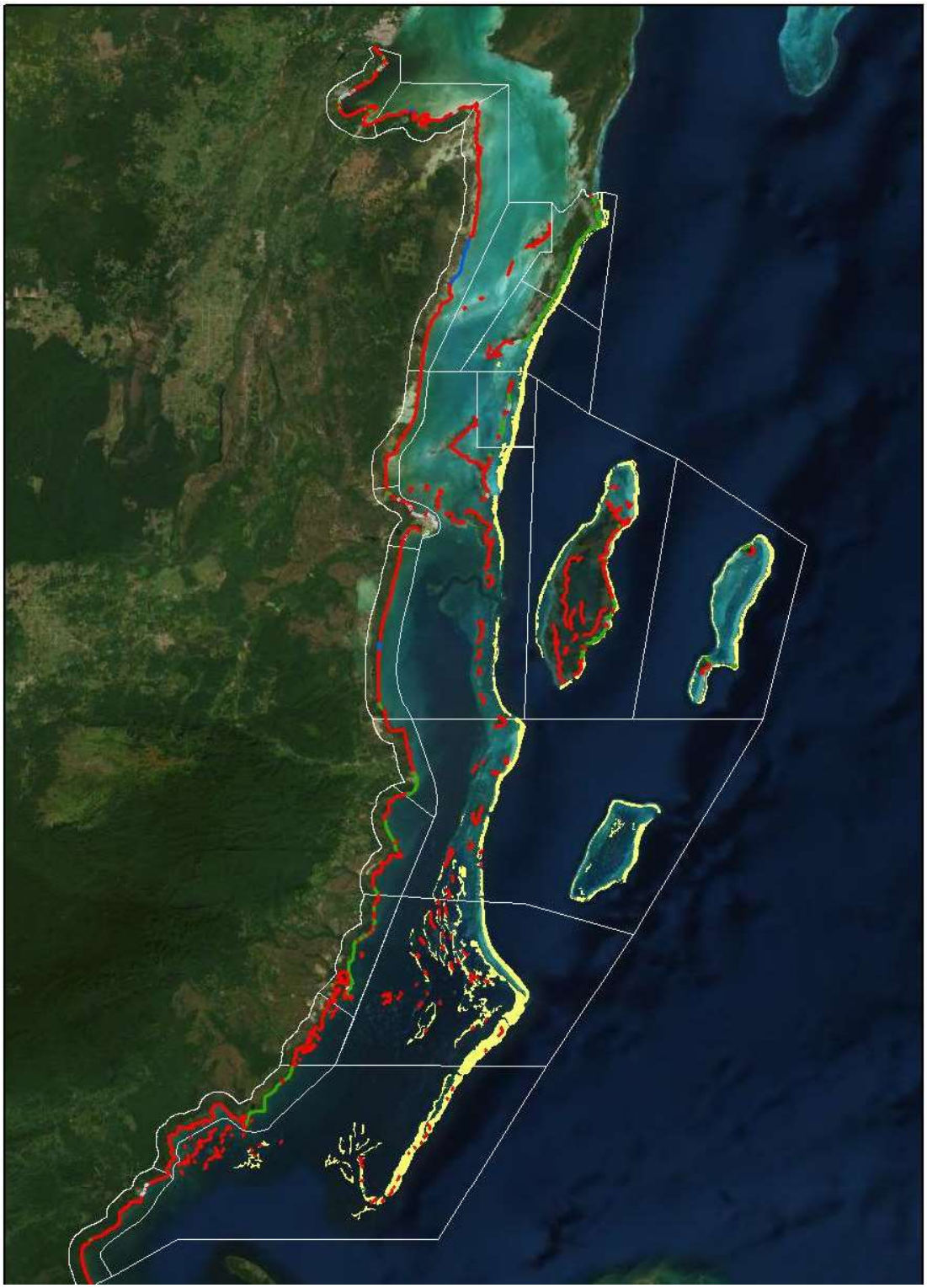

Two kinds of hard structures (type 1) have been considered in this study (see Figure 19):

- Rip-rap structures such as longshore revetments or cross-shore groins.
- Vertical concrete or sheet-pile seawalls.

Figure 19. Vertical Seawall and Rip-Rap Protection in San Pedro (Belize).

Rip-rap structures can be damaged by tropical cyclones if the wave height at the foot of the structure exceeds the design wave height of the armor pieces. The XBEACH numerical modelling yields the maximum wave height at the foot of coastal structures in each CU (where coastal structures are present) for each one of the 309 TCs in the database. The well-known Hudson's formula (USACE, 1984; Ciria-CUR, 2007) has been used to estimate potential damages of these coastal structures as a function of the wave height. Accordingly, the design weight of pieces in rip-rap protections to withstand TC impacts have been obtained for different return periods (10, 50, 100 and 500 years). The following figure shows an example of the statistical fit to the GPD for the wave height and the weight of rip-rap revetment at one particular location.

Figure 20. Distribution Function of Wave Height at the Foot of the Coastal Structures (Left) and Design Weight of Armor Rocks (Right) in AC-South (CU6).

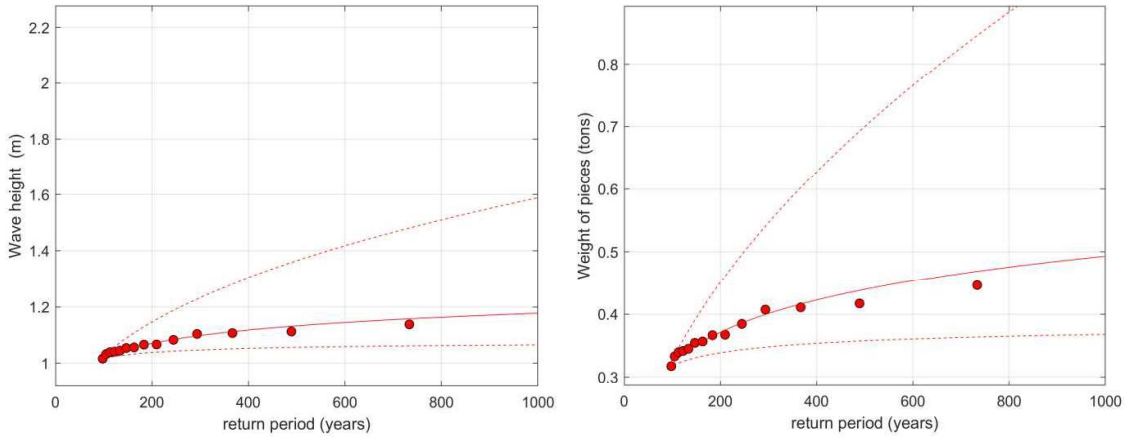

As for the vertical seawalls, collapse of these structures takes place when the scour depth exceeds the base of the seawall foundation. XBEACH provides the scour depth (vertical erosion in front of the structure) at each CU (where coastal structures are present) for each one of the 309 TCs in the database. An example of the scour results for a historical and synthetic hurricane at a particular location is shown in the following figure.

Figure 21. Example of Modeled Scour at the Foot of a Seawall Associated with Hattie (Left) and a Synthetic Hurricane (Right) in the SC-North (CU17). Beach Profile Before (Thin Black Line) and After the Event (Red Line), Seawall (Thick Black Line) and Wave Height (Blue Line).

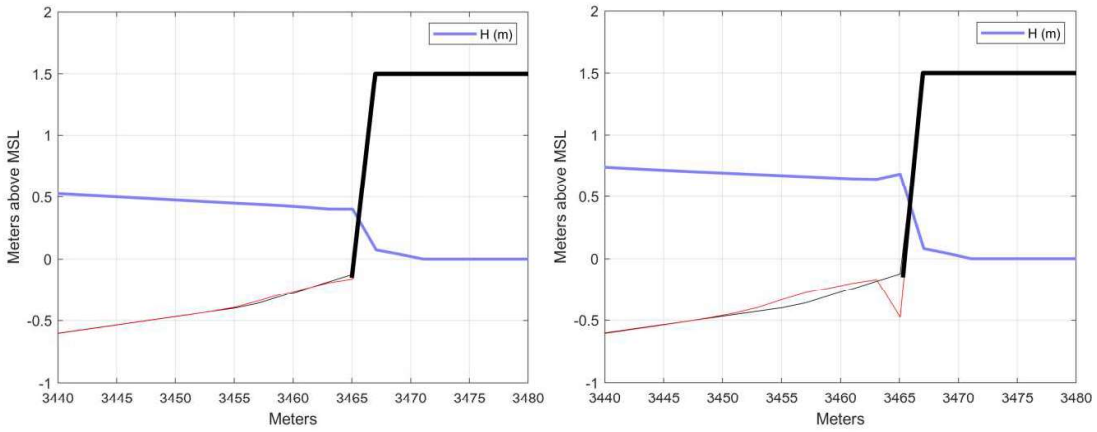

Model results show over 35 cm of scour (vertical erosion) at the foot of the seawall for the synthetic hurricane and negligible scour for the historical hurricane Hattie, in the particular

case of the example in Figure 21. As per the corresponding distribution function (see Figure 22), the return period of these scours are 500 years and 100 years, respectively, which exemplifies the need of synthetic events in the developed database in order to obtain results for high return periods.

Figure 22. Example of the Distribution Function of Modeled Scour at the Foot of a Seawall in the SC-North (CU17).

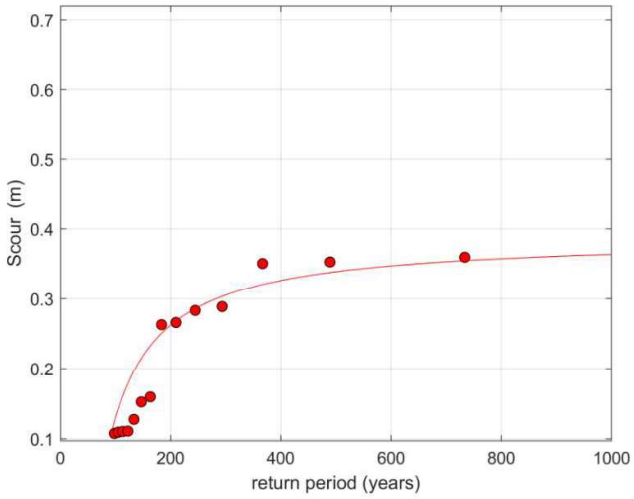

The erosion of sandy beaches back by vegetation and mangroves (types 2 and 3) has been characterized by the loss of land after a TC on the beach front up to a height of 1 m above the mean sea level. Regular vegetation at the back of the beach has been included in XBEACH as vertically uniform vegetation situated 10 m landward of the shoreline and inland, whereas mangroves have been included in XBEACH as vertically non-uniform vegetation located on the shoreline and inland, including three vertical layers for the consideration of roots, trunks and branches (see Figure 23).

Figure 23. Conceptual Modelling of Mangroves in XBEACH (Left), Mangroves in Caye Caulker (Right).

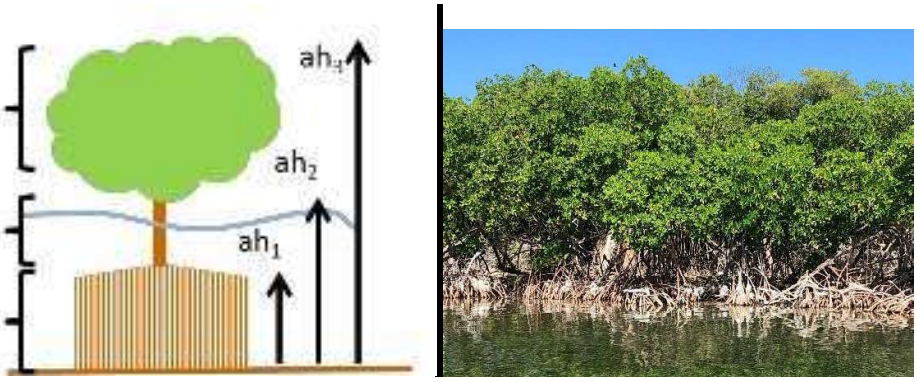

As an example, the following figure shows an example of the modelled erosion of mangroves and of the beach backed by vegetation.

Figure 24. Example of modeled erosion of mangroves (left) and beach backed by vegetation (right) associated with Hurricane Keith in the AC-North (CU6). Beach profile before (thin black line) and after the event (red line), vegetation/mangroves (thick green line) and wave height (blue line).

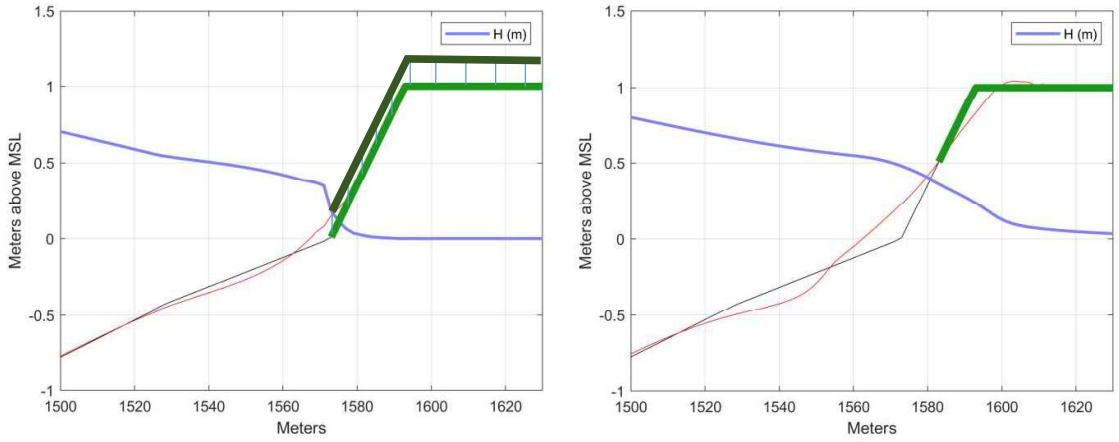

It shows no erosion above the shoreline, whereas part of the vegetation located at the back of the beach is lost. In the submerged beach similar erosional pattern is observed with and without mangroves, nevertheless mangroves attenuate morphological changes in this area.

In Belize, all beaches are either backed by vegetation or by some sort of coastal structure. However, for the purpose of comparison, a non-vegetated beach profile has been modeled. The following figure shows the modelled erosion of a sandy beach in Ambergris Caye - South

following hurricane Keith. Comparison of Figure 24 and Figure 25 exemplifies the potential for erosion reduction of vegetated coastal areas and mainly mangroves.

Figure 25. Example of Modeled Erosion of a (Non-Existent) Sandy Beach Associated with Hurricane Keith in the AC-North (CU6). Beach Profile Before (Thin Black Line) and After the Event (Red Line) and Wave Height (Blue Line).

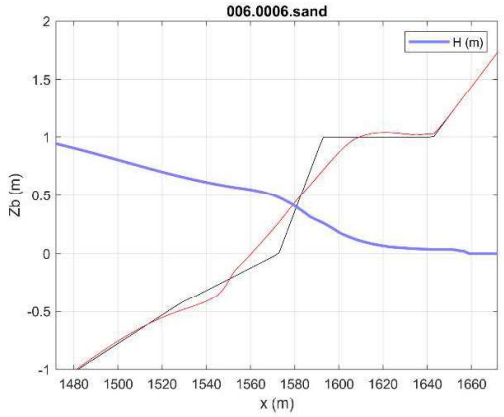

The numerical modelling approach based on XBEACH model is not able to correctly simulate the erosion of coral reefs under a storm and, to our knowledge, this is an unprecedented challenge. Thus, in this study, the assessment of coral reef erosion under TC is based on the hypothesis of no damages in the current situation and a homogeneous reduction of reef crest height of 1 m in the horizon year 2050, due to climate change-derived coral bleaching. Chapter 3 includes the assessment of the expected damages due to the hypothesized degradation of coral reefs.

The effect of climate change has been calculated modelling the same geometries under the RCP8.5 climate change scenario by 2050 (SLR= 0.275 m). Figure 26 shows that the presence of SLR produces more scour in front of the structures. Figure 26 indicates that the design weight of pieces for rip-rap protections does not vary for these scenarios. Figure 28 and Figure 29 show increasing erosion in the case of SLR for sandy beaches backed by vegetation and mangroves respectively.

Figure 26. Example of the Distribution Function of Modeled Scour at the Foot of a Seawall at SC-North (CU17).

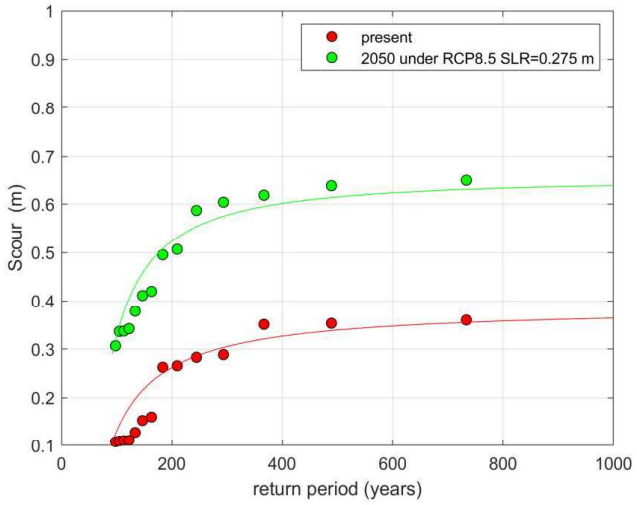

Figure 27. Example of the Distribution Function of Modeled Design Weight of Pieces in Rip-Rap Protections in the AC-South (CU6).

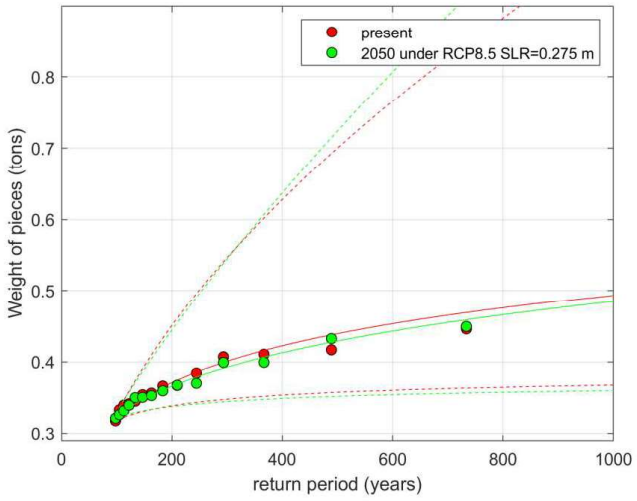

Figure 28. Example of the Distribution Function of Modeled Erosion at a Sandy Beach Backed by Vegetation at SR-North (CU20).

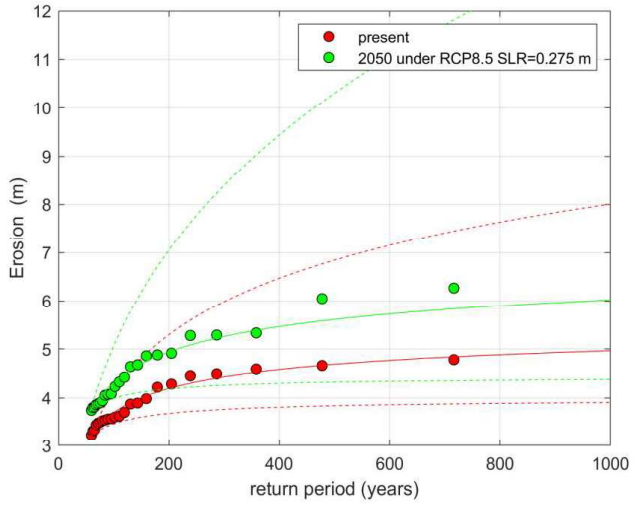

Figure 29. Example of the Distribution Function of Modeled Erosion at a Coast Protected With Mangroves at CR-South (CU9).

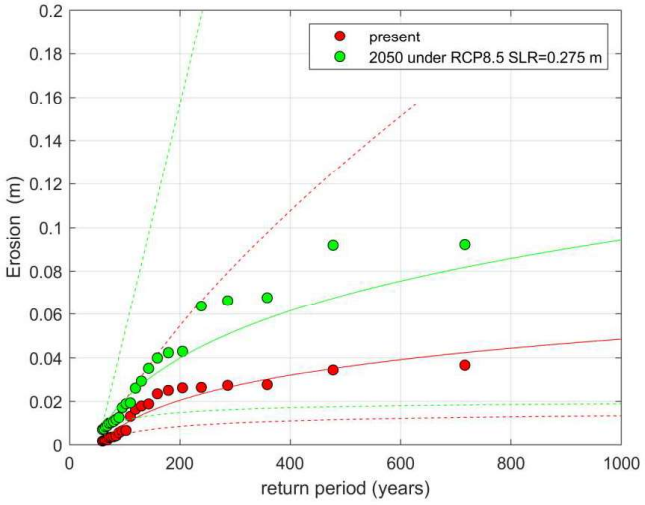

2.5 Results

In this section coastal flooding and coastal erosion return period maps are shown.

2.5.1 Coastal flooding

The maps in this section show the flood extent and flood height with respect to the current mean sea level for various return periods (10, 50, 100 and 500 years) in the current situation (see) and in the horizon year 2050 under RCP8.5 scenario (SLR=27.5 cm).

Figure 30. Maps Eith the 10, 50, 100 and 500 Years Return Periods of Extent and Flood Height (i.e. Respect to the Current Mean Sea Level) for the Present Conditions.

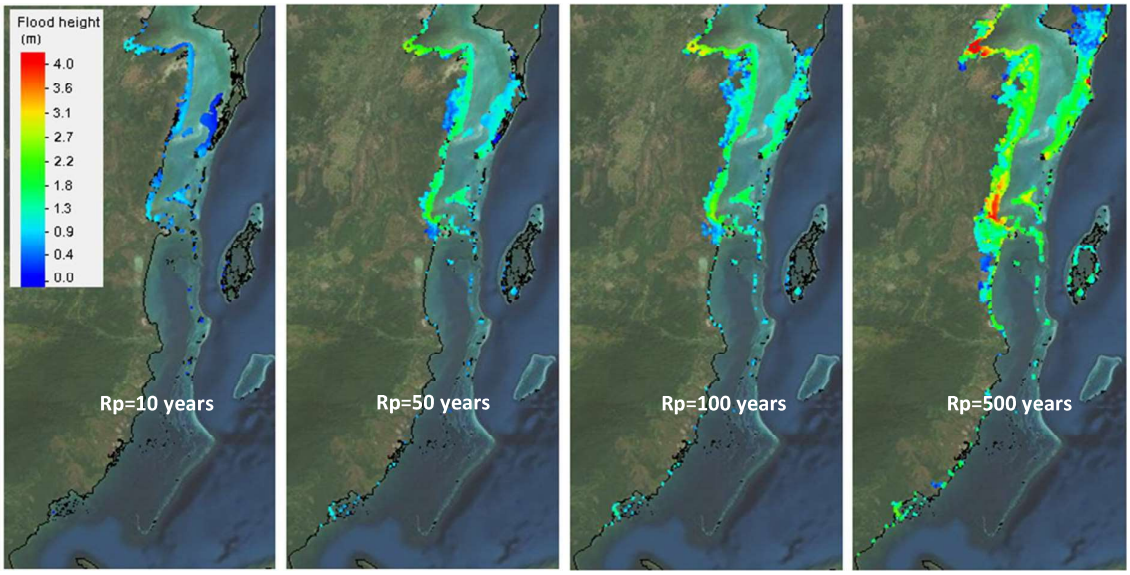

Figure 31. Maps with the 10, 50, 100 and 500 Years Return Periods of Extent and Depth of Flooding for the RCP8.5 Climate Change Scenario by 2050 (SLR= 0.275 m).

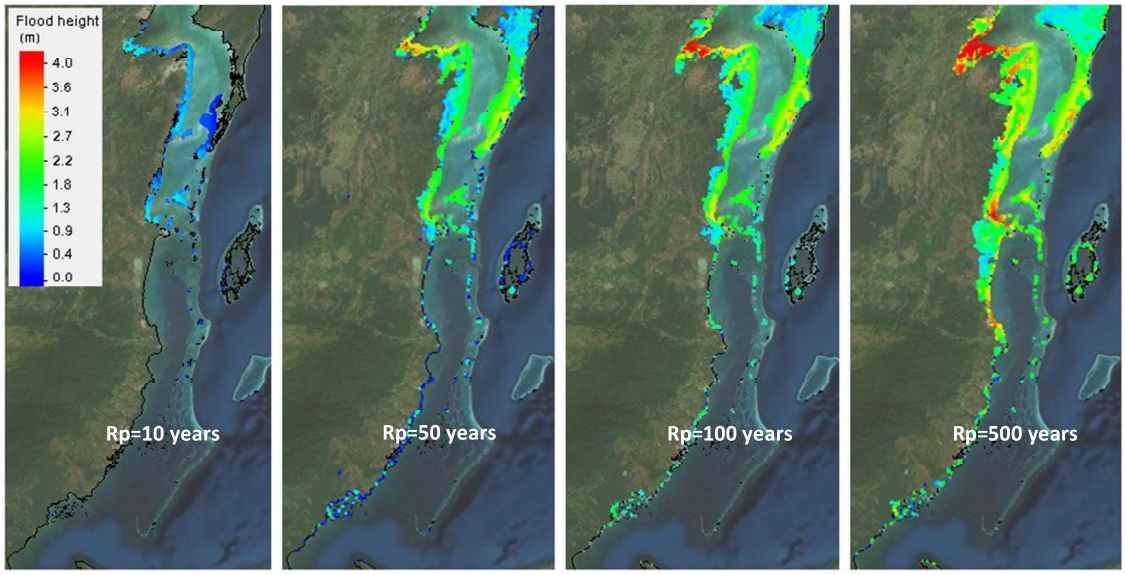

2.5.2 Coastal erosion

The maps in this section show the erosion and scour simulated with XBEACH for each CU for various return periods (10, 50, 100 and 500 years) in the current situation and in the horizon year 2050 under RCP8.5 scenario (SLR=27.5 cm). Figures have been generated for each of the typologies of vegetation found in Figure 18 (hard structure, sandy beach backed by vegetation and mangrove).

Figure 32. Maps with the 10, 50, 100 and 500 Years Return Periods of Scour in Front of Hard Structures for the Present Conditions.

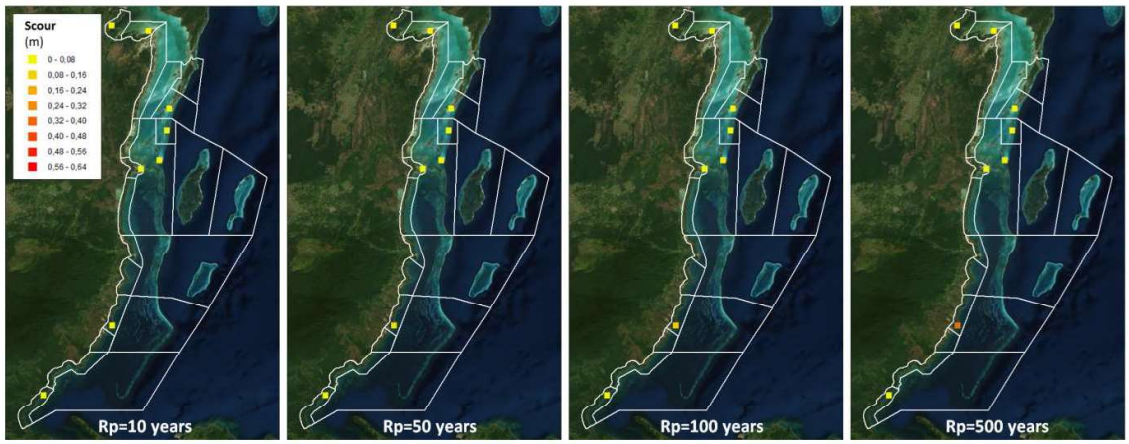

Figure 33. Maps with the 10, 50, 100 and 500 Years Return Periods of Scour in Front of Hard Structures for the RCP8.5 Climate Change Scenario by 2050 (SLR= 0.275 m).

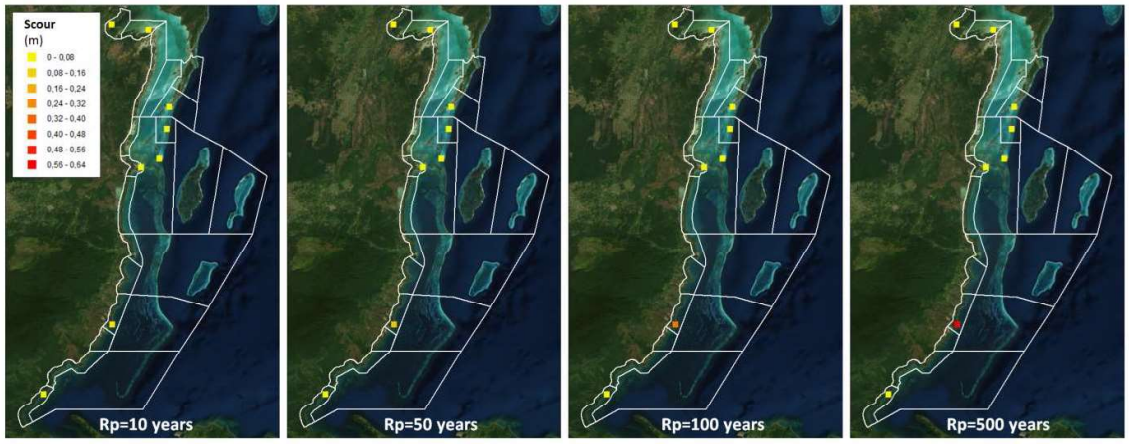

Figure 34. Maps with the 10, 50, 100 and 500 Years Return Periods of Coastal Erosion of a Sandy Beach Backed by Vegetation for the Present Conditions.

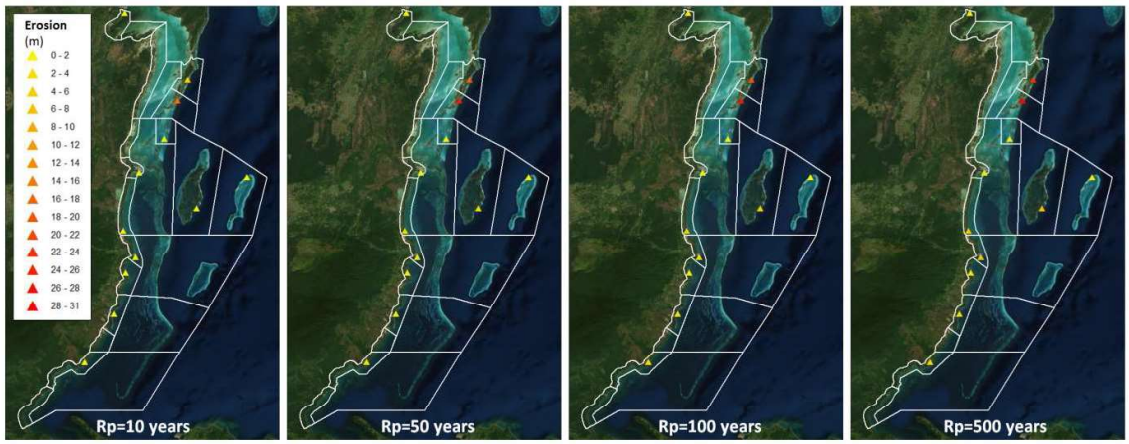

Figure 35. Maps with the 10, 50, 100 and 500 Years Return Periods of Coastal Erosion of a Sandy Beach Backed by Vegetation for the RCP8.5 Climate Change Scenario by 2050 (SLR= 0.275 m).

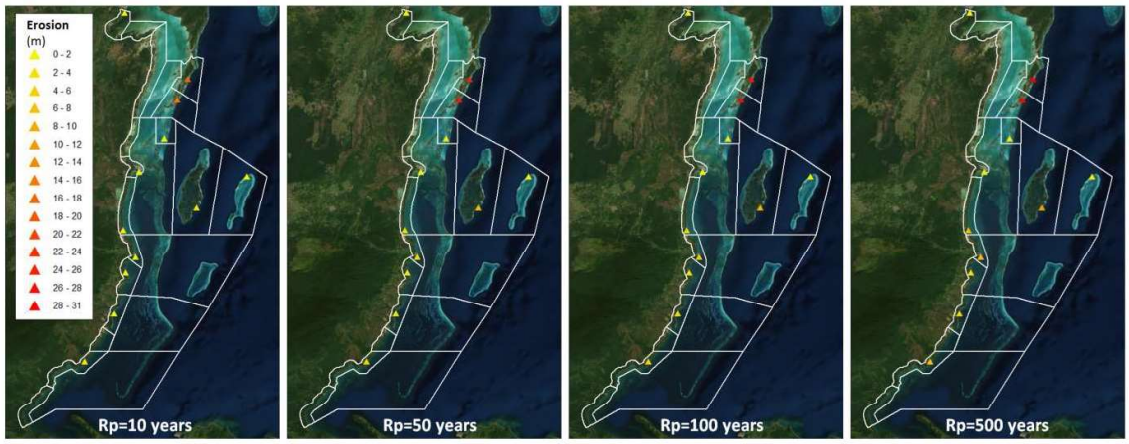

Figure 36. Maps with the 10, 50, 100 and 500 Years Return Periods of Coastal Erosion of a Coast With Mangroves for the Present Conditions.

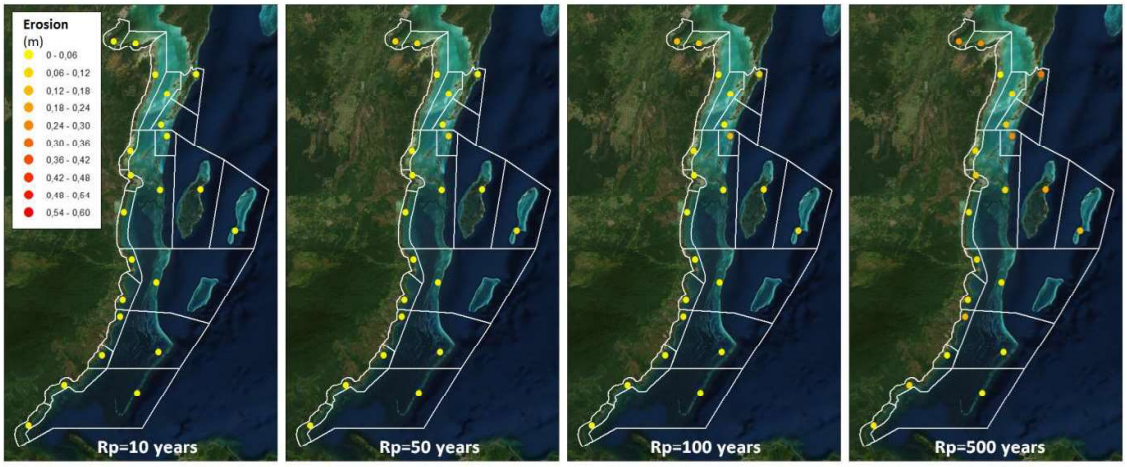

Figure 37. Maps with the 10, 50, 100 and 500 Years Return Periods of Coastal Erosion of a Coast With Mangroves for the RCP8.5 Climate Change Scenario by 2050 (SLR= 0.275 m).

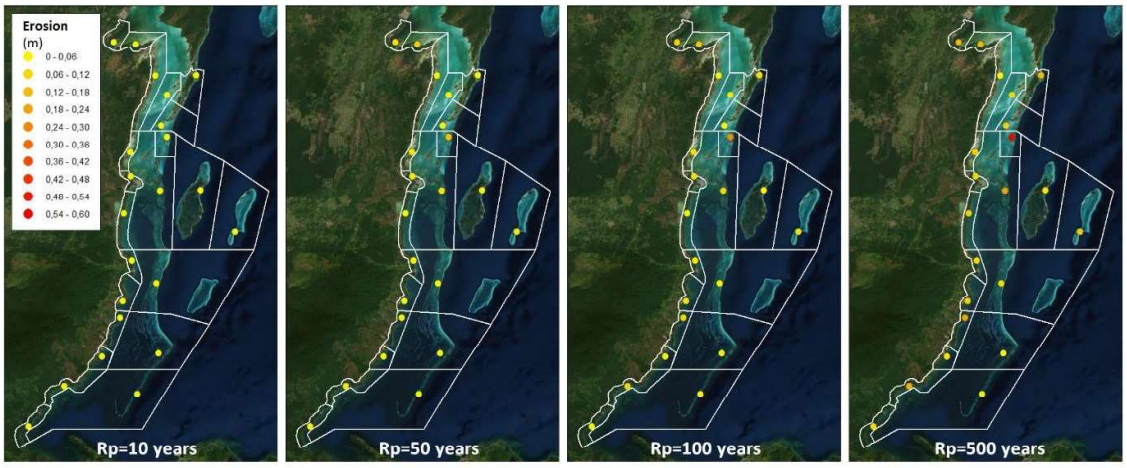

The design weight of pieces in rip-rap protections for the present situation is shown in Figure 38 and in Figure 29 for the RCP8.5 climate change scenario by 2050 (SLR= 0.275 m).

Figure 38. Maps With the 10, 50, 100 and 500 Years Return Periods of Design Weight of Pieces in Rip-Rap Protections for the Present Conditions.

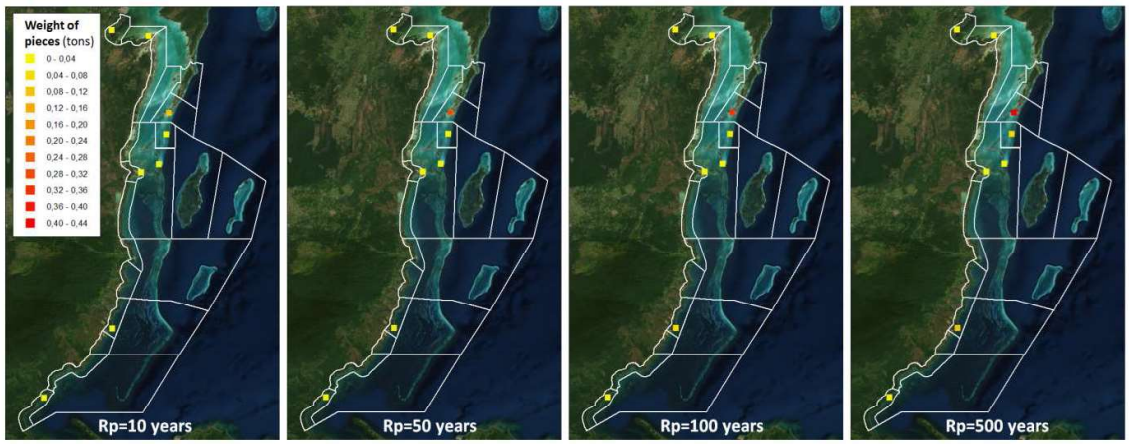

Figure 39. Maps with the 10, 50, 100 and 500 Years Return Periods of Design Weight of Pieces in Rip-Rap Protections for the RCP8.5 Climate Change Scenario by 2050 (SLR= 0.275 m).

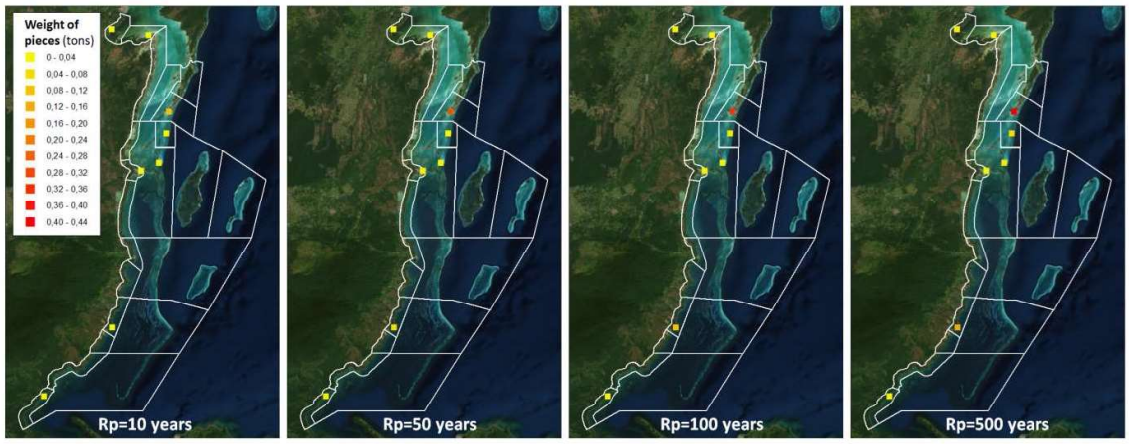

3. COASTAL PROTECTION SERVICE BY ECOSYSTEMS

3.1 Introduction

Coral reefs and mangroves are natural ecosystems grown in coastal areas, typically in the tropical and subtropical regions, such as Belize. They provide several services such as coastal protection, habitat and source of food to different fish species, jobs and incomes to regional economies from fishing, recreation and tourism and they also play a relevant cultural role in many regions around the world, like in Polynesia.

Particularly, in the case of coral reefs, their great richness contrasts with their high vulnerability, heavily exposed to natural hazards and very sensitive to human activity. The two main issues affecting coral reef health are the excess of nutrients and the excess of water temperature. The first one induces an environmental balance disturbance, causing eutrophication of the coral reef area and forcing fishes to move away. The excess of temperature supposes an increment of the acidification of water and, as a consequence, coral bleaching development and degradation process.

Both effects, nutrients and temperature increments, are linked to human activity and closely related to climate change. According to AR5 IPCC (2014), human influence on the climate system is clear and evident, mainly induced by the increase of emissions of greenhouse gases. The atmosphere and the ocean have warmed since 1950 and this fact directly affects coral reefs.

Coral reef degradation has obviously a significant impact in the services provided, especially in protection services, such us flooding reduction, whose value is rarely accounted and difficult to measure unless the ecosystem disappears.

Figure 40. Belize Coral Barrier. Source: NASA.

This chapter focuses on coral reefs and their coastal flood protection role. The current flood protection service by coral reefs along Belize coastline is assessed, along with the comparison with other ecosystems such as mangroves.

3.2 Methodology

The evaluation of the flood protection service of coral reefs in Belize is based on the World Bank guidelines (Beck & Lange, 2016). This methodology (Figure 41) has been widely applied at global (Beck et al., 2017), national (Menéndez et al., 2018) and local scale (Menéndez et al., 2019).

Two scenarios are compared: with and without coral reefs. The difference between both scenarios is the current value of the flood protection service. For the without-coral-reef scenario, 1 meter reduction in reef height (and the associated component of friction) is considered. The loss of 1m of living coral is assumed, with little (if any) loss of the underlying limestone. Hence, a dead or dying reef is reproduced and loss of a significant component of the living coral reef, not the underlying limestone structure. Most of the 1m in loss that is assumed comes from the loss of the top-most layer of living corals, including in particular the branching, table and (small) boulder forming corals. The underlying limestone structure is assumed to remain intact and is not lost (or is eroded only slowly).

The multistep methodology is based on five stages, from offshore wave climate to socioeconomic risk and risk reduction:

- **Stage 1**: Oceanographic data are combined to assess offshore sea states (waves and sea level).
- **Stage 2**: Downscaling from offshore to nearshore (before the ecosystem). Waves are modified by nearshore hydrodynamics.
- **Stage 3**: Wave's propagation through the habitat. The effects of habitat on wave run-up are estimated.
- **Stage 4**: Flood heights are extended inland along profiles (every 2 km) for four locally generated, storm events (10, 25, 50, 100-yr events) with and without coral reefs.
- **Stage 5**: The land, people and built capital damaged under the flooded areas are estimated, with and without coral reef scenarios. The benefit provided by the ecosystem is the difference between both scenarios.

Figure 41. Key Steps and Data for Estimating the Flood Protection Benefits Provided by Reefs. Source: Beck et al. (2017).

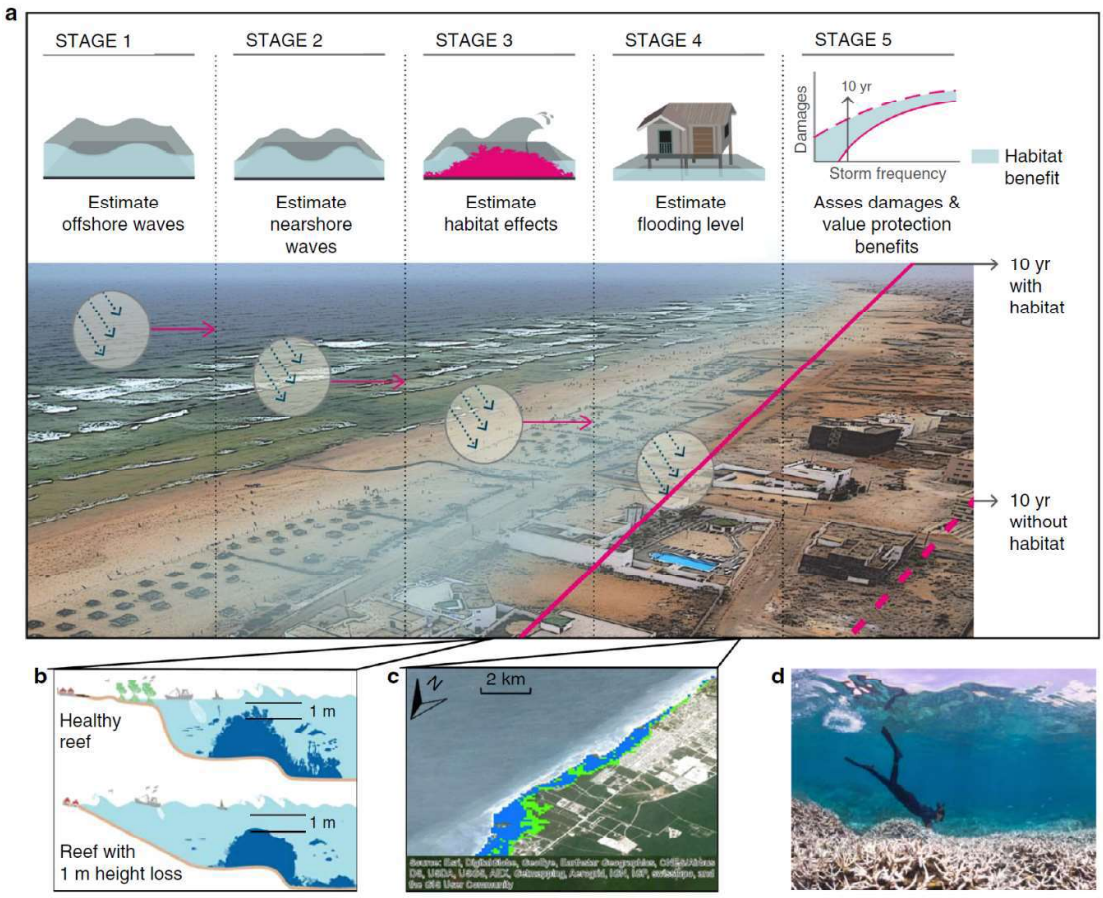

3.3 Results

3.3.1 Value of the flood protection service in Belize

Coral reefs provide direct protection to 702 people in Belize every year, and prevent 9 US$ millions of annual losses. Without coral reefs, an additional 400 Ha of land would be annually flooded.

While these values highlight the annual expected benefits, coral reefs in Belize provide the highest flood protection facing to high intensity events (i.e. tropical cyclones). The benefits of preserving the current coral reefs in Belize increase with the storm intensity. For example, 1-in-10-year event would affect additional 1789 people and produce 53 US$ millions more losses if coral reefs wouldn't exist, while the flood protection against 1-in-100-year event rises to 14259 people and 282 US$ millions. The people flooded and the built capital lost under both, with and without coral reefs scenarios in Belize, and for different return period events are shown in Figure 42 and Figure 43.

Figure 42. Number of People Flooded With and Without Coral Reefs in Belize Under Different Return Period Events.

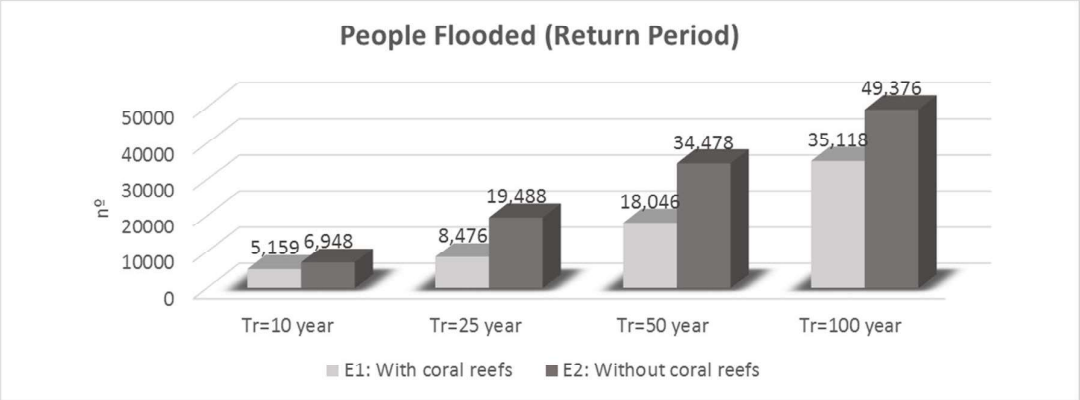

Figure 43. US$ Million Lost by Coastal Flooding With and Without Coral Reefs in Belize Under Different Return Period Events.

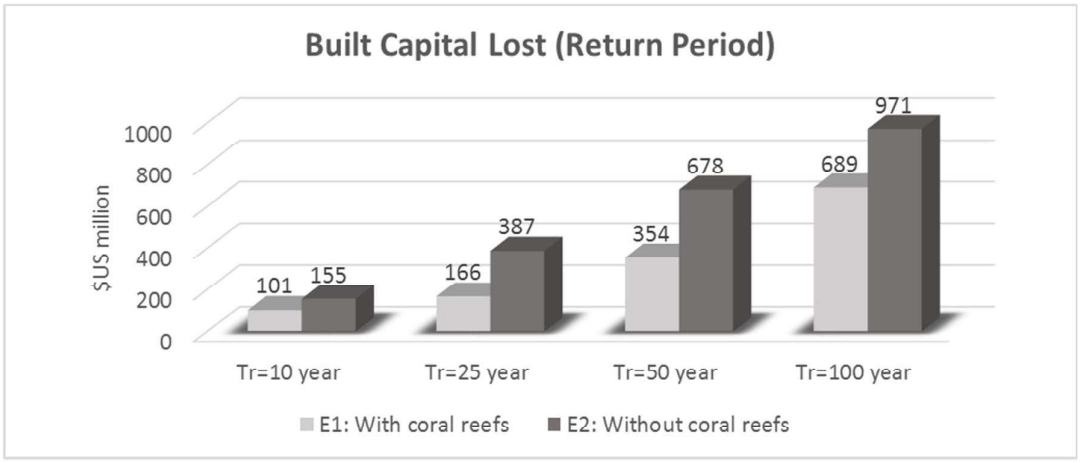

3.3.2 Comparing Belize with the rest of the world

Belize is one of the coral reef most protected countries in the world. It ranks 9th in terms of annual land protected from flooding, 11th in terms of people and 15th in terms of built capital protected. However, the most relevant point is the significant value of the flood protection service with respect to the national GDP. If we compare the percentage of GDP protected by coral reefs, Belize ranks 2nd overall countries in the world, only behind the Cayman Islands. Nowadays, 0.37% of the total GDP of Belize is protected by coral reefs (Table 6).

Table 6. Countries that Rceive the Most Flood Protection Benefits from Reefs. Source: Beck et al. (2017).

	Annual averted damages ($ millions)		Annual averted damages/GDP	
1	Indonesia	639	Cayman Islands	0.98
2	Philippines	590	Belize	0.37
3	Malaysia	452	Grenada	0.30
4	Mexico	452	Cuba	0.25
5	Cuba	401	Bahamas	0.16
6	Saudi Arabia	138	Jamaica	0.14
7	Dom. Republic	96	Philippines	0.13
8	United States	94	Antigua & Barbuda	0.13
9	Taiwan	61	Dom. Republic	0.11
10	Jamaica	46	Malaysia	0.09
11	Vietnam	42	Seychelles	0.06
12	Myanmar	33	Turks & Caicos	0.06
13	Thailand	32	Guadeloupe	0.05
14	Bahamas	14	Indonesia	0.04
15	Belize	9	Solomon Islands	0.04

Annual expected benefit of reefs for flood protection in terms of annual averted damages to built capital ($ millions per year) and relative to Gross Domestic Product (GDP). The values are the difference in expected damages to built capital with and without reefs

3.3.3 Comparing coral reefs with other ecosystems

Coral reefs are not the only ecosystem that contributes to reduce flooding along the coastline of Belize. Mangroves are also very effective, especially in storm surge dissipation. Other analysis carried out with mangroves allows us to compare the relative benefits of each ecosystem in Belize.

The unitary benefit (per hectare of ecosystem) of coral reefs is greater than mangrove's in terms of annual expected people protected (Figure 44) and annual expected economic losses avoided (Figure 45).

Figure 44. Annual Expected Unitary Benefits to People (People/Ha) Provided by Coral Reefs (Green) and Mangroves (Brown).

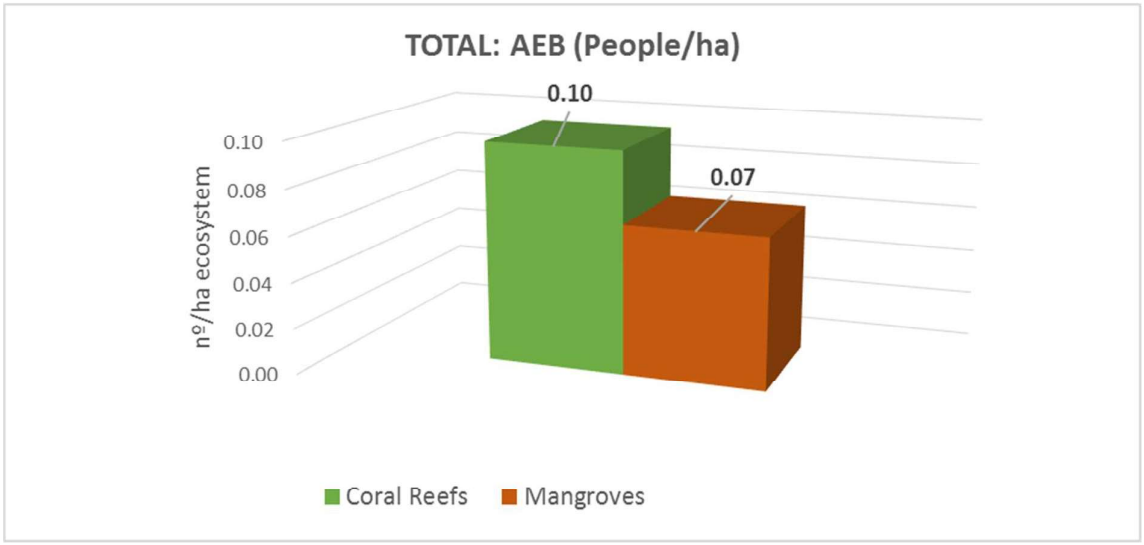

Figure 45. Annual Expected Unitary Benefits to Build Capital (People/ha) Provided by Coral Reefs (Green) and Mangroves (Brown).

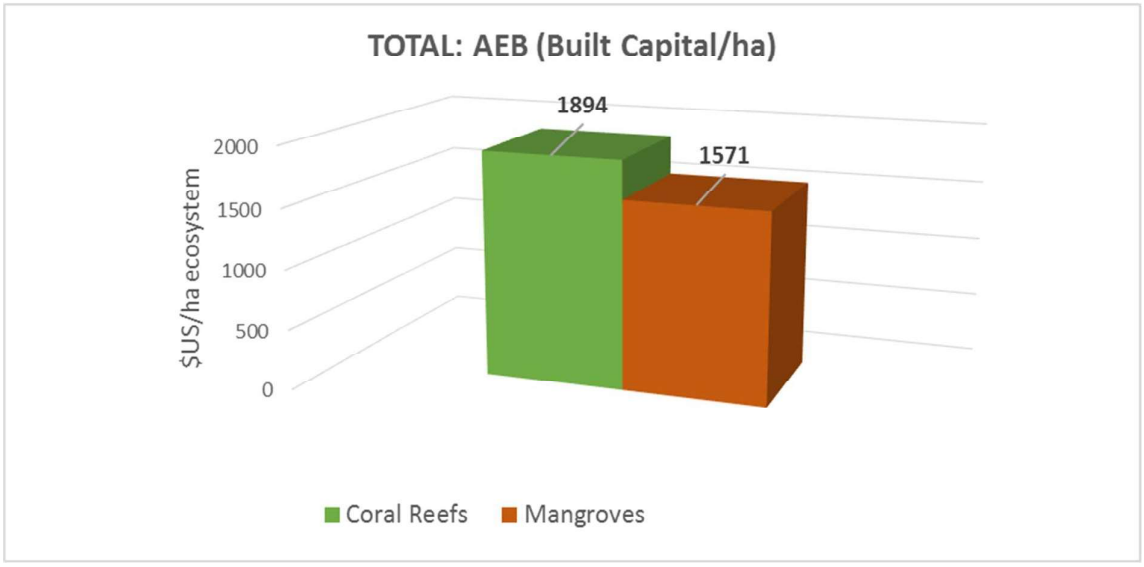

4. RISK ASSESSMENT

4.1 Introduction

Risk assessment aims at analyzing, identifying and describing areas, communities and assets that may suffer serious negative consequences as a result of facing certain natural or human-induced hazards. This is an essential step towards an appropriate implementation of site-specific and target-oriented disaster risk management strategies and risk reduction measures. Accordingly, its major goal is to strengthen disaster risk governance and enhancing disaster preparedness for an effective response as emphasized by the Sendai Framework for Disaster Risk Reduction (UNDRR, 2015), by mainstreaming disaster risk reduction into development policies, planning and programming at all levels including prevention, mitigation, preparedness and vulnerability reduction, as highlighted by the previous Hyogo Framework for Action (UNDRR, 2005).

In this study, according to the explanation detailed in chapter 2, two different natural hazard phenomena are considered within the risk assessment: (i) coastal flooding and (ii) coastal erosion, with both storm surges and waves caused by tropical cyclones as drivers. These hazards have been assessed by a probabilistic approach, intended to answer the question of when a certain intensity of flooding or erosion can be exceeded (e.g., probability of exceeding 50 cm of flooding or 1 m of coastal retreat).

4.2 Conceptual framework

Given the wide variety of terms related to risk management and the different approaches used to assess it, both the conceptual framework and the different risk components are defined below to understand the approach carried out in this work.

Risk is understood in this study as the potential for negative consequences or impacts due to the interaction between one or more natural or human-induced hazards, exposure of humans, infrastructures, and ecosystems, and their vulnerability (adapted from UNDRR, 2016; UNDRR Terminology, 2020).

Following the UNDRR terminology, the hazard is a process, phenomenon or human activity that may cause loss of life, injury or other health impacts, property damage, social and economic disruption or environmental degradation. On the other hand, exposure relates to the situation of people, infrastructure, housing, production capacities and other tangible human

assets located in hazard-prone areas whereas vulnerability refers to the conditions determined by physical, social, economic and environmental factors or processes which increase the susceptibility of an individual, a community, assets or systems to the impacts of hazards.

Accordingly, the risk is addressed in this study as a function of hazard and vulnerability of the elements exposed to the hazard, $R= f (H, V_{(E)})$.

As noted in the introductory section of this chapter, the natural hazards addressed in this work are coastal flooding and erosion, with storm surges and waves caused by tropical cyclones being the driving factors. Both hazards have been assessed from a probabilistic approach, considering the following return periods: 10, 50, 100 and 500 years. Additionally, the RCP 8.5 climate change scenario has been considered in terms of sea-level rise, applying the projections defined in Slangen et al. (2014) with the selection of the 27.5 cm sea-level rise scenario (see chapter 0 for more details).

In terms of risk and vulnerability, this study focuses on the impacts that the coastal society may potentially suffer due to both hazards considered. To perform this human-centred approach, several variables have been analyzed and a set of indicators has been defined to evaluate the characteristics of the diverse elements exposed that may increase their susceptibility to the hazards considered. These elements have been split into three different dimensions called human, infrastructures and environmental.

The human dimension addresses the intrinsic characteristics of the population which make them more susceptible to suffer from the impact of the hazards analyzed.

The infrastructure dimension includes households, critical and emergency facilities and coastal structures, to consider their potential worsening implications for the populations due to existing feedback loops. For example, the increase in the number of victims due to the loss of emergency services during the event or the loss of recovery capacity of the country due to the loss of strategic socio-economic infrastructures such as ports.

The environmental dimension considers the relevance and status of ecosystems. Losses in the extent or number of ecosystems will hinder recovery from a disaster, as well as the development of livelihoods and social well-being associated with various ecosystem services.

As a result, the risk assessment performed considers:

- three components, namely hazard, exposure and vulnerability,
- three dimensions, namely human, infrastructures and environmental,

- study area / spatial scale: Coastal Unit (CU),
- four return periods and,
- two scenarios (current sea-level rise and RCP 8.5 climate change scenario)

Accordingly, several results have been obtained. Figure 46 illustrates the general conceptual framework including the different risk components, dimensions, scenarios and results obtained Due to the scale of the work and the inherent complexity of the erosion processes, it should be noted that in the case of coastal erosion risk assessment, coastal structures and beach surfaces have been considered instead of three dimensions. It is understood that those areas in which coastal structures are damaged, collapsed or significant beach surface is lost will have a subsequent impact on coastal society. The following sections explain the details of the method applied for each hazard based on this conceptual framework.

Figure 46. Conceptual Framework. Components, Dimensions and Scenarios Addressed and Results Obtained.

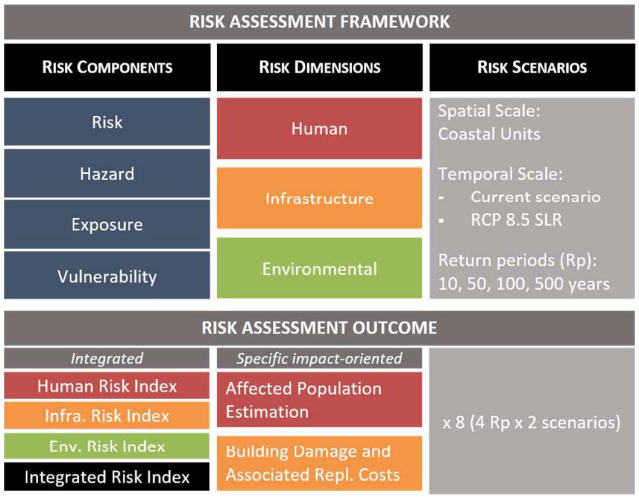

4.2.1 Coastal flooding risk assessment

The coastal flooding risk assessment has considered all the risk components, dimensions and scenarios explained in Figure 46.

The assessment included two analyses. On the one side, an integrated assessment, based on an indicator-based and semi-quantitative approach that has been developed to obtain two types of results: partial risk indexes for each of the dimensions evaluated and an integrated risk index

(IRI) that includes the three dimensions. This approach allows understanding the impacts separately for the different risk dimensions, components, indicators and variables as well as to identify areas where major problems may arise as a combination of the different dimensions that comprise the system. In addition, the method allows for the understanding of the precise cause of the results obtained, thus providing essential information for risk management (Aguirre-Ayerbe et al., 2018).

The use of indices has the advantage of simplifying the complexity of the information that must be communicated while simultaneously indicating the interaction of multiple, spatially homogeneous indicators through a single aggregated vulnerability score (Abson, 2012). At the same time, to minimize the loss information inherent to an indicator-based method, the structure developed permits easily to trace back the real data so that the utility for the policymakers can be found in both ways: first a broader insight of where are the exposed elements more susceptible to suffer the impact of the hazard and secondly to identify and know the reason with real data.

Figure 47. Complexity and Completeness of Information Available for Decision Making (Source: Abson, 2012).

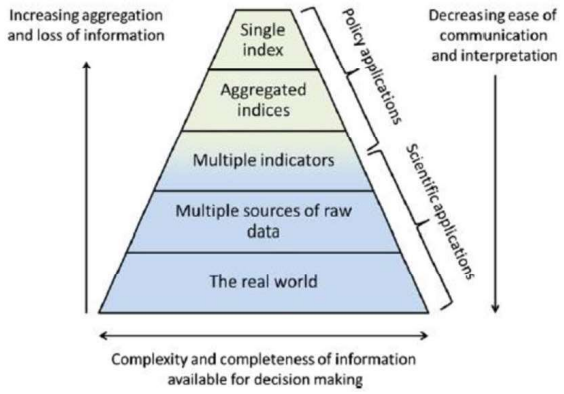

Furthermore, a specific impact-oriented analysis has been developed. Estimates of coastal flood damage to buildings and related replacement costs per CU have been analyzed. In addition, an analysis has been carried out, consistent with the scale and scope of the study, to estimate the degree of impact that the coastal flooding hazard obtained in this study could have on the exposed population.

4.2.2 Exposure and Vulnerability

4.2.2.1 Integrated risk assessment

The conceptual framework explained above considers that the first condition for a person, area or asset to be vulnerable is to be exposed to the analyzed hazard. Therefore, only the exposed elements are included in the vulnerability assessment.

The method for the indicator-based vulnerability assessment has the following steps:

– *Variables and indicators selection.* A set of indicators has been developed to calculate the exposure and vulnerability of the three dimensions considered. These indicators are supported by a Geographic Information System (GIS) which allows every decision with geo-referenced information. Based on previous relevant experience in terms of risk and vulnerability assessment, considering the scope and objectives of the study and the particular characteristics of Belize, a preliminary set of 22 indicators was developed, based on a preliminary list presented to relevant stakeholders at the First Workshop of the project (for additional information see Annex 1 "First Workshop Report" of the document Deliverable 2. Data Collection Report). During this workshop, in addition to the agreement on the final set of indicators, the different sources of the information were identified. Further limitations during the data collection process reduced this initial list to 11 indicators. Nevertheless, it permitted to develop a good framework for the analysis covering the three dimensions defined and the major issues related to the vulnerability of the country.

The table below presents the final set of indicators developed and the variables used for the vulnerability assessment.

Table 7. Exposure and Vulnerability Indicators.

INDICATORS		VARIABLES
Human Exposure	H1 - Exposed population	Number of persons exposed.
Human Vulnerability	H2 - Sensitive age groups	Number of persons under 9 years old.
		Number of persons over 65 years old.
	H3 – Disability	Number of disabled persons (physical/intellectual).
	H4 – Illiteracy	Number of illiterate persons.
Infrastructure Exposure	I1 - Exposed built up area	Area of settlements exposed.
Infrastructure Vulnerability	I2 - Critical buildings	Number of critical buildings (health, educational, hotels, cultural).
	I3 – Emergency	Number of emergency infrastructures (police and fire stations).
	I4 –Transport	Number of strategic transport infrastructures (ports and airports) and length of roads.
Environmental Exposure	E1- Ecosystems exposed	Area of ecosystems exposed.
Environmental Vulnerability	E2 - Protected areas	Area of ecosystems under a protection figure.
	E3 - Relevance of Ecosystems	Area of relevant ecosystems (corals, mangroves, littoral forests, wetlands and seagrass).

Indicators that correspond with the Exposure are coded H1, I1 and E1 for human, infrastructure and environmental dimensions respectively.

The vulnerability indicators are oriented to measure the following:

The Human Vulnerability indicators (H2-H4) are oriented to measure the CUs weaknesses in terms of response, evacuation and recovery capacities of the exposed population.

Indicators H2 and H3 are related to dependency and mobility issues, whereas H3-intellectual disability and H4 relate to difficulties in responding to and understanding hazard situations and warning messages, as well as reduced adaptive capacity.

The Infrastructure Vulnerability indicators (I2-I4) measure the number of critical and emergency facilities that would be affected by CU considering the implications to the affected system. Indicator I2 considers the buildings that would require a coordinated and previously planned evacuation due to the high number of people in them (in many cases sensitive population), such as hospitals, schools, hotels, cultural sites). Through the indicator I3, it is analyzed the loss of emergency services, which are essential during the event. Finally, indicator I4 relates to strategic transport infrastructures, such as ports and airports, in addition to the road network, all of them essential for the normal function and the economy of the country and the local livelihoods.

The Environmental Vulnerability indicators (E2-E3) are defined to measure the relevance and condition of ecosystems. Indicator E2 relates to the existing protected areas since the protection of a given space is an explicit recognition of the environmental value of the resources it contains and their relevance to the country. On the other hand, indicator E3 is related to the ecosystems that have a significant value for the country considering the cultural, provisioning and regulating services provided. This indicator includes the relevant ecosystems shown in Table 7, if not included in an official protection figure.

The indicators system developed allows managing the information at the index level as well as separating them into the different indicators and working directly with the base data which is essential for not losing information while aggregating results, and for the formulation of adequate risk reduction measures.

– *Data collection and validation*. The data collection task focused on the collection of all existing information needed for carrying out the risk assessment, e.g. georeferenced data, tables, scientific papers or technical reports. During the first workshop, several sources of the information were identified for the data collection process. Detailed information on data collection and validation is described in the document *Deliverable 2. Data Collection Report*. In summary, after the data collection and validation phase, the data provided by the following sources of information were finally used:

- Human dimension: Statistical Institute of Belize (SIB).
- Infrastructure dimension: Coastal Zone Management Authority and Institute (CZMAI) and Land Information Centre (LIC).
- Environmental dimension: The Biodiversity and Environmental Resource Data System of Belize (BERDS) and Land Information Centre (LIC)

– *Building indicators through normalization of variables.* Several mathematical-statistical procedures are applied to the variables to produce comparable and combinable indices. Based on OECD (2008), to correct the imbalance caused by the different variable units thus allowing for their comparison and combination, the transformation of the variables range of values is carried out through the minimum-maximum (Min-Max) method, which normalizes the indicators to obtain an identical range [0,1].

$$Indicator_{MM} = \frac{x - X_{\min}}{X_{\max} - X_{\min}}$$

where:

MM = normalization via Min-Max method

x = variable value in the analyzed CU

$X_{\min}$ = minimum value of analyzed variable*

$X_{\max}$ = maximum value of analyzed variable*

* For the exposure indicators (H1, I1 and E1), the normalization was performed using the minimum/maximum value of the corresponding variable. However, when building the vulnerability indicators for the human and environmental dimensions (H2 to H4 and E2 to E3), normalization is based on the minimum/maximum value of the range of values considering all the variables of the same dimension, to avoid uncontrolled weighting (over- or underweighting), as each of the variables has a very different range of values. For the infrastructure dimension, due to the significant diversity of variables and value ranges, the normalization was performed using the minimum/maximum value of each corresponding variable, similar to the procedure used to obtain the exposure indicators.

– *Building indices through weighted aggregation.* Once every indicator is normalized, a weighted aggregation is applied to the individual indicators to build the partial and aggregated indices as shown in Table 8. Through the use of weighting, management and social priorities can be addressed, as well as technical factors related to the reliability of the data used.

$$Index = \sum_{i=1}^{n} W_i \cdot I_i$$

where:

Wi = weight of analyzed indicator *i*; ΣWi=1

Ii = normalized indicator *i* (i= 0-1)

n = number of indicators aggregated

Table 8. Aggregated indices and Indicators Construction and Weights Applied to the Vulnerability.

AGGREGATED INDICES	W	PARTIAL INDICES	W	INDICATORS
Human Vulnerability Index	0,5	HEI - Human Exposure	1	H1 - EXPOSED POPULATION
	0,5	HVI - Human Vulnerability	0,4	H2 - SENSITIVE AGE GROUPS
			0,4	H3 – DISABILITY
			0,2	H4 – ILLITERACY
Infrastructure Vulnerability Index	0,5	IEI - Infra. Exposure	1	I1 - EXPOSED BUILT UP AREA
	0,5	IVI - Infra. Vulnerability	0,4	I2 - CRITICAL BUILDINGS
			0,4	I3 – EMERGENCY
			0,2	I4 –TRANSPORT
Environmental Vulnerability Index	0,5	EEI - Env, Exposure	1	E1- ECOSYSTEMS EXPOSED
	0,5	EVI - Env. Vulnerability	0.5	E2 - PROTECTED AREAS
			0.5	E3 - RELEVANCE OF ECOSYSTEMS

– *Index classification.* The indices are then classified considering the data distribution through the Natural Breaks method and translated into five classes. Similar procedures may be found, for instance in Aguirre-Ayerbe et al. (2018), Damm (2010) and the World Risk Report (Alliance Development Works, 2012).

The Jenks Natural Breaks classification method has been selected after testing other methods (such as the equal interval, defined interval, quantile, geometrical interval, standard deviation, etc.). This method is designed to provide the best arrangement of values into different classes by minimizing the variance within classes and maximizing the variance between classes (Jenks, 1967), as it groups within the same class those CU that have similar values, i.e. those that behave in the same way and which are expected to need similar risk reduction measures.

To obtain comparable results among all the CUs, the establishment of the thresholds of classes has been performed taking into account the index values of all CUs. Since this method of classification depends on the distribution of the data, the study of any index evolution over time (for comparable purposes) must maintain the ranges established in the initial analysis.

The following figure (Figure 48) summarizes schematically the process followed to build each indicator and the vulnerability index.

Figure 48. Vulnerability Index Construction.

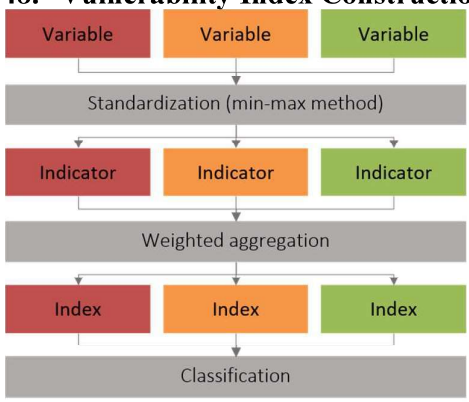

4.2.2.2 Degree of impact on the population (serious injuries/loss of life estimation)

There are several attempts to define a mortality function based on water depth and the combination of water depth and flow rate (see Jonkman, 2007 for further details). However, based on empirical evidence, it is shown that in addition to flood depth and flow velocity, many other factors contribute to flood mortality, many of which are related to the vulnerability of the exposed population and its behaviour, which greatly complicates the equation and increases the uncertainty of purely quantitative estimates.

In this study, an estimation of the degree of damage to the population due to flooding caused by tropical cyclones has been addressed taking into account the existing limitations related to the scope and scale of work of this study, as well as the varying scale, detail and distribution of data across the country.

The method, which is based on the works of Penning-Rowsell et al. (2005) and Jonkman (2007) attempts to estimate the potentially serious injuries or fatalities of the exposed population. According to Graham (1999) and Penning-Rowsell et al. (2005), the main contributing factors that can cause death or serious injury to people during floods are flood characteristics/intensity (flow velocity, flow depth), the exposure of people (their location), and their behaviour/response, the latter often conditioned by their vulnerability (population characteristics).

Several assumptions and simplifications have been made in this work regarding the complexity of an in-depth analysis of the three main contributing factors mentioned above. On the other side, no historical detailed data has been found relating water depth and mortality in the country, thus the approximation should be further reviewed and adjusted. However, this preliminary estimation is reasonably adequate to determine the areas where more management effort should be made to avoid possible loss of life.

Concerning the characteristics of the flood, only flow depth (associated with tropical cyclones) has been considered for each Rp (10, 50, 100 and 500 years) and two SLR scenarios (current sea level situation and RCP 8.5 scenario +0.275 m). Accordingly, the flooding area has been zoned considering a threshold of 1 meter.

In terms of population exposure, due to the uncertainty associated with addressing the probability of exact population location and a management-oriented approach, the worst-case

scenario is addressed. The entire potentially exposed population is considered to be exposed, i.e. people are not located high up or indoors, but are assumed to be outdoors at ground level. It should be noted that the information regarding the population is at the level of the Electoral Division (ED) and a homogeneous distribution by the area of each ED is assumed.

Finally, in terms of the characteristics and behaviour of the population, this work considers the group over 65 years old as the most vulnerable in terms of possible serious flood injuries, due to their potential mobility issues. It is assumed that the youngest population (those under 9 years old) is accompanied by adults. As for the disabled population group, the data provided do not specify the degree of disability and therefore it is difficult to estimate the possible decrease in their mobility and/or behaviour. Therefore, in order not to exaggerate and generate an overestimate of the already proposed worst-case scenario, this variable has not been applied. Lastly, the illiterate population group is not included, as it is not considered a relevant variable for this purpose.

4.2.2.3 Building damage and associated replacement costs

Damage to buildings and related replacement costs constitute relevant information for proper management and preparedness for hazardous events and thus this estimate has been developed, with the following considerations.

The available information on building stock is related to households by Electoral Division (ED). Although the exact location of each household is not known, it is reasonably good information for a country-level analysis. The information also includes building materials for outer walls, which is relevant for the estimation of flood damage.

Two main types of buildings have been defined according to the outer wall materials: concrete and wood. Based on previous analysis developed in the country (*Baseline study for Belize City*, 2017, and *Cost-Benefit Analysis of the Proposed Measures for Caye Caulker and Goff's Caye*, 2017), the following damage functions have been applied to estimate the structural damage that these buildings may suffer as a function of the intensity of the hazard, i.e., the flood depth (see Figure 49).

Damage function wooden facade buildings

$$D_C = 1 - e^{(-0.33 \cdot h^3)}$$

$$if\ h < 2.8;\ D_B = 0.5 \cdot e^{(-0.33 \cdot h^3)}$$

Damage function wooden facade buildings

$$if\ h > 2.8;\ D_B = 0.5 + 0.5 \cdot e^{(-0.33 \cdot (h-2.8)^3)}$$

Figure 49. Functions to Estimate Building Damage.

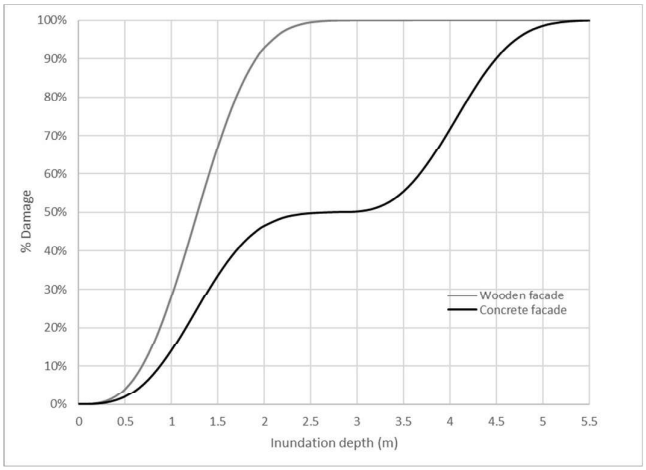

In addition, two different types of building quality have been assumed according to the outer wall materials and replacement values have been assigned for each of them based on the above-mentioned previous work, resulting in 145000 USD and 60000 USD for the concrete and wooden facade buildings respectively.

Finally, replacement costs results (*RC*) are obtained by combining exposed households, the related replacement value and the damage function as $RC = HE * D * HV$, where *HE* relates to the households exposed, *D* is the damage ratio and *HV* is the replacement value for each type of building.

4.2.3 Risk assessment

According to the risk assessment conceptual framework (see Figure 46) and the above descriptions, the risk outcomes are grouped into (i) integrated risk indexes and (ii) specific impact-oriented results.

As for the integrated risk indexes, once the human, infrastructure and environmental vulnerability indices are evaluated and classified into five vulnerability classes, risk is calculated for the human, infrastructure and environmental dimensions through a risk matrix (Aguirre-Ayerbe et al., 2018, González-Riancho et al., 2012; IH Cantabria-MARN, 2010 and 2012 projects; Jelínek et al., 2009; Greiving et al., 2006; ESPON, 2006) by combining the classes obtained for the hazard (x-axis) and the vulnerability indices (y-axis) (see Figure 50).

Figure 50. Risk Matrix (VL: Very low, L: Low, M:Medium; H: High; VH: Very High).

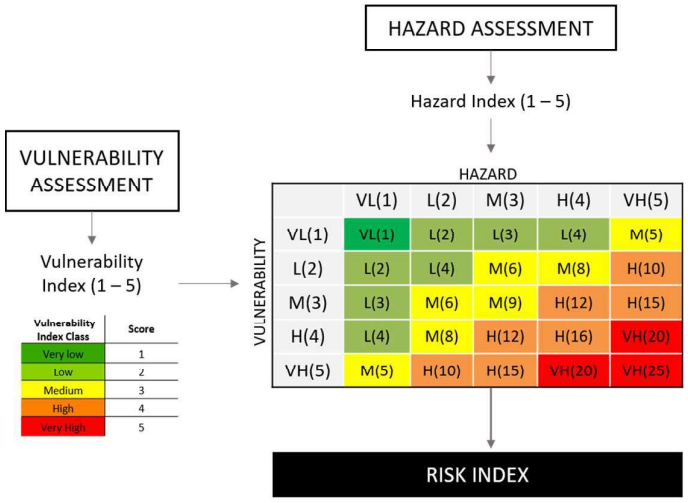

This matrix materializes the equation $R = H \times V_{(E)}$ (see section 0) to calculate the risk as the product of the hazard classes by the vulnerability classes.

The results of the risk matrix allow the identification of the areas of each CU with higher risk values, in other words, those which are expected to have serious negative consequences due to the combination of the hazard and the vulnerability conditions. The qualitative risk values are assigned to each CU based on the combination of hazard and vulnerability indices so that a risk class is the result of different possible combinations, i.e. the medium class may be the result of

a very low hazard but very high vulnerability, the medium values for both or the result of a very high hazard but very low vulnerability.

As illustrated in the conceptual framework (see Figure 46), two types of results are obtained, partial risk results for each dimension and a combined risk result by weighted aggregation of all dimensions, called integrated risk index (IRI).

Finally, IRI is ranked to identify and prioritize the CU where special attention should be paid in terms of disaster risk management. As there are 22 CUs, the rank goes from 1 to 22, with number 1 being the worst situation and number 22 the best. This ranking is based on the amount of area at each risk level, sorted class by class.

As for the specific impact-oriented assessment, on the one hand, the estimation of serious injuries/loss of life estimation will result from the combination of the intensity of the hazard (i.e., flow depth), the population exposure and their vulnerability conditions. CUs with a higher probability of serious injuries or loss of life should be prioritized for preparedness strategies and actions. Similarly, building damages and associated replacement costs will result from the combination of the flow depth, the buildings exposed and their vulnerability conditions, by means of damage functions.

4.3 Erosion Risk Assessment

Following the method and complexities related to erosion processes and modelling, described in section 2.4 Erosion Modelling, the approach for conducting the risk assessment has been developed as follows. Following the conceptual framework for risk assessment described above, in the specific case of erosion hazard and exposure have been predefined and linked in advance. That is, the erosion assessment has been conducted for specific assets. Following the results of the hazard analysis (see section 2.5.2 Coastal Erosion Results), the erosion risk described in this study has been focused on (i) hard structures (vertical concrete or sheet-pile seawalls and rip-rap structures such as longshore revetments or cross-shore groins) and (ii) sandy/beach areas.

The predefinition described above is related to the definition of the impact to analyze. The objective of this analysis is to identify the main coastal typologies that may be affected and to what extent, by the erosion processes associated with tropical cyclones.

Accordingly, the vulnerability of the exposed assets is related to their foundation structure and the focus is on identifying the characteristics of assets at erosion risk that may increase their susceptibility to the harmful consequences of the hazard.

The collapse of vertical seawalls occurs when the scour depth exceeds the base of the seawall foundation. An average depth in Belize of 0.3 m below ground has been assumed for these structures. The scour depth in front of the seawall has been computed for each CU, different return periods (10, 50, 100 and 500 years) and two scenarios (see section 2.4 Erosion Modelling).

As for hard rip-rap structures, they can be damaged by tropical cyclones if the design weight of the structure pieces is greater than the actual weight of the pieces. A rip-rap with rocks of nominal weight of 50 kg has been assumed as the average typology for this kind of coastal structures in Belize and the design weight of rocks has been calculated for each CU, different return periods (10, 50, 100 and 500 years) and two scenarios (see section 2.4 Erosion Modelling).

Final results are obtained according to the combination of hazard and vulnerability characteristics of the assets exposed.

For vertical seawalls, when the scour exceeds a depth of 0.3 m, the wall is assumed to be lost and as a result of this loss, other elements/infrastructure/buildings immediately behind it can suffer serious damage.

As for rip-rap hard structures, whenever the required weight of the parts exceeds 50 kg, it is assumed that the structure collapses and consequently other elements/infrastructure/buildings immediately behind it can suffer severe damage too.

Sand/beach areas are assessed slightly differently. In this case, the objective is to estimate the loss of sandy surface, so the shoreline retreat has been analyzed for each CU, different return periods (10, 50, 100 and 500 years) and two scenarios (see section 2.4 Erosion Modelling). Results are obtained by combining the shoreline retreat with the length of the beach to estimate the surface that may be lost for each CU, return period and scenario mentioned. Losses in beach areas are directly related to potential monetary losses associated with tourism activities and damage to buildings and infrastructures.

4.4 Results

This section includes the results organized according to the different analyses carried out. First, for floods associated with tropical cyclones, the integrated risk assessment is explained, starting with the Integrated Risk Index (IRI) to get a comprehensive view of the overall result of the integrated analysis. Then, each of the individual dimensions (human, infrastructure and environmental) that contribute to the IRI is shown and explained. Finally, the results of the impact-specific assessment are described: the estimation of serious injuries/loss of life estimation and the estimate of damage to households and associated replacement costs.

Last, results from the erosion risk assessment on hard coastal structures and sandy/beach areas are included.

4.4.1 Integrated risk assessment

4.4.1.1 Integrated Risk Index (IRI)

The integrated risk index is the result of the combination of hazard classes and vulnerability indexes for all the dimensions analyzed (human, infrastructure and environmental) per CU, return period and scenario, as explained in the methodology described in chapter 3. It is important to note this when reviewing the results below. Overall results are shown in Table 9 and Figure 51, where it is shown the integrated risk index ranking per CU, return period and scenario.

Table 9. Integrated Risk Index ranking per CU, Scenario (RCP 8.5 SLR Scenario and Current SL Scenario) and Return Period. Red Colour is Assigned for the Worst-Case (Value 1) and Green for the Best Situation (Value 22).

CU		Integrated Risk Index Ranking							
		RCP 8.5 SLR scenario				Current SL scenario			
#	Location	Rank_s10	Rank_s50	Rank_s100	Rank_s500	Rank_10	Rank_50	Rank_100	Rank_500
1	NR-North	2	6	4	4	2	5	6	4
2	NR-Central	6	5	6	7	8	4	5	7
3	NR-South	3	1	1	1	5	1	1	1
4	NR-Cayes	7	9	9	12	7	8	9	12
5	AC-North	9	2	2	3	12	9	8	6

6	AC-South	1	4	5	9	3	7	3	8
7	CR-North	13	13	16	16	11	16	11	16
8	CR-Central	4	3	3	2	6	2	2	2
9	CR-South	8	7	7	5	1	3	4	3
10	CR-Cayes	20	15	10	6	13	12	12	9
11	CC	5	8	8	10	4	6	7	5
12	TA	10	10	13	11	10	10	10	13
13	LA	21	21	21	21	21	21	21	21
14	SN-North	19	16	11	8	14	17	15	10
15	SN-South	17	19	18	13	15	20	18	15
16	SN-Cayes	12	11	14	17	9	11	13	14
17	SC-North	15	14	15	15	17	18	20	17
18	SC-South	16	17	20	18	18	19	16	18
19	SC-Cayes	22	22	22	22	22	22	22	22
20	SR-North	11	12	12	14	16	13	14	11
21	SR-South	18	18	17	19	19	14	17	19
22	SR-Cayes	14	20	19	20	20	15	19	20

Figure 51. (Top) Integrated Risk Index ranking per CU, all Scenarios: RCP 8.5 SLR Scenario ("s") and Current SL Scenario, and All Return Periods. (Bottom) Coloured Map Showing the Ranking, With Red Being Assigned for the Worst-Case Value and Dark Green for the Best Situation.

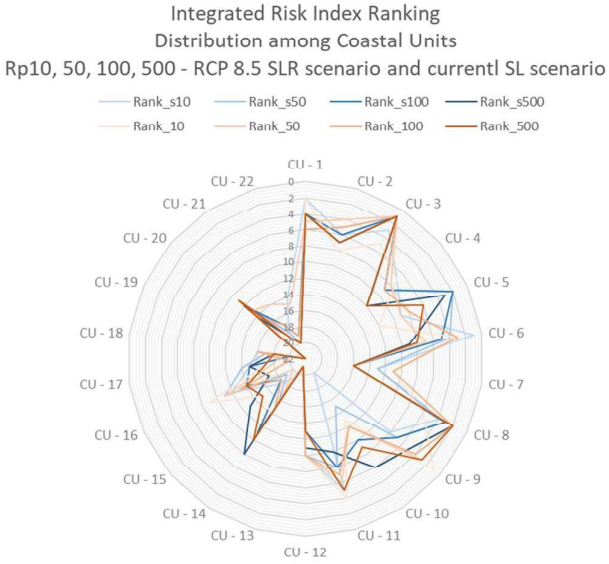

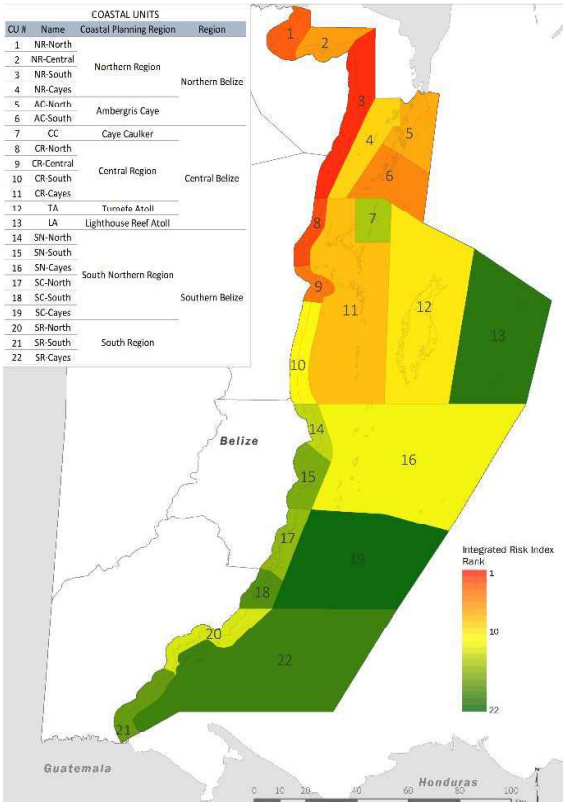

The rank goes from 1 to 22 (there are 22 CUs defined), at each column in the table, with number 1 being the worst situation and number 22 the best. This ranking is based on the amount of area at each risk level, sorted class by class (from very high to very low IRI). In addition, the graph in Figure 51, shows the index distribution by CU, clearly differentiating those CUs with the highest and the lowest risk index rankings. On the other hand, the map represents the classification considering all return periods and scenarios, as an overall view, regardless of the probability of occurrence. Considering this aggregation, CUs with highest IRI ranking values are, in this order CU-3 (NR-South), CU-8 (CR-Central), CU-1 (NR-North), CU-9 (CR-South), CU-6 (AC-South), CU-2 (NR-Central), CU-5 (AC-North), CU-11 (Caye Caulker), CU-4 (NR-Cayes) and CU-12 (Turnefe Atoll). Different reasons are explaining these results for each of the different CUs, based on the combination of hazard and vulnerability classes, as explained above. These factors are addressed in the corresponding sections concerning the analysis of the partial results for each dimension (sections 4.4.1.2, 4.4.1.3 and 4.4.1.4).

Before the individual analysis by dimension, Figure 52 and Figure 53 show the contribution of each vulnerability index (human, infrastructure and environmental) to the integrated risk index per CU, scenario (RCP 8.5 sea-level rise scenario and current sea level scenario) and return period (10, 50, 100 and 500 years). Therefore, graphs highlight the relevance of each dimension in the overall risk outcome for each CU.

Figure 52. Contribution of the Vulnerability Indices to the Integrated Risk Index per CU and Return Period at Current Sea Level Scenario (HVI: Human Vulnerability Index; IVI: Infrastructure Vulnerability Index; EVI: Environmental Vulnerability Index).

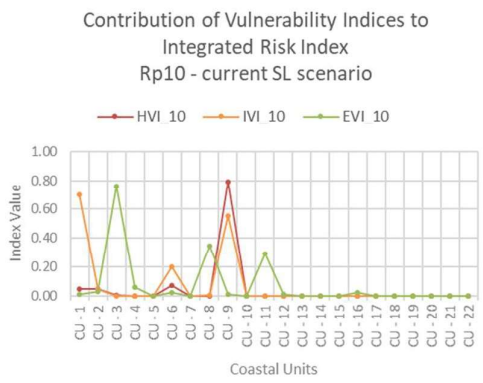

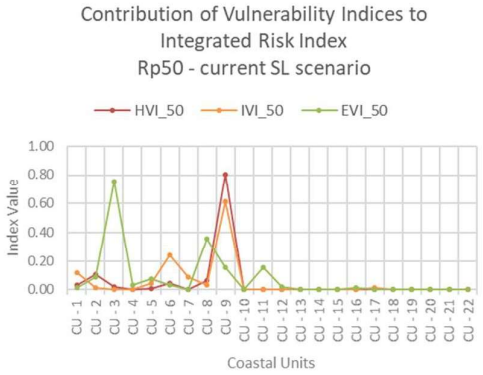

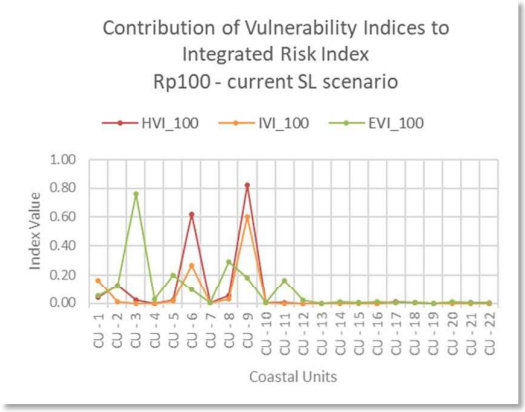

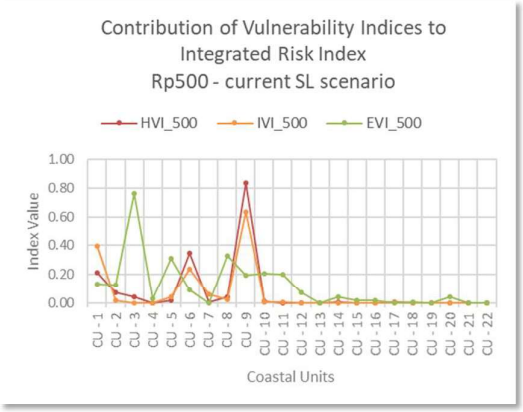

Figure 53. Contribution of the vulnerability Indices to the Integrated Risk Index per CU and Return Period at RCP 8.5 SLR Scenario (+0.275 m) (HVI: Human Vulnerability Index; IVI: Infrastructure Vulnerability Index; EVI: Environmental Vulnerability Index).

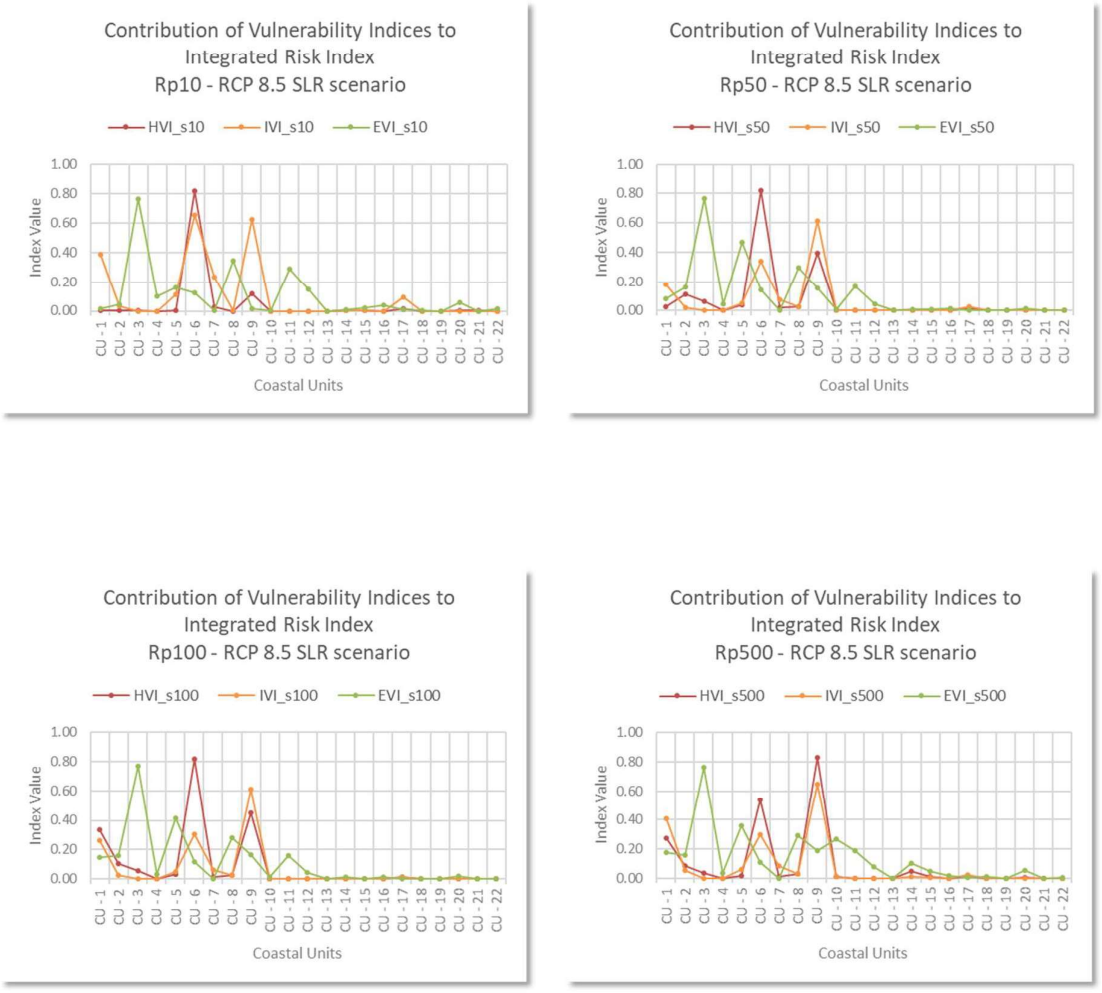

As shown in Figure 52 and Figure 53, for every return period and scenario, EVI is the vulnerability index with the highest relevance in IRI results in CU-3 (NR-South), CU-8 (CR-Central), CU-2 (NR-Central), CU-5 (AC-North), CU-11 (Caye Caulker), CU-4 (NR-Cayes) and CU-12 (Turnefe Atoll), whereas IVI is more relevant in CU-1 (NR-North) and HVI in CU-9 (CR-South) and CU-6 (AC-South), where the highest number of exposed population is found. It is also interesting to consider the differences in the contribution of each index, being in some CUs much more relevant than in others. For example, there is a big difference in the CU-3 (NR-South) regarding the contribution of the EVI compared to the other vulnerability indices, whereas in CU-9 (CR-South) and CU-6 (AC-South), the contribution of HVI and IVI is quite

similar (with some differences in different return periods). Particularities of each dimension are described in the corresponding sections.

Finally, Figure 54 and Figure 55 show the area exposed to the different classes of risk in each CU to identify, in combination with all the above information, the areas where special attention should be paid concerning disaster risk management.

Figure 54. Area per Integrated Risk Index Class, CU and Rp 10, 50, 100 and 500 yr. (Current Sea Level Scenario).

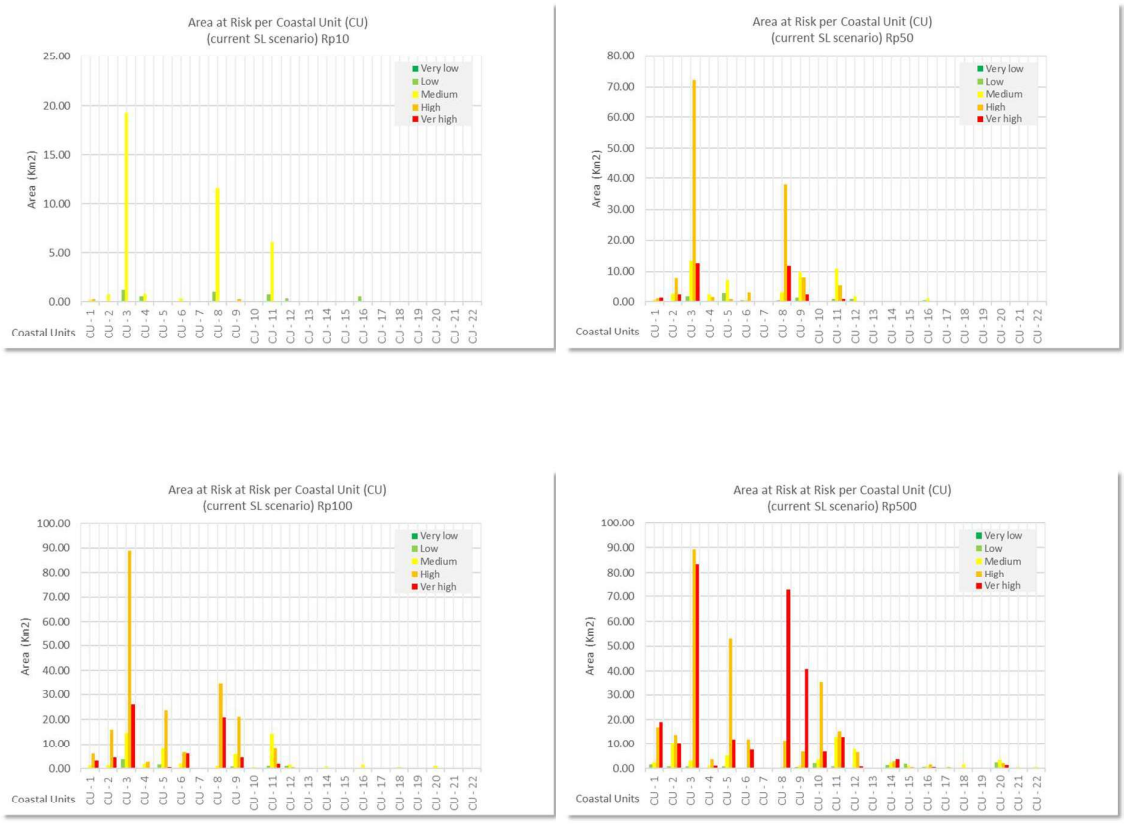

Figure 55. Area Per Integrated Risk Index Class, CU and Rp 10, 50, 100 and 500 yr. RCP 8.5 Sea Level Rise Scenario (+0.275 cm).

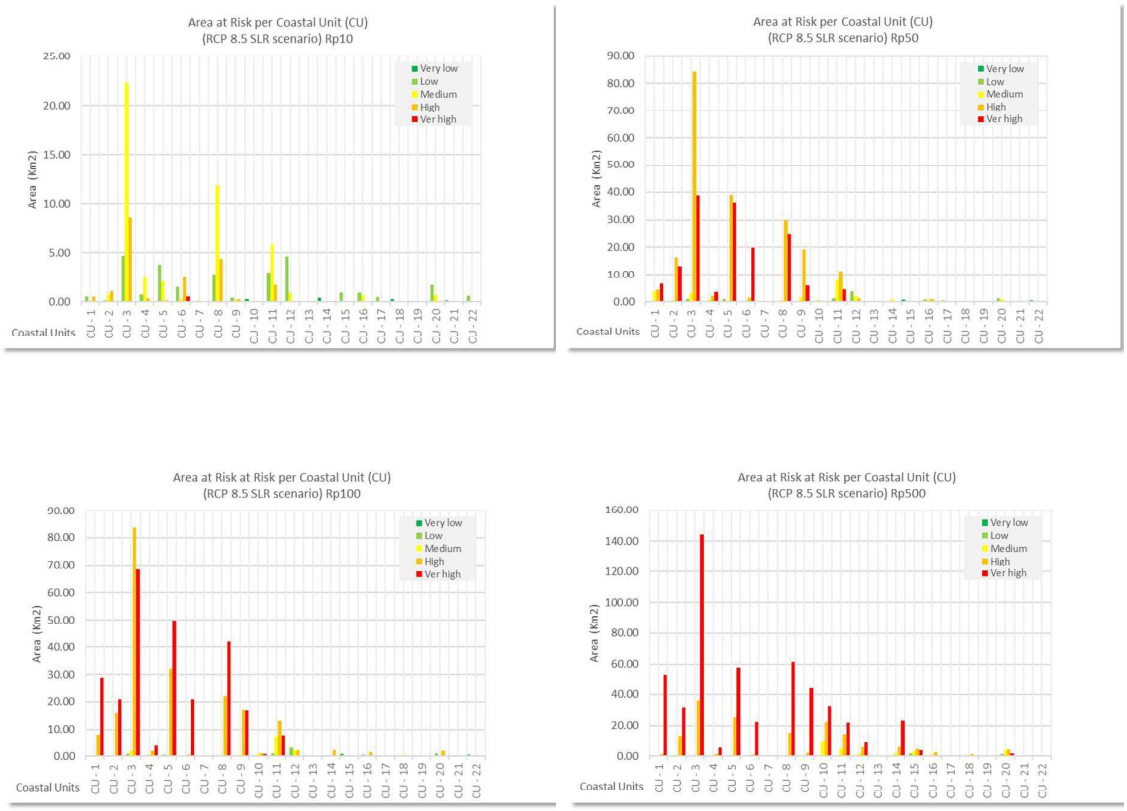

Within these graphs, in addition to the information regarding general ranks and contribution of partial vulnerability indices of previous figures, it is shown the area by risk level in every CU. This information is useful to prioritize action in terms of establishing risk management measures. It must be noted that these figures are showing exposed area by risk level which means that it is possible to find some CUs with relatively big areas exposed at certain return periods but at medium or low levels of risk (for example CU-5, AC-North, and CU-11, Caye Caulker), due to the minor grade of vulnerability. Conversely, some CUs can also be found with a smaller exposed area but higher levels of risk (e.g. CU-1: NR-North). For this reason, the information provided in these figures must be complementary to the previous ones. Therefore, following the ranking shown in Table 9 and Figure 51, it may be seen that CU-3 (NR-South) is still the most exposed one and at the highest risk levels, followed by CU-8 (CR-Central). The CUs with the smallest flooded area, as indicated previously, correspond to the southern part of the country, where the impact of tropical cyclones, in terms of coastal flooding, is lower than in the north.

Next sections address the partial risk indices (by dimension) and the specific impact-oriented results.

4.4.1.2 Human dimension

Human Exposure and Vulnerability

Human exposure and vulnerability results are presented showing the population exposed and the human vulnerability index (HVI) in each CU. Figure 56 and Figure 57 show the return periods analyzed for each scenario.

The CUs with greater human exposure and vulnerability index for each return period and scenario analyzed are CU-9 (CR-South), CU-6 (AC-South), CU-1 (NR-North) and CU-2 (NR-Central). From CU-10 (CR-Cayes) onwards there is almost no human exposure and consequently no vulnerability.

Figure 56. Human Exposure and Vulnerability Index per CU at the Current Sea Level Scenario.

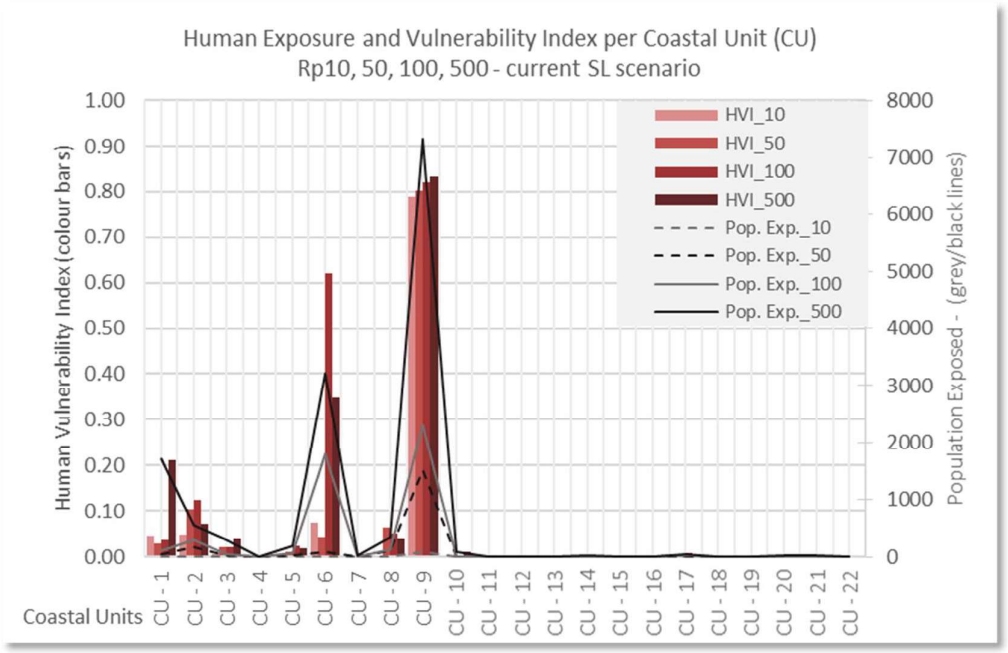

Table 10. Human Exposure and Vulnerability Index per CU at Current Sea Level (HVI: Human Vulnerability Index; Pop_Exp_s#: Population Exposed Current Sea Level Scenario Return Period.

HUMAN EXPOSURE AND VULNERABILITY INDEX

CU		Current SLR scenario							
		Rp10		Rp50		Rp100		Rp500	
#	Location	HVI_10	Pop. Exp._10	HVI_50	Pop. Exp._50	HVI_100	Pop. Exp._100	HVI_500	Pop. Exp._500
1	NR-North	0.05	5	0.03	52	0.04	99	0.21	1714
2	NR-Central	0.05	5	0.10	165	0.12	298	0.07	546
3	NR-South	0.01	1	0.02	33	0.02	50	0.04	305
4	NR-Cayes	0.00	0	0.00	0	0.00	0	0.00	0
5	AC-North	0.00	0	0.01	22	0.02	74	0.02	185
6	AC-South	0.07	8	0.04	80	0.62	1793	0.35	3208
7	CR-North	0.00	0	0.00	0	0.00	13	0.00	25
8	CR-Central	0.00	0	0.06	108	0.05	132	0.04	341
9	CR-South	0.79	87	0.80	1527	0.82	2304	0.83	7335
10	CR-Cayes	0.00	0	0.00	1	0.00	8	0.01	79
11	CC	0.00	0	0.00	0	0.00	1	0.00	1
12	TA	0.00	0	0.00	0	0.00	0	0.00	0

13	LA	0.00	0	0.00	0	0.00	0	0.00	0
14	SN-North	0.00	0	0.00	0	0.00	4	0.00	33
15	SN-South	0.00	0	0.00	0	0.00	1	0.00	12
16	SN-Cayes	0.00	0	0.00	0	0.00	0	0.00	0
17	SC-North	0.00	0	0.00	1	0.01	25	0.01	43
18	SC-South	0.00	0	0.00	0	0.00	1	0.00	2
19	SC-Cayes	0.00	0	0.00	0	0.00	0	0.00	0
20	SR-North	0.00	0	0.00	1	0.00	3	0.00	19
21	SR-South	0.00	0	0.00	3	0.00	4	0.00	14
22	SR-Cayes	0.00	0	0.00	0	0.00	0	0.00	0
	TOTAL		**106**		**1992**		**4808**		**13864**

Figure 57. Human Exposure and Vulnerability Index per CU at the Current Sea Level Scenario.

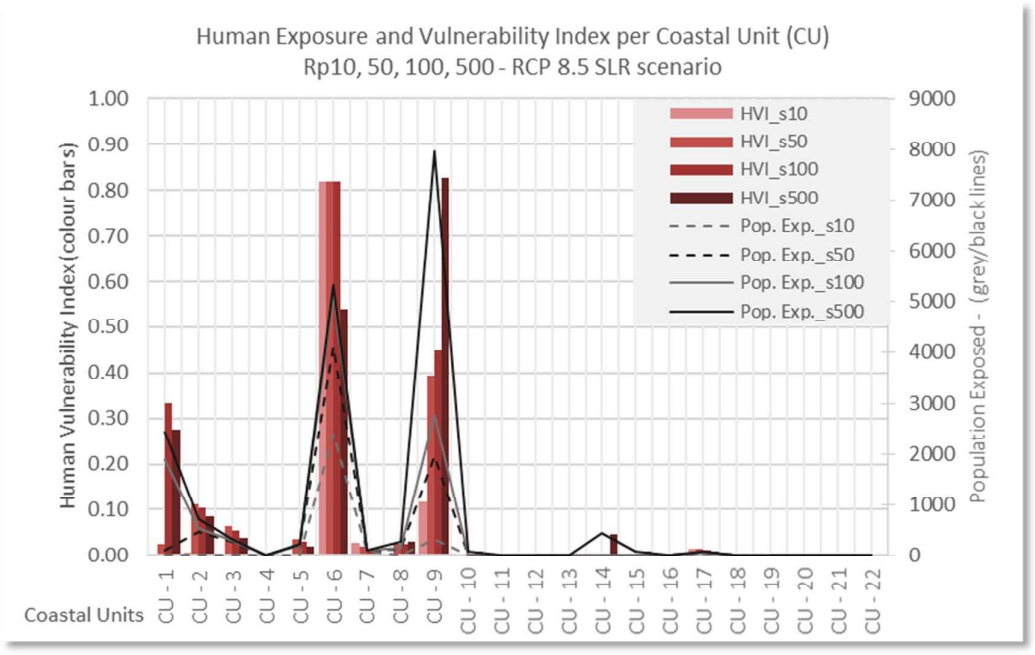

Table 11. Human Exposure and Vulnerability Index per CU at RCP 8.5 SLR Scenario (HVI: Human Vulnerability Index; Pop_Exp_s#: Population Exposed_RCP 8.5 SLR Scenario_Return Period).

CU		RCP 8.5 - SLR scenario (+0.274 cm)							
		Rp10		Rp50		Rp100		Rp500	
#	Location	HVI_s10	Pop. Exp._s10	HVI_s50	Pop. Exp._s50	HVI_s100	Pop. Exp._s100	HVI_s500	Pop. Exp._s500
1	NR-North	0.00	11	0.02	109	0.33	1878	0.28	2438
2	NR-Central	0.01	15	0.11	466	0.10	542	0.09	721
3	NR-South	0.00	4	0.07	270	0.05	284	0.04	308
4	NR-Cayes	0.00	0	0.00	0	0.00	0	0.00	0
5	AC-North	0.00	12	0.04	197	0.03	210	0.02	212
6	AC-South	0.82	2377	0.82	4112	0.82	5137	0.54	5318
7	CR-North	0.03	81	0.02	94	0.01	94	0.01	106
8	CR-Central	0.00	1	0.03	118	0.03	148	0.03	264
9	CR-South	0.12	324	0.39	1954	0.45	2762	0.83	7968
10	CR-Cayes	0.00	0	0.00	1	0.00	11	0.01	72
11	CC	0.00	0	0.00	1	0.00	1	0.00	1
12	TA	0.00	0	0.00	0	0.00	0	0.00	0

13	LA	0.00	0	0.00	0	0.00	0	0.00	0
14	SN-North	0.00	2	0.00	4	0.00	10	0.05	436
15	SN-South	0.00	6	0.00	7	0.00	7	0.01	76
16	SN-Cayes	0.00	0	0.00	0	0.00	0	0.00	0
17	SC-North	0.02	39	0.01	64	0.01	65	0.01	86
18	SC-South	0.00	0	0.00	1	0.00	1	0.00	2
19	SC-Cayes	0.00	0	0.00	0	0.00	0	0.00	0
20	SR-North	0.00	2	0.00	2	0.00	5	0.00	17
21	SR-South	0.00	3	0.00	3	0.00	4	0.00	11
22	SR-Cayes	0.00	0	0.00	0	0.00	0	0.00	0
	TOTAL		**2879**		**7402**		**11159**		**18036**

Human Risk

Human risk results are presented by combining the area exposed to different risk classes in each CU and the number of people estimated to be at those risk levels. This allows identifying the CU to which special attention should be paid in terms of human risk management. Figure 58 and Figure 59 show all the return periods analyzed for each scenario. According to the vulnerability results, CUs with higher human risk index values are CU-9 (CR-South), CU-6 (AC-South), CU-1 (NR-North) and CU-2 (NR-Central).

Figure 58. Population and Area per Human Risk Class, CU and Rp 10, 50, 100 and 500 yr. (Current Sea Level Scenario).

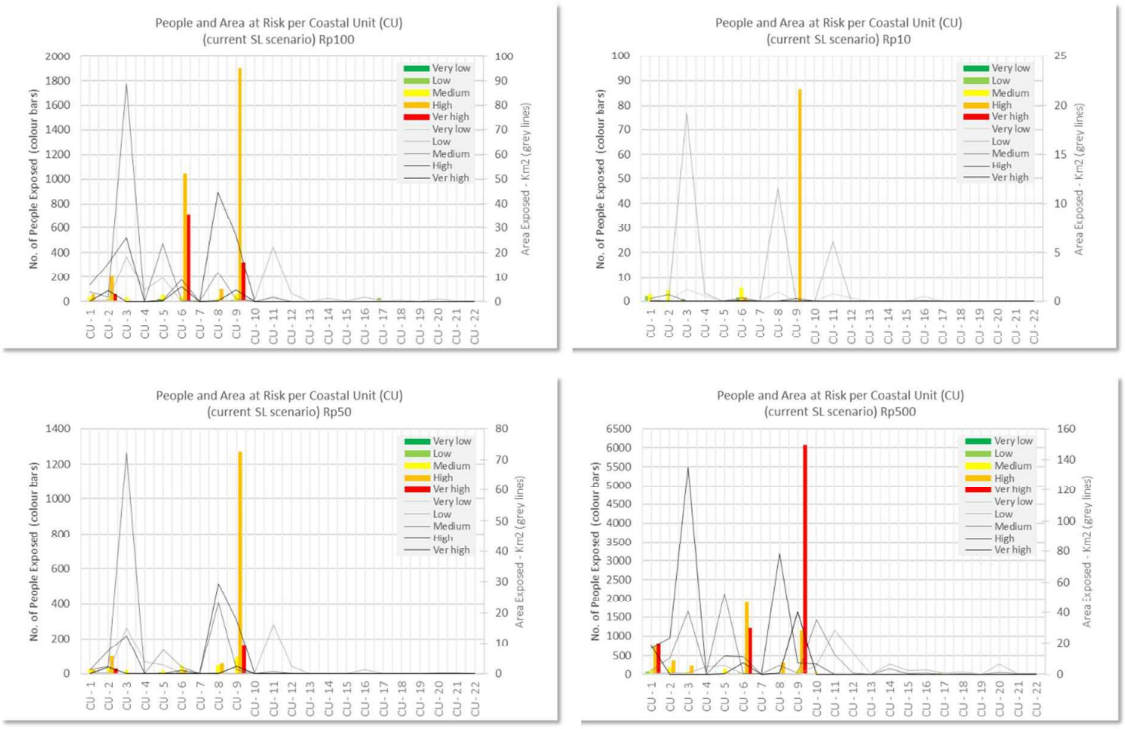

Figure 59. Population and Area per Human Risk Class, CU and Rp 10, 50, 100 and 500 yr. RCP 8.5 Sea Level Rise Scenario (+0.275 cm).

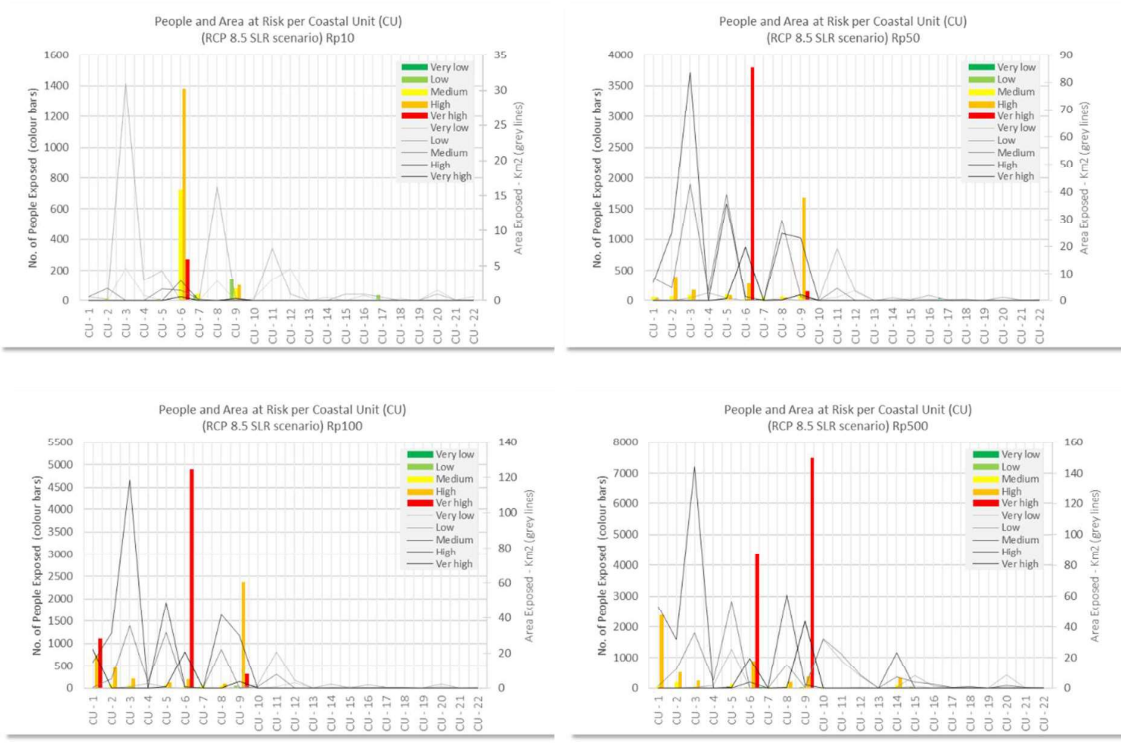

4.4.1.3 Infrastructure dimension

Infrastructure Exposure and Vulnerability

Infrastructure exposure and vulnerability results are presented showing, on the one hand, the critical infrastructures, roads and transport facilities exposed by at each CU (Figure 60 and Figure 61) and on the other, the exposed area of the settlements together with the infrastructure vulnerability index (IVI) per CU and return period (Figure 62 and Figure 63).

CUs with the largest number of critical infrastructures exposed are the CU-6 (AC-South), CU-1 (NR-North) and CU-5 (AC-North), while the largest number of roads and transport facilities exposed are in the CU-9 (CR-South), CU-8 (CR-Central), CU-1 (NR-North and CU-2 (NR-Central). Concerning the overall results of the IVI, the CU-9 (CR-South), CU-6 (AC-South) and CU-1 (NR-North) are the most vulnerable.

Figure 60. Critical Infrastructures, Roads and Transport Facilities Exposure per CU at Current Sea Level Scenario.

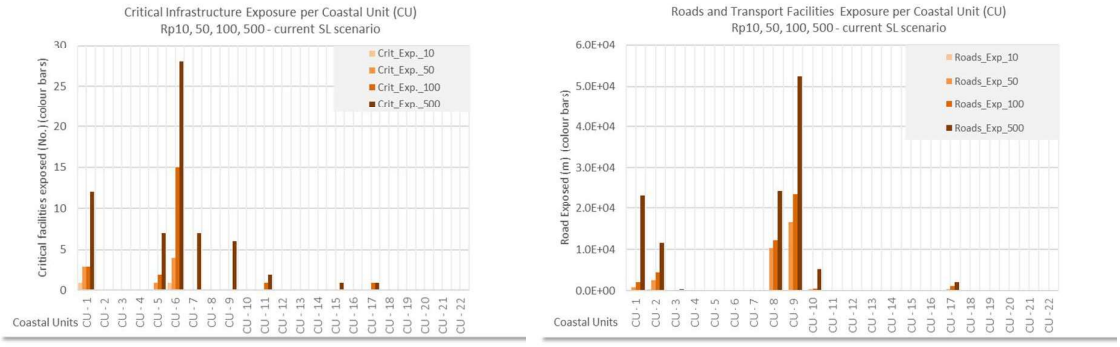

Figure 61. Critical Infrastructures, Roads and Transport Facilities Exposure per CU. RCP 8.5 Sea Level Rise Scenario (+0.275 cm).

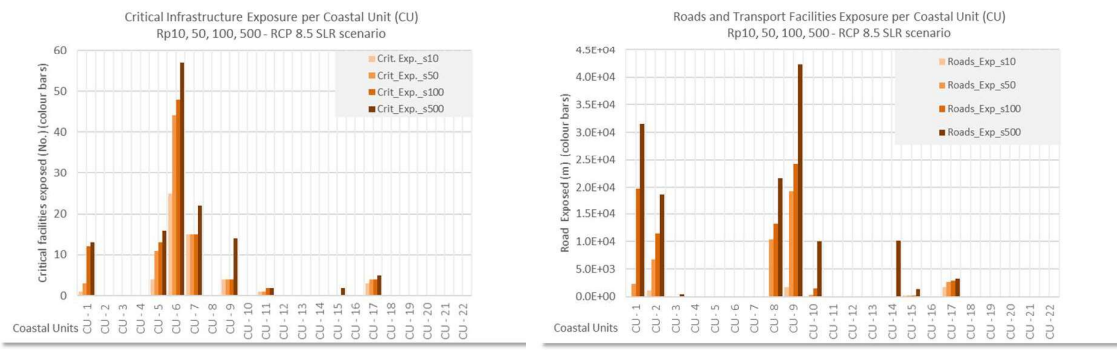

Figure 62. Infrastructure Exposure (Area of Settlements) and Vulnerability Index per CU at The Current Sea Level Scenario.

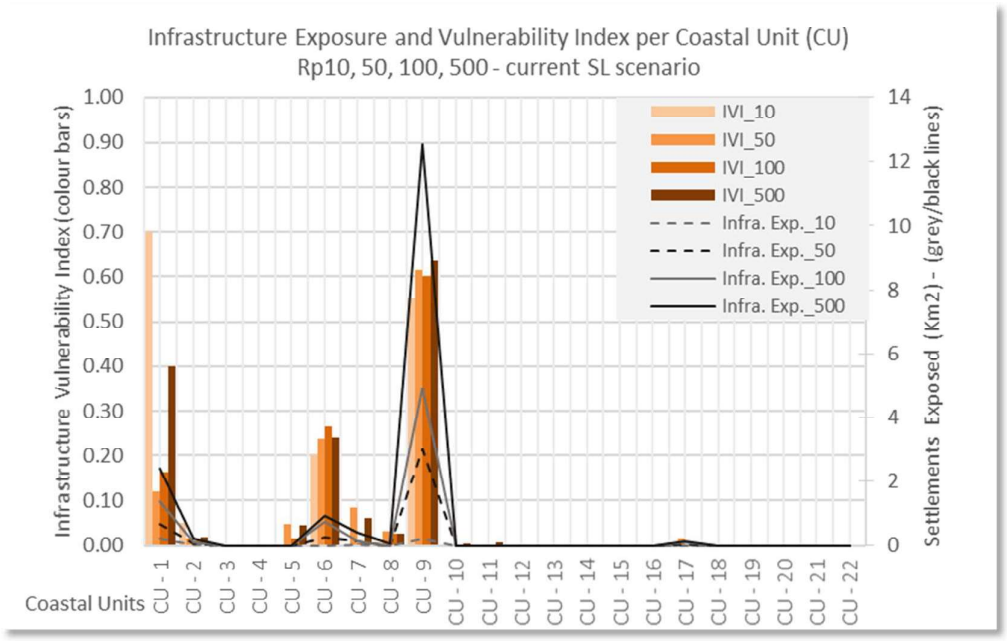

Table 12. Infrastructure Exposure and Vulnerability Index per CU at Current Sea Level (IVI: Infrastructure Vulnerability Index; Infra_Exp_s#: Area of Settlements Exposed_Current Sea Level Scenario_Return Period).

CU		Current SLR scenario							
		Rp10		Rp50		Rp100		Rp500	
#	Location	IVI_10	Infra. Exp._10	IVI_50	Infra. Exp._50	IVI_100	Infra. Exp._100	IVI_500	Infra. Exp._500
1	NR-North	0.70	0.22	0.12	0.67	0.16	1.37	0.40	2.41
2	NR-Central	0.05	0.01	0.02	0.08	0.01	0.11	0.02	0.20
3	NR-South	0.00	0.00	0.00	0.00	0.00	0.00	0.00	0.00
4	NR-Cayes	0.00	0.00	0.00	0.00	0.00	0.00	0.00	0.00
5	AC-North	0.00	0.00	0.05	0.00	0.01	0.00	0.04	0.00
6	AC-South	0.20	0.00	0.24	0.26	0.26	0.72	0.24	0.94
7	CR-North	0.00	0.01	0.09	0.15	0.00	0.15	0.06	0.39
8	CR-Central	0.01	0.00	0.03	0.00	0.03	0.00	0.03	0.06
9	CR-South	0.55	0.21	0.61	2.99	0.60	4.92	0.64	12.56
10	CR-Cayes	0.00	0.00	0.00	0.00	0.00	0.00	0.00	0.00
11	CC	0.00	0.00	0.00	0.00	0.00	0.00	0.01	0.00
12	TA	0.00	0.00	0.00	0.00	0.00	0.00	0.00	0.00
13	LA	0.00	0.00	0.00	0.00	0.00	0.00	0.00	0.00

14	SN-North	0.00	0.00	0.00	0.00	0.00	0.00	0.00	0.00
15	SN-South	0.00	0.00	0.00	0.00	0.00	0.00	0.00	0.00
16	SN-Cayes	0.00	0.00	0.00	0.00	0.00	0.00	0.00	0.00
17	SC-North	0.00	0.00	0.01	0.03	0.00	0.11	0.01	0.12
18	SC-South	0.00	0.00	0.00	0.00	0.00	0.00	0.00	0.00
19	SC-Cayes	0.00	0.00	0.00	0.00	0.00	0.00	0.00	0.00
20	SR-North	0.00	0.00	0.00	0.00	0.00	0.00	0.00	0.00
21	SR-South	0.00	0.00	0.00	0.00	0.00	0.00	0.00	0.00
22	SR-Cayes	0.00	0.00	0.00	0.00	0.00	0.00	0.00	0.00

Figure 63. Infrastructure Exposure and Vulnerability Index per CU. RCP 8.5 Sea Level Rise Scenario (+0.275 cm).

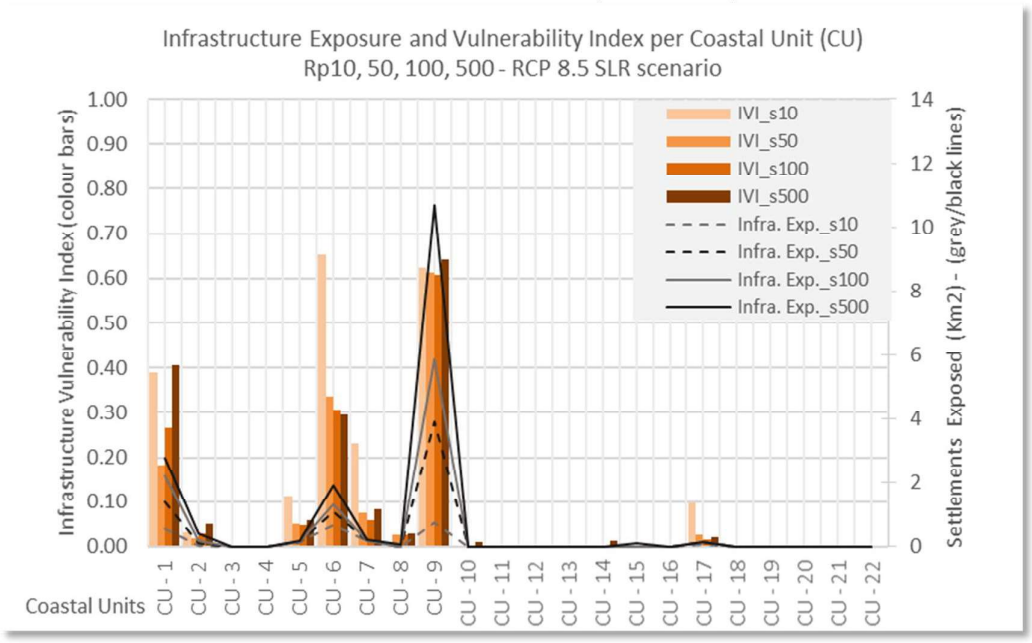

Table 13. Infrastructure Exposure and Vulnerability Index per CU at RCP 8.5 SLR Scenario (IVI: Infrastructure Vulnerability Index; Infra_Exp_s#: Area of Settlements Exposed_RCP 8.5 SLR Scenario_Return Period).

CU		RCP 8.5 - SLR scenario (+0.275 cm)							
		Rp10		Rp50		Rp100		Rp500	
#	Location	IVI_s10	Infra. Exp._s10	IVI_s50	Infra. Exp._s50	IVI_s100	Infra. Exp._s100	IVI_s500	Infra.Exp._s500
1	NR-North	0.39	0.57	0.18	1.37	0.27	2.22	0.41	2.78
2	NR-Central	0.03	0.02	0.02	0.11	0.03	0.20	0.05	0.42
3	NR-South	0.00	0.00	0.00	0.00	0.00	0.00	0.00	0.00
4	NR-Cayes	0.00	0.00	0.00	0.00	0.00	0.00	0.00	0.00

5	AC-North	0.11	0.15	0.05	0.15	0.05	0.15	0.06	0.19
6	AC-South	0.65	0.67	0.34	1.10	0.31	1.30	0.30	1.93
7	CR-North	0.23	0.19	0.08	0.19	0.06	0.19	0.08	0.23
8	CR-Central	0.00	0.00	0.03	0.00	0.03	0.00	0.03	0.06
9	CR-South	0.62	0.74	0.61	3.91	0.61	5.85	0.64	10.70
10	CR-Cayes	0.00	0.00	0.00	0.00	0.00	0.00	0.01	0.00
11	CC	0.00	0.00	0.00	0.00	0.00	0.00	0.00	0.00
12	TA	0.00	0.00	0.00	0.00	0.00	0.00	0.00	0.00
13	LA	0.00	0.00	0.00	0.00	0.00	0.00	0.00	0.00
14	SN-North	0.00	0.00	0.00	0.00	0.00	0.00	0.01	0.01
15	SN-South	0.00	0.00	0.00	0.00	0.00	0.00	0.01	0.10
16	SN-Cayes	0.00	0.00	0.00	0.00	0.00	0.00	0.00	0.00
17	SC-North	0.10	0.06	0.03	0.15	0.02	0.15	0.02	0.15
18	SC-South	0.00	0.00	0.00	0.00	0.00	0.00	0.00	0.00
19	SC-Cayes	0.00	0.00	0.00	0.00	0.00	0.00	0.00	0.00
20	SR-North	0.00	0.00	0.00	0.00	0.00	0.00	0.00	0.00

21	SR-South	0.00	0.00	0.00	0.00	0.00	0.00	0.00	0.00
22	SR-Cayes	0.00	0.00	0.00	0.00	0.00	0.00	0.00	0.00

Infrastructure risk

Infrastructure risk results are presented showing the area exposed at different risk classes in each CU. The following figures (Figure 64 and Figure 65) identify the CUs to which special attention should be paid in terms of infrastructure risk management. Figures show all the return periods analyzed for each scenario.

Figure 64. 1.Area per Infrastructure Risk Class, CU and Rp 10, 50, 100 and 500 yr (Current Sea Level Scenario).

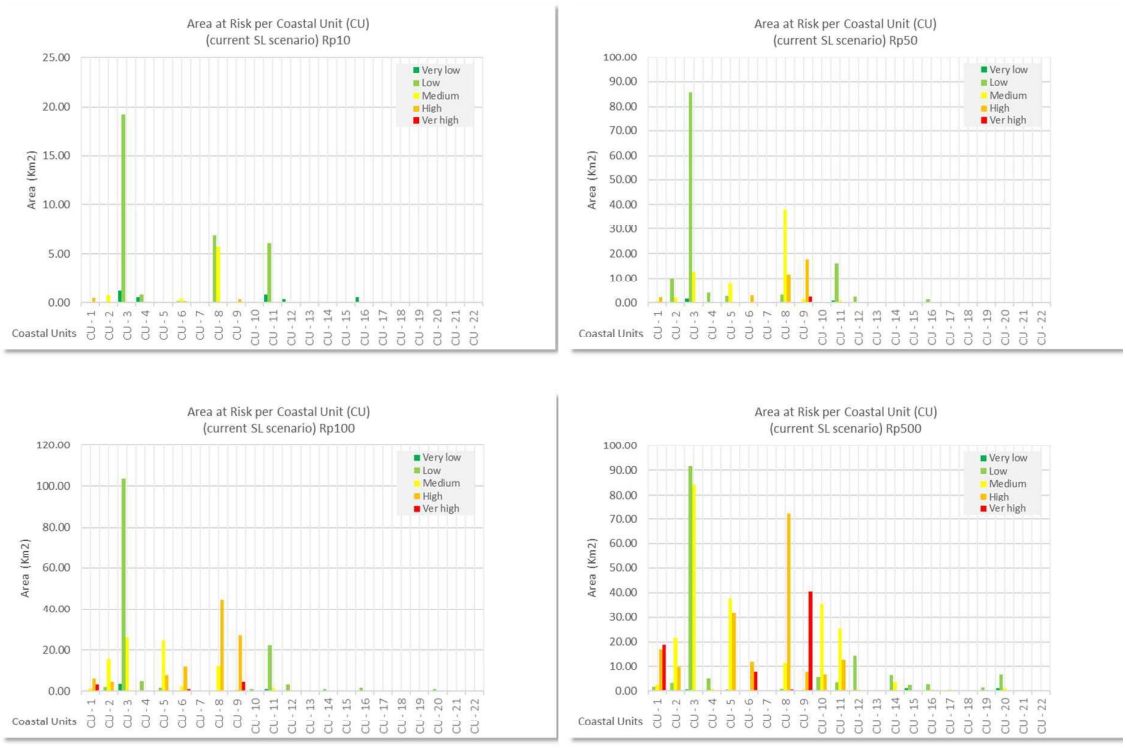

Figure 65. Area per Infrastructure Risk Class and CU. RCP 8.5 Sea Level Rise Scenario (+0.275 cm).

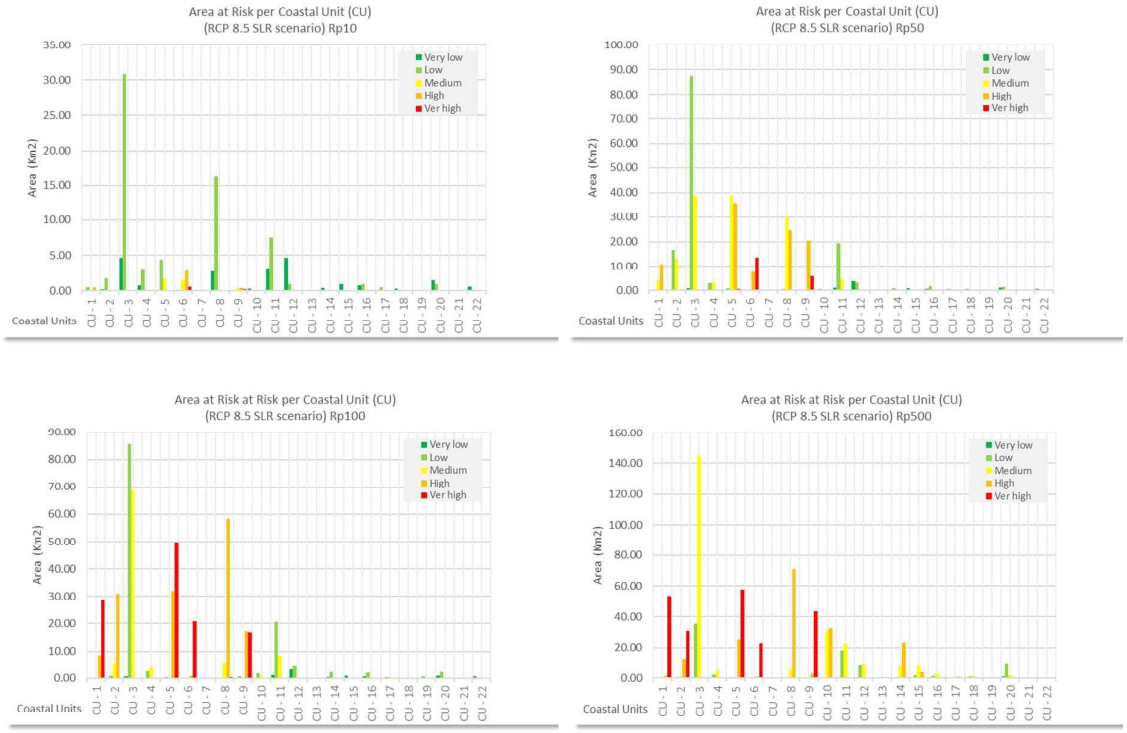

4.4.1.4 Environmental dimension

Environmental Exposure and Vulnerability

Environmental exposure and vulnerability results are presented showing, on the one hand, the ecosystems with a protection figure and the relevant ecosystems without any protection figure, exposed by at each CU (Figure 66 and Figure 67). On the other hand, Figure 69 and Figure 70 show the exposed area of all the ecosystems considered together with the environmental vulnerability index (EVI) per CU and return period.

Figure 66. Protected (Left) and Relevant (Non-Protected) (Right) Ecosystems Exposure per CU at Current Sea Level Scenario.

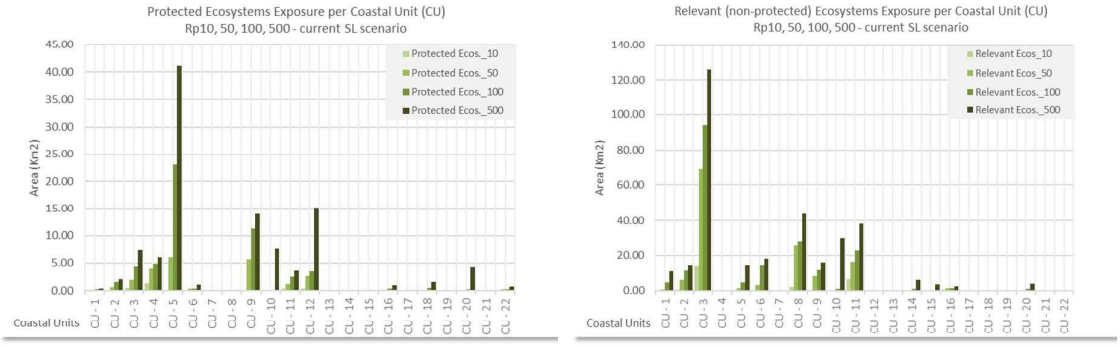

Figure 67. Protected (left) and Relevant (Non-Protected) (Right) Ecosystems Exposure per CU. RCP 8.5 Sea Level Rise Scenario (+0.275 cm).

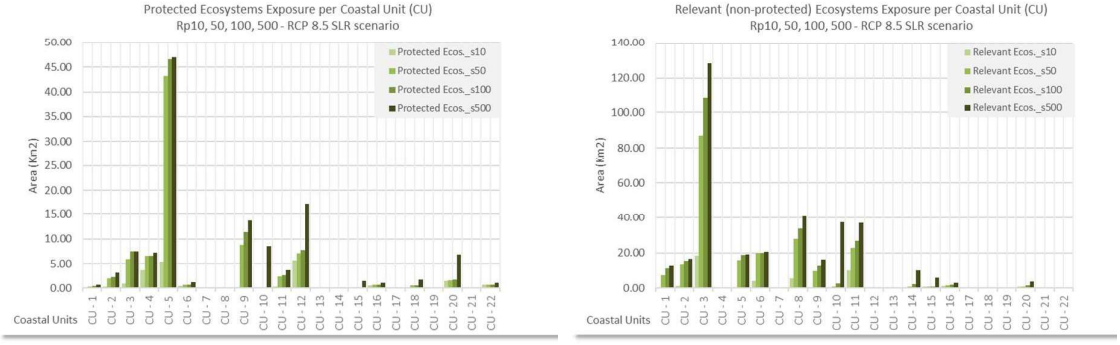

Figure 68. Environmental Exposure (Area of Ecosystems) and Vulnerability Index per CU at Current Sea Level Scenario.

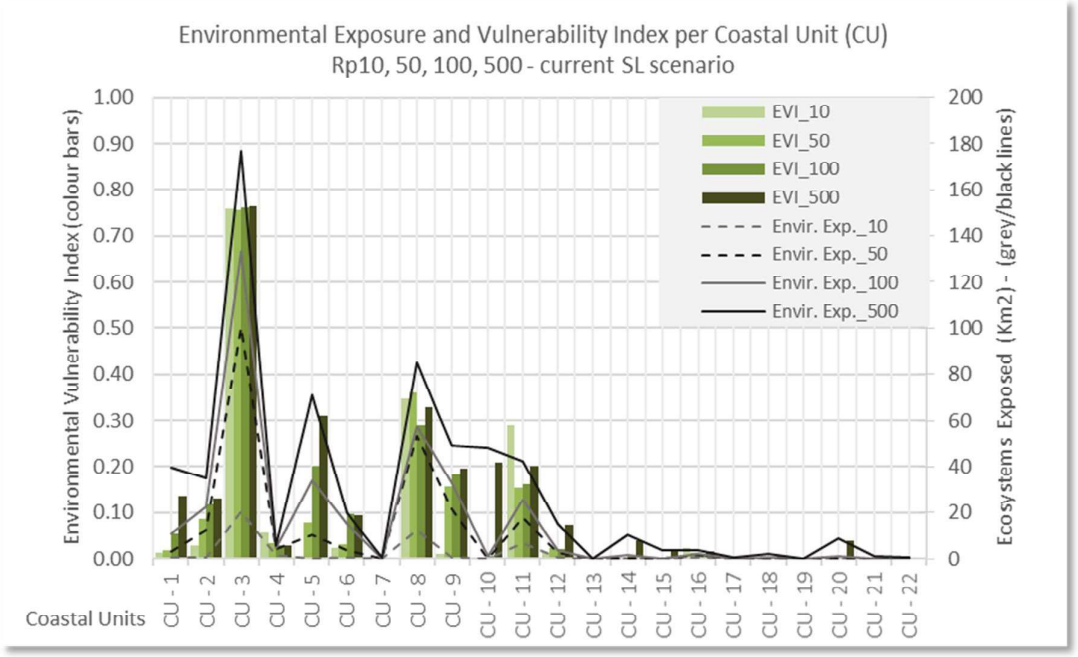

Table 14. Environmental Exposure and Vulnerability Index per CU at Current Sea Level (EVI: Environmental Vulnerability Index; Envir_Exp_s#: Area of Ecosystems Exposed_Current Sea Level Scenario_Return Period).

CU		Current SLR scenario							
		Rp10		Rp50		Rp100		Rp500	
#	Location	EVI_10	Envir. Exp._10	EVI_50	Envir. Exp._50	EVI_100	Envir. Exp._100	EVI_500	Envir. Exp._500
1	NR-North	0.01	0.48	0.02	2.89	0.05	11.04	0.13	39.83
2	NR-Central	0.03	0.76	0.09	12.35	0.12	22.27	0.13	34.93
3	NR-South	0.76	20.38	0.76	100.12	0.76	133.26	0.76	176.66
4	NR-Cayes	0.06	1.38	0.03	4.00	0.03	4.80	0.03	6.00
5	AC-North	0.00	0.00	0.08	10.48	0.20	34.12	0.31	70.82
6	AC-South	0.02	0.59	0.03	3.69	0.10	15.40	0.09	20.08
7	CR-North	0.00	0.02	0.00	0.16	0.00	0.25	0.00	0.53
8	CR-Central	0.35	12.57	0.36	53.11	0.29	57.41	0.33	85.18
9	CR-South	0.01	0.31	0.16	21.23	0.18	32.63	0.20	48.82
10	CR-Cayes	0.00	0.00	0.00	0.27	0.01	1.03	0.21	47.97
11	CC	0.29	6.85	0.15	17.71	0.16	25.33	0.20	42.05
12	TA	0.01	0.33	0.02	2.66	0.02	3.54	0.07	15.20

13	LA	0.00	0.00	0.00	0.00	0.00	0.00	0.00	0.00
14	SN-North	0.00	0.00	0.00	0.13	0.01	1.33	0.04	10.23
15	SN-South	0.00	0.00	0.00	0.00	0.00	0.21	0.02	3.70
16	SN-Cayes	0.02	0.59	0.01	1.46	0.01	1.85	0.02	3.43
17	SC-North	0.00	0.00	0.00	0.03	0.00	0.25	0.00	0.60
18	SC-South	0.00	0.00	0.00	0.00	0.00	0.55	0.01	1.85
19	SC-Cayes	0.00	0.00	0.00	0.00	0.00	0.00	0.00	0.00
20	SR-North	0.00	0.00	0.00	0.22	0.01	1.10	0.04	8.94
21	SR-South	0.00	0.00	0.00	0.22	0.00	0.25	0.00	0.96
22	SR-Cayes	0.00	0.00	0.00	0.20	0.00	0.20	0.00	0.67

Figure 69. Environmental Exposure and Vulnerability Index per CU. RCP 8.5 Sea Level Rise Scenario (+0.275 cm).

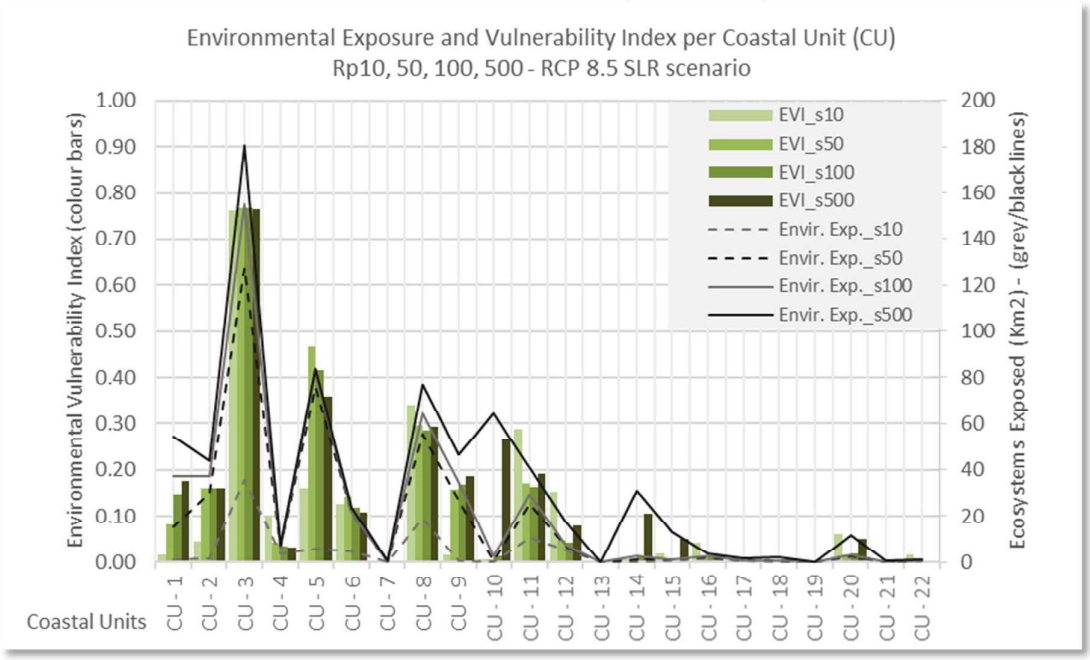

Table 15. Environmental Exposure and Vulnerability Index per CU at RCP 8.5 SLR Scenario (EVI: Environmental Vulnerability Index; Envir_Exp_s#: Area of Ecosystems Exposed _RCP 8.5 SLR Scenario_Return Period).

CU		RCP 8.5 - SLR scenario (+0.275 cm)							
		Rp10		Rp50		Rp100		Rp500	
#	Location	EVI_s10	Envir. Exp._s10	EVI_s50	Envir. Exp._s50	EVI_s100	Envir. Exp._s100	EVI_s500	Envir. Exp._s500
1	NR-North	0.02	1.09	0.08	15.13	0.15	37.20	0.18	54.53
2	NR-Central	0.04	1.97	0.16	29.84	0.16	36.99	0.16	43.93
3	NR-South	0.76	35.57	0.77	127.19	0.77	154.86	0.76	180.75
4	NR-Cayes	0.10	3.75	0.04	6.50	0.04	6.50	0.03	7.26
5	AC-North	0.16	6.02	0.47	76.03	0.42	82.39	0.36	83.42
6	AC-South	0.13	4.97	0.14	21.43	0.12	21.80	0.11	23.64
7	CR-North	0.00	0.27	0.00	0.37	0.00	0.37	0.00	0.45
8	CR-Central	0.34	19.08	0.30	55.26	0.28	64.35	0.29	77.09
9	CR-South	0.02	0.95	0.16	26.59	0.17	34.70	0.19	46.49
10	CR-Cayes	0.01	0.31	0.01	0.88	0.01	2.91	0.27	64.34
11	CC	0.29	10.54	0.17	25.06	0.16	29.52	0.19	40.73
12	TA	0.15	5.55	0.05	6.99	0.04	7.71	0.08	17.19

13	LA	0.00	0.00	0.00	0.00	0.00	0.00	0.00	0.00
14	SN-North	0.01	0.43	0.01	1.11	0.01	2.90	0.10	31.08
15	SN-South	0.02	0.93	0.01	1.03	0.00	1.03	0.05	13.02
16	SN-Cayes	0.04	1.65	0.02	2.34	0.01	2.61	0.02	3.92
17	SC-North	0.01	0.52	0.00	0.75	0.00	0.86	0.00	1.48
18	SC-South	0.00	0.30	0.00	0.74	0.00	0.74	0.01	2.15
19	SC-Cayes	0.00	0.00	0.00	0.00	0.00	0.00	0.00	0.00
20	SR-North	0.06	2.43	0.02	2.53	0.02	3.51	0.05	11.42
21	SR-South	0.00	0.23	0.00	0.23	0.00	0.27	0.00	0.84
22	SR-Cayes	0.02	0.67	0.00	0.71	0.00	0.71	0.00	1.12

Environmental Risk

Environmental risk results are presented showing the area exposed at different risk classes in each CU. The following figures (Figure 70 and Figure 71) identify the CUs to which special attention should be paid in terms of environmental risk management. Figures show all the return periods analyzed for each scenario.

Figure 70. Area per Environmental Risk Class and CU (Current Sea Level Scenario).

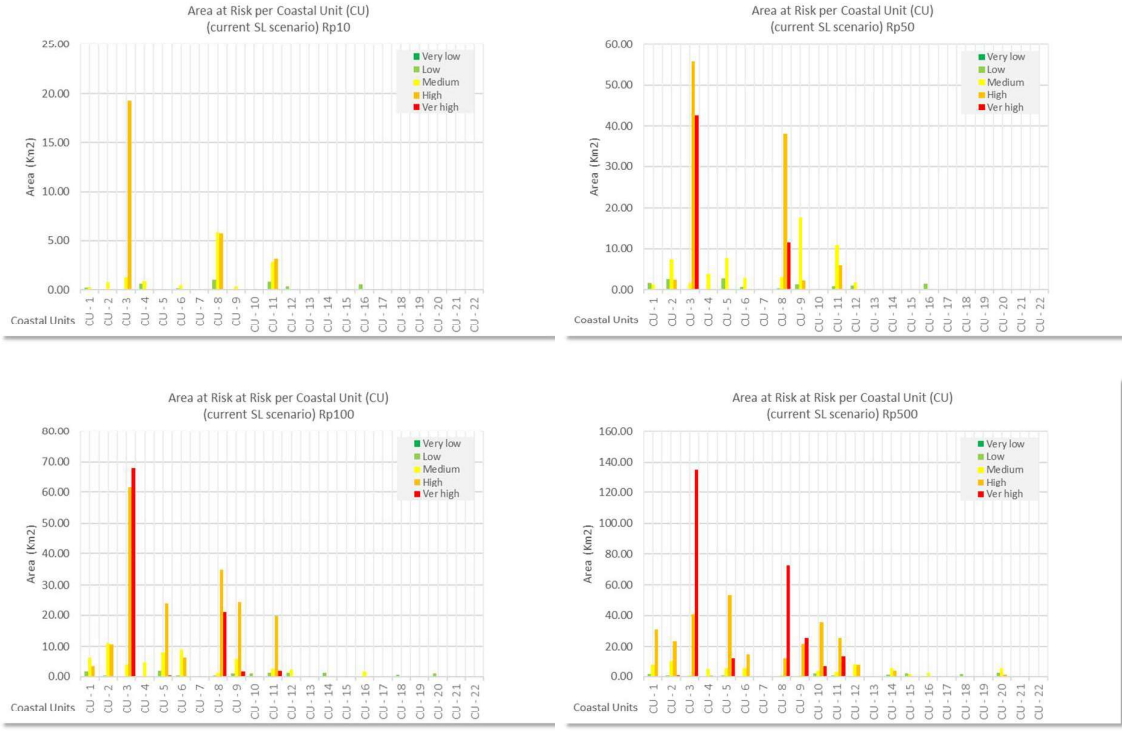

Figure 71. Area per Environmental Risk Class and CU. RCP 8.5 Sea Level Rise Scenario (+0.275 cm).

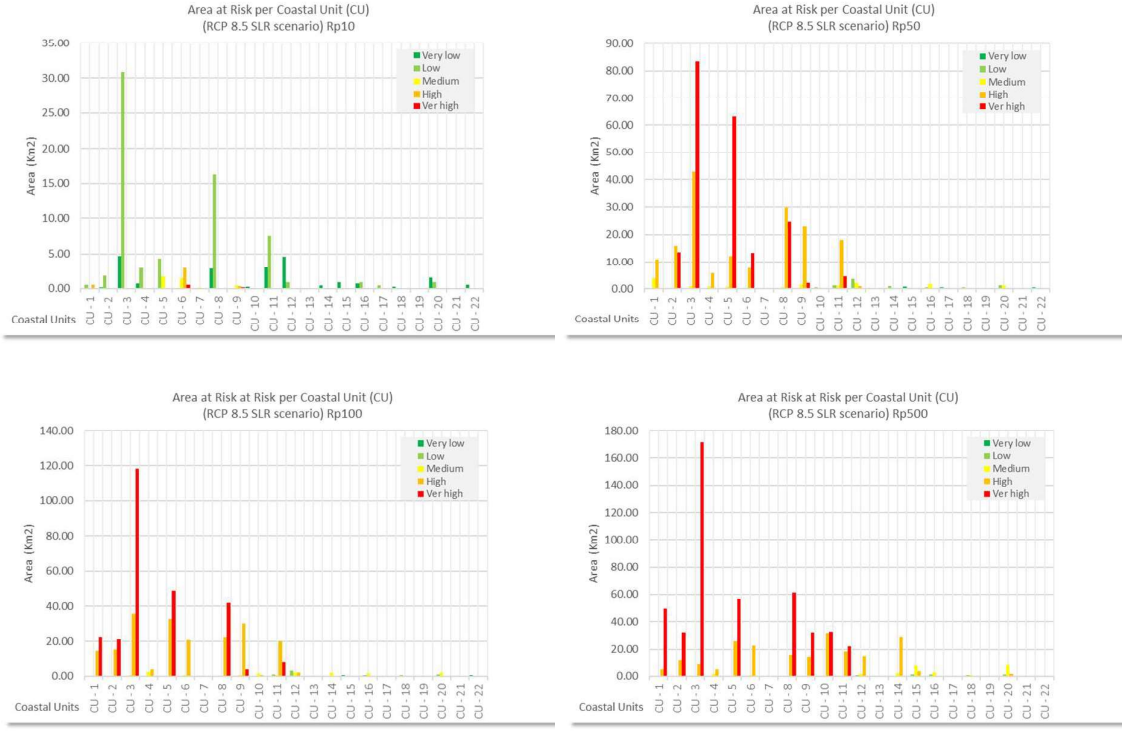

The CUs with the largest area of exposed protected ecosystems are CU-5 (AC-North), CU-9 (CR-South) and CU-12 (Turnefe Atoll), while the largest exposed area of relevant ecosystems without a protection figure is in CU-3 (NR-South), CU-8 (CR-Central) and CU-11 (Caye Caulker), especially wetlands, mangroves and littoral forest. In terms of the overall results of the EVI (aggregating protected and relevant non-protected ecosystems), among the CU that show higher values and are therefore more vulnerable are CU-3 (NR-South), CU-8 (CR-Central), CU-9 (CR-South), CU-5 (AC-North) and CU-11 (Caye Caulker). Accordingly, once hazard and environmental vulnerability classes are combined, the three CUs that show a greater area at high-risk levels are CU-3 (NR-South), CU-8 (CR-Central), and CU-5 (AC-North). From CU-12 (Turnefe Atoll) onwards the exposure decreases significantly and so does vulnerability and risk, with several CU having EVI values equal to zero.

4.4.2 Specific impact-oriented results

Degree of impact on the population (serious injuries/loss of life estimation)

According to the method described in 4.2.2.2, the degree of impact on the population (serious injuries/loss of life estimation) has been estimated through the calculation of the exposure of the most sensitive population group to an inundation depth of 1 meter. The approach simplifies complex interactions between population dynamics, behaviour patterns, warning systems, hazard intensity variables and availability of empirical data. However, it is a reasonable approach to identify areas with an actual higher probability of serious injuries and/or loss of life of the population exposed.

Jonkman (2007) describes a first rule of thumb of 1% of the exposed population for estimating mortality from large-scale coastal floods, based on empirical data. The approach followed in this study reduces the one percent mentioned for the 10 years return period, increasing slightly in the 50, 100 and 500 years return period considering the current sea level scenario (maximum value reached in the Rp 500 with 2.7% of the exposed population). When considering the RCP 8.5 sea-level rise scenario, as it was expected, this percentage has a higher increase, being higher the longer the return period, up to 3.7% in the 500 Rp.

Figure 72 shows the estimated expected losses in terms of serious injuries/loss of life for the exposed population to coastal flooding caused by cyclones in each CU across Belize, whereas Figure 73 represents the estimated expected average annual losses (AAL) per year, founded on the mentioned curve.

Figure 72. Probability Curve of Serious Injury/Mortality Considering Return Periods of 10, 50, 100 and 500 years for the RCP 8.5 SLR Scenario (+0.275 m) and the Current Sea Level Scenario.

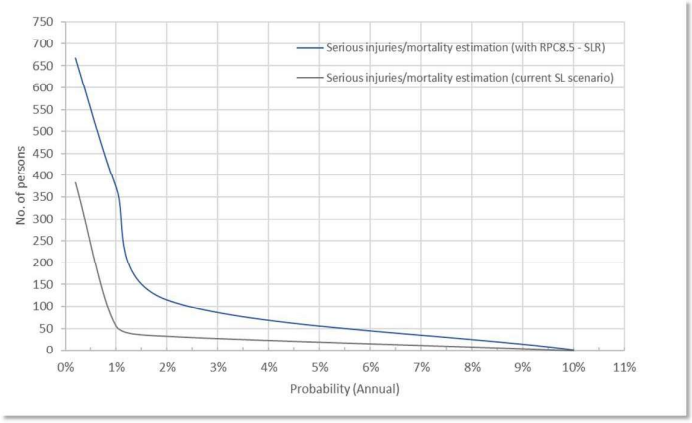

Figure 73. Estimated Population Serious Injuries/Mortality Estimation Annual Average Losses (AAL) Considering 10, 50, 100 and 500 Years Return Periods for RCP 8.5 SLR Scenario (+0.275 m) and Current Sea Level Scenario.

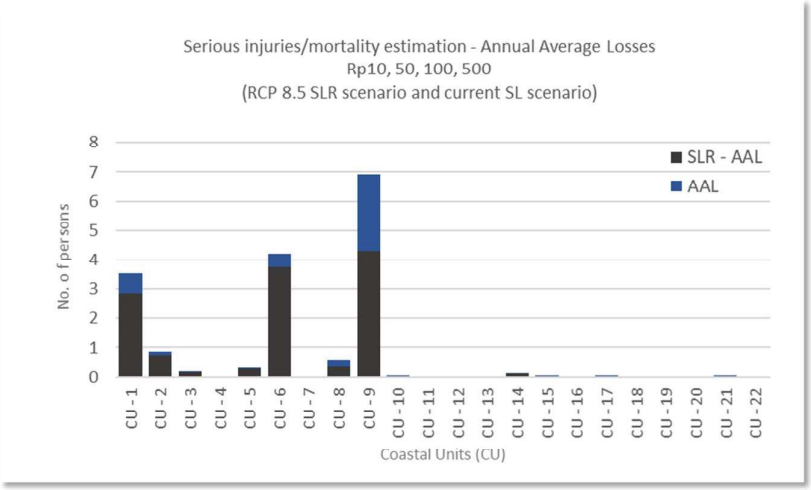

Building damage and associated replacement costs

According to the method described in 4.2.2.3, building damage and associated replacement costs have been calculated. Figure 74 and Figure 75 show the estimation of the replacement costs associated with building damage due to coastal floods caused by cyclones. The information is shown per CU, return period and sea-level scenario. CUs where building damage is more relevant are noticeably identified.

Figure 74. Estimated Building Damage Replacement Costs per CU and Return Period at Current Sea Level Scenario.

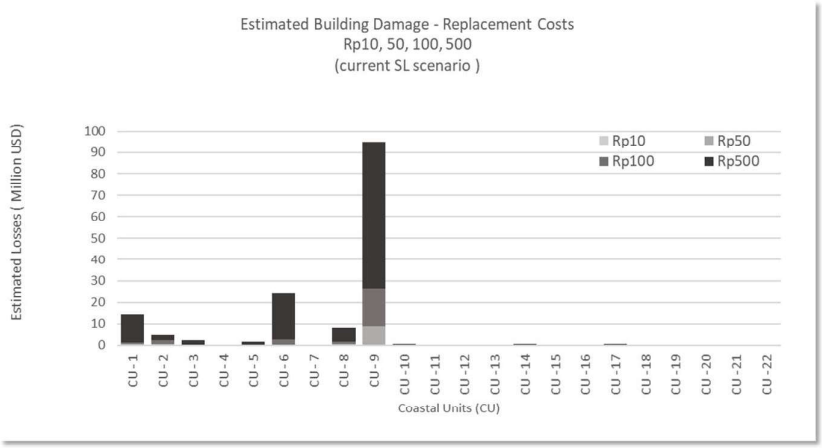

Figure 75. Estimated Building Damage Replacement Costs per CU and Return Period. RCP 8.5 Sea Level Rise Scenario (+0.275 cm).

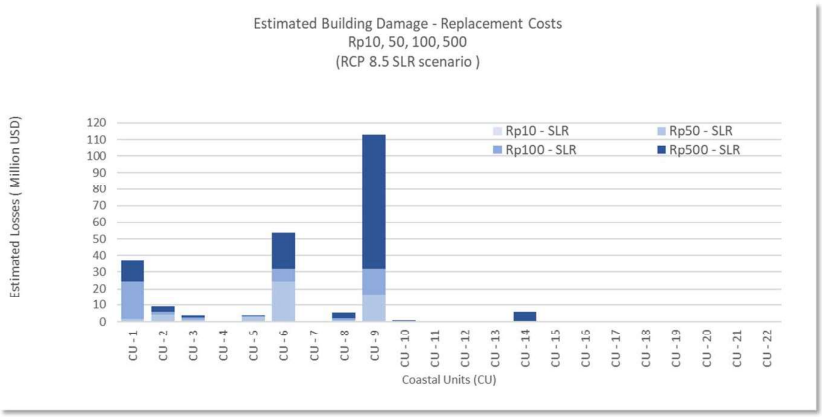

Following Figure 76 and Table 16 show the probability of potential monetary losses due to the replacement costs of damage that coastal flooding due to cyclones can cause to buildings. Finally, Figure 77shows the expected annual average losses (AAL) associated with the curve in Figure 76, showing visibly the CUs with higher expected losses. Information on AAL is useful to develop a cost-benefit analysis, allowing to test the efficiency (in monetary terms) of implementing certain risk reduction measures.

Figure 76. Loss Exceedance Estimation Curve for Replacement Costs Sssociated with Building Damage.

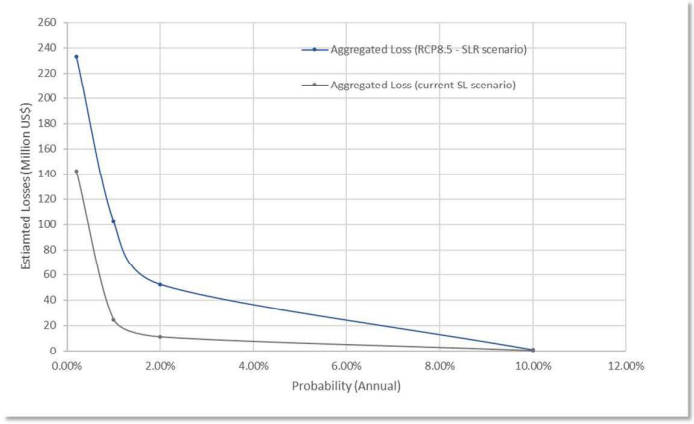

Table 16. Estimation of Replacement Costs Associated With Building Damage for Each Return Period and Sea-Level Scenario Considered.

Return Periods	10	50	100	500
Associated replacement costs (RCP8.5 - SLR scenario) – (Millions USD)	0.97	52.43	102.33	233.35
Associated replacement costs (current SL scenario) – (Millions USD)	0.28	11.11	24.65	142.19

Figure 77. Estimation of Annual Average Losses (AAL) per CU, Return Period and Sea-Level Scenario (AAL: Current Sea Level Scenario; AAL-SLR: RCP 8.5 SLR Scenario). Gross Domestic Product is 1.88 USD Billion for Year 2019.

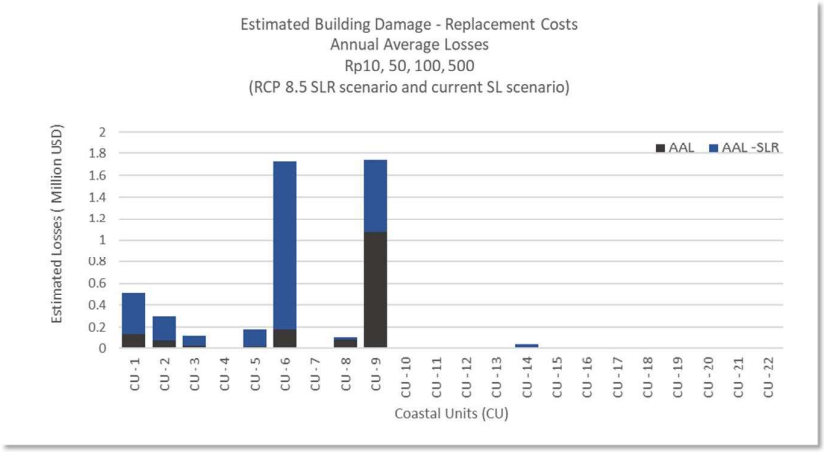

4.4.3 Erosion Risk Assessment

Hard structures

According to the method and assumptions described in section 0, hard structures results are presented in Figure 78 and Figure 79. Both graphs include the assessment for all CU, return periods (10, 50, 100 and 500 years) and two scenarios (current sea level and RCP 8.5 sea-level rise scenario, considering a rise of +0.275 m). Graphs include a red line indicating the threshold above which the collapse of structures is expected. For vertical seawalls, this is 0.3 m of scour depth and for rip-rap structures 50 kg of design weight. Structures of CUs above the threshold are expected to be seriously damaged or collapsed.

Regarding the collapse of the seawalls, it is estimated to occur in CU-17 associated with the 100 and 500 years Rp in both sea-level scenarios. As for the rip-rap structures, collapse is estimated to occur in CU-6 (AC-South) for all return periods and both sea-level scenarios, and in CU-17, related to Rp of 100 and 500 years in both sea-level scenarios.

Figure 78. Scour Depth Estimated per CU, Return Period (10, 50, 100 and 500 years) for Current Sea Level Scenario and RCP 8.5 Sea-Level Rise Scenario (+0.275 m).

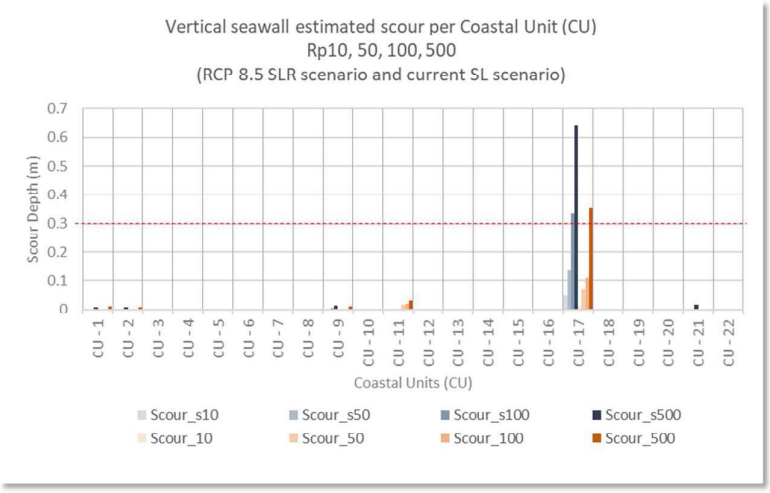

Figure 79. Design Weight for Rip-Rap Structures Estimated per CU, Return Period (10, 50, 100 and 500 years) for Current Sea Level Scenario and RCP 8.5 Sea-Level Rise Scenario (+0.275 m).

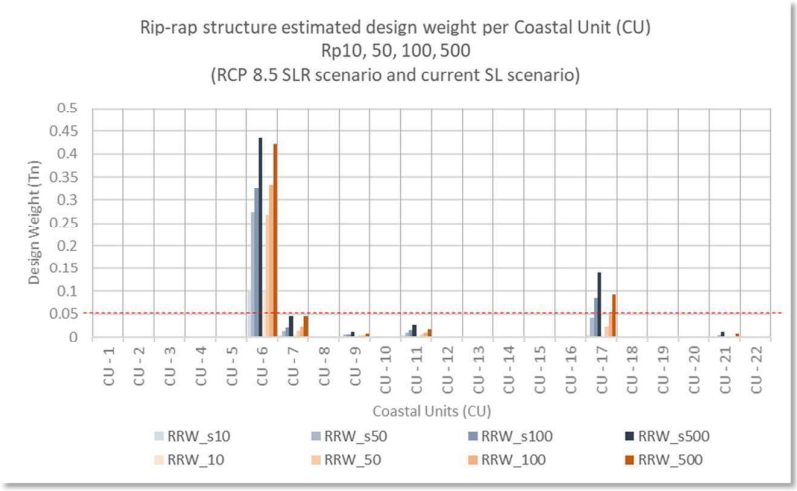

Sandy/ beach areas

Erosion risk assessment results in beaches are focused to obtain the potential loss of sandy areas due to erosion processes associated with tropical cyclones. Shoreline retreat per CU, return period (10, 50 100 and 500 years) for current sea level scenario and RCP 8.5 sea-level rise scenario (+0.275 m). Figure 80. shows the shoreline retreat estimated in each CU, for every return period analyzed and both sea-level scenarios. The CUs where the erosion processes will have the greatest impact on the beaches of Belize are well defined regardless of the scenario

considered, being CU-5 (AC-North) and CU-6 (AC-South) the ones with highest values of shoreline retreat.

Figure 80. Shoreline Retreat per CU, Return Period (10, 50, 100 and 500 years) for Current Sea Level Scenario and RCP 8.5 Sea-Level Rise Scenario (+0.275 m).

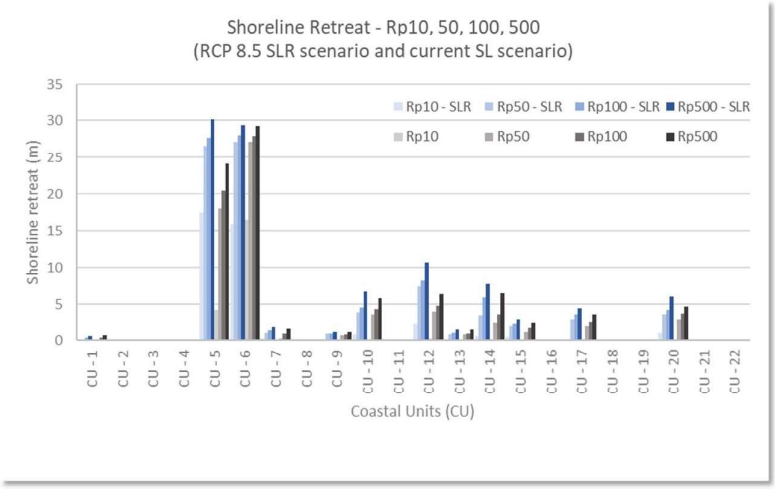

As shown in Figure 81, the estimated shoreline retreat is greater, as expected, for longer return periods. However, it is notable that even with higher probabilities of occurrence there is significant shoreline retreat (20 and 40 meters for current sea level and RCP 8.5 SLR scenarios and 10 years Rp., respectively).

Figure 81. Sand Loss Exceedance Curve Considering 10, 50, 100 and 500 years Return Periods and Two Scenarios (Current Sea Level and RCP 8.5 SLR + 0.275 m).

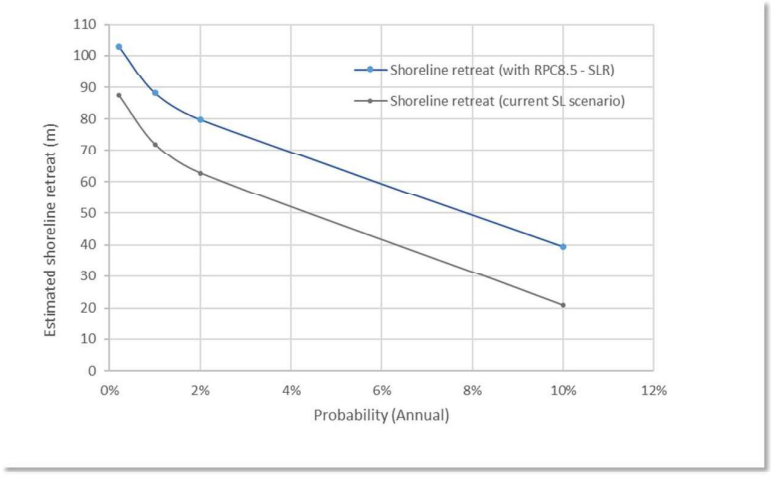

As for the beach surface loss, Figure 82 shows the loss in each CU, for every return period analyzed and for the two sea-level scenarios. The CUs where surface losses will be greater are well identified. In addition, Figure 83 shows the loss ratio, i.e., the percentage of area that it is estimated to be lost for each of the scenarios and return periods described. This information enriches the analysis by relativizing the loss data for each specific initial status, highlighting areas in which, although the area lost may not be as relevant in raw data, it may represent a significant percentage of its own current area (e.g. CU-14, SN-North, with a low value of gross area loss but which loses about 65% of its own beach area in the worst-case scenario; or CU-6 (AC-South) which will lose 100% for all return periods and scenarios considered).

Figure 82. Beach Surface Loss per CU, Return Period (10, 50, 100 and 500 Years) for Current Sea Level Scenario and RCP 8.5 Sea-Level Rise Scenario (+0.275 m).

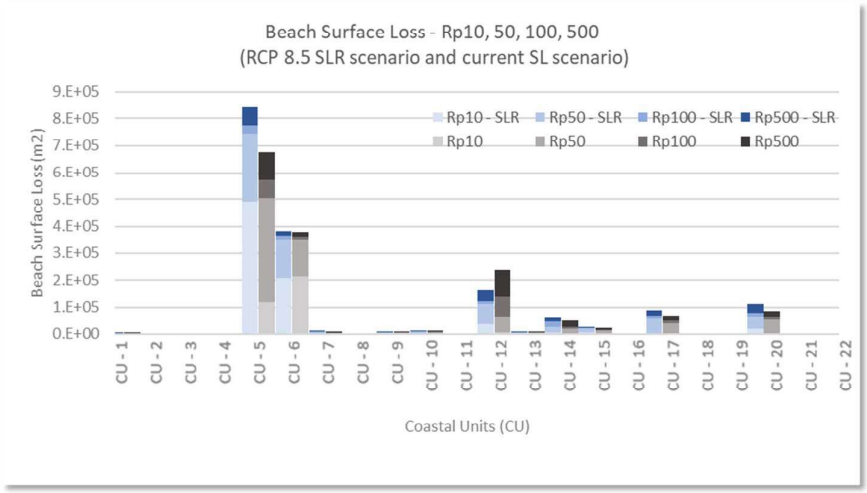

Figure 83. Beach Loss Ratio per CU, Return Period (10, 50, 100 and 500 Years) for Current Sea Level Scenario and RCP 8.5 sea-Level Rise Scenario (+0.275 m).

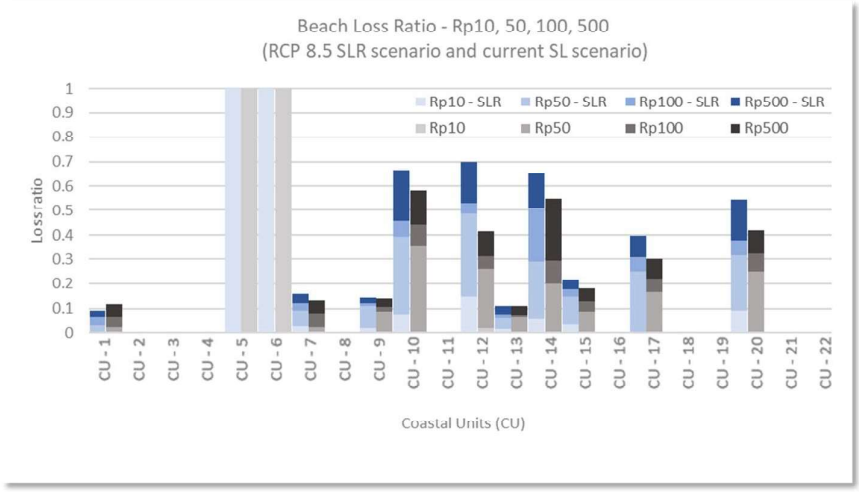

5. CONCLUSION

The hazard analysis has revealed the efficacy of mangroves and coral reefs to protect the coastal system from the impacts of tropical cyclones, particularly coastal erosion and coastal flooding. Coral reefs provide direct flood protection to 702 people in Belize every year and prevent 9 US$ millions of annual losses. Without coral reefs, an additional 400 Ha of land would be annually flooded and the benefits of preserving the current coral reefs in Belize increase with the storm intensity: the flood protection against 1-in-100-year event rises to 14259 people and 282 US$ millions. Although the unitary benefit (per hectare of the ecosystem) of coral reefs is greater than mangrove's (0.1 annual expected people protected and US$ 1894 of annual expected economic losses avoided per hectare of coral reefs and 0.07 people and US$ 1571 per hectare of mangroves), mangroves also contribute to reducing flooding along the coastline of Belize.

Flood Protection Provided by Ecosystems

Coral reefs provide direct flood protection to 702 people in Belize every year. They prevent flooding of 400 Ha of land and 9 US$ millions of annual losses.

Every year, per 1 hectare of coral reefs:

- 0,1 people is protected.
- 1894 US$ of losses are avoided.

Every year, per 1 hectare of mangroves:

- 0,07 people is protected.
- 1571 US$ of losses are avoided.

Coastal Flood Risk Assessment

Results show a greater impact across the northern area of the country, whereas the southern part of the country is less exposed to coastal flooding associated with tropical cyclones.

In terms of population and infrastructure, Belize City, Ambergris Caye and Corozal Town are the most exposed and vulnerable areas, showing higher estimates of serious injuries/loss of life and damage to households and associated replacement costs.

As for the environmental component, relevant and protected ecosystems play an important role in the northern and central regions not only due to their protection services but also due the cultural, provisioning and regulatory services they provide.

The results of the integrated coastal flood risk assessment developed this study show a greater impact across the northern area of the country, especially

in areas where higher exposure to coastal flooding associated with tropical cyclones is combined with high levels of vulnerability. In terms of population and infrastructure, the most exposed and vulnerable areas are in the most populated areas of Belize City, Ambergris Caye and Corozal Town and their surroundings. With regard to the environmental component, it has been shown that relevant and protected ecosystems play an important role in the integrated risk outcome, especially in the northern and central regions, which should be taken into account in the process of disaster risk management, considering not only the protection services but also the cultural, provisioning and regulatory services they provide. In general terms, the southern part of the country is less exposed to coastal flooding associated with tropical cyclones, so none of the dimensions considered provides a significant integrated risk outcome compared to the northern area.

According to estimates on serious injuries/loss of life of the population as well as for damage to households and associated replacement costs, main findings show that impact will be higher in the populated areas of Belize City, Ambergris Caye and Corozal Town and their surroundings, in line with the individual human and infrastructures risk results. It is estimated that more than 650 people could be seriously injured in the worst-case scenario, the 500 years Rp and CPR 8.5 SLR +0.275 m, a number that decreases as the probability of occurrence increases, with an estimate of about 3 people for the 10 year Rp under the same sea-level rise scenario. Damage to households is estimated to be between US$ 275,500, in the best scenario, the 10 year Rp under the current sea level scenario and over US$ 230 million if the worst-case studied is considered (500-year Rp and RCP 8.5 SLR +0.275 m). The average losses associated with replacement costs are estimated at around US$ 1.5 and US$ 4.8 million for the current situation and the 2050 horizon considering the 0.275 m sea-level rise scenario, respectively.

As for coastal erosion, results reveal that in those areas covered with mangroves, this is less than 0.5 m for all return periods (10, 50, 100 and 500) and scenarios analyzed (current situation and horizon year 2050 under climate change effects). Looking at the effect of erosion on coastal structures, few areas of the country present serious problems. The highest scour of vertical structures and associated collapse estimates are detected in the Southern Central Region, around Placencia, for the 100 and 500 year return periods. In this area, the possible collapse of the rip-rap structures is also estimated for the same return periods, which also occurs in the Ambergris Caye area, in this case for all return periods and both sea-level scenarios analyzed.

Erosion effects on shoreline retreat and beach surface loss are more significant in terms of their magnitude. Nevertheless, usually the erosion caused by tropical cyclones on beaches is naturally recovered only a few months after the erosive event due to natural morphodynamic processes during calm weather conditions. The area of the country where the erosion processes will have the greatest impact on the beaches of Belize is well defined regardless of the scenario considered, having Ambergris Caye the highest values for both shoreline retreat and beach surface losses. Nevertheless, although with a lower impact, there is also a significant shoreline retreat in the sandy coastal areas of the country, as well as a significant loss of beach surface in the beaches of Central and Southern Belize.

Coastal erosion derived from tropical cyclones

Mangroves almost completely avoid coastal erosion derived from tropical cyclones all across Belize.

A significant shoreline retreat is estimated in all sandy coastal areas of the country, but this beach erosion derived from tropical cyclones can be naturally recovered (beach resilience not addressed, though).

Shoreline retreat and beach surface loss is estimated to be the highest in Ambergris Caye and, second, in the beaches of Central and Southern Belize.

The effect on coastal structures of coastal erosion derived from tropical cyclones is very limited and it has been estimated to be relevant only in Placencia and Ambergris Caye.

6. REFERENCES

Abson, D. J., Dougill, A. J., and Stringer, L. C. Using Principal Component Analysis for information-rich socio-ecological vulnerability mapping in Southern Africa. Applied Geography, 35 (1–2), 515 – 524, 2012.

Aguirre-Ayerbe, I., Martínez Sánchez, J., Aniel-Quiroga, Í., González-Riancho, P., Merino, M., Al-Yahyai, S., González, M., and Medina, R.: From tsunami risk assessment to disaster risk reduction – the case of Oman, Nat. Hazards Earth Syst. Sci., 18, 2241-2260, https://doi.org/10.5194/nhess-18-2241-2018, 2018.

Bates, P. D., R. J. Dawson, J. W. Hall, M. S. Horritt, R. J. Nicholls, J. Wicks, and M. A. A. M. Hassan (2005). Simplified two-dimensional numerical modelling of coastal flooding and example applications, Coastal Eng., 52, 793–810.

Beck, M. W. ., & Lange, G. M. (2016). World Bank (2016). Managing Coasts with Natural Solutions: Guidelines for Measuring and Valuing the Coastal Protection Services of Mangroves and Coral Reefs. In Washington DC: The World Bank.

Beck, M. W., Losada, I. J., Mendendez, P., Reguero, B. G., Díaz-Simal, P., & Fernandez, F. (2017). The global flood protection savings provided by coral reefs. Nature Communications, (2018). https://doi.org/10.1038/s41467-018-04568-z

Bender, M.A., Knutson, T.R, Tuleya, R.E, Sirutis, J.J, Vecchi, G. A., Garner, S.T. and Held, I. (2010). Modeled impact of anthropogenic warming on the frequency of intense Atlantic hurricanes. Science, 327(5964), doi:10.1126/science.1180568.

Booij, N., Ris, R.C., Holthuijsen, L.H. (1999). A third-generation wave model for coastal regions. Part I: model description and validation. Journal of Geophysical Research, 104 (C4), 7649–7666.

Damm, M.: Mapping Social-Ecological Vulnerability to Flooding. Graduate Research Series, Ph.D. Dissertations, Publication Series of UNU-EHS Vol. 3, ISBN: 978-3-939923-46-6. United Nations University – Institute for Environment and Human Security (UNU-EHS), Bonn, 2010.

Fleming, J. G, Fulcher, C. W., Luettich, R. A., Estrade, B. D., Allen, G. D. and Winer, H. S. (2008). A Real Time Storm Surge Forecasting System using ADCIRC. Proceedings of the International Conference on Estuarine and Coastal Modeling, pp. 893-912.

Dietrich, J. C., Tanaka, S., Westerink, J. J., Dawson, C. N., Luettich Jr., R. A., Zijlema, M., Holthuijsen, L. H., Smith, J. M., Westerink, L. G., and Westerink, H. J (2012). Performance of the unstructured-mesh, SWAN+ADCIRC model in computing hurricane waves and surge, J. Sci. Comput., 52, 468–497, 2012

Fuller, C, Green, E, and Gordon, A. (2011). Second National Communication. United Nations Framework convention on Climate Change. Belmopan (Belize); Belize's National Meteorological Service (www.hydromet.gov.bz).

Goldenberg, S.B., Landsea, C. W. , Mestas-Nuñez, A. M., and Gray, W. M. (2001). The recent increase in Atlantic hurricane activity: Causes and implications. Science,293, 474–479.

González-Riancho, P., Aguirre-Ayerbe, I., García-Aguilar, O., Medina, R., González, M., Aniel-Quiroga, I., Gutiérrez, O. Q., Álvarez-Gómez, J. A., Larreynaga, J., and Gavidia, F.: Integrated tsunami vulnerability and risk assessment: application to the coastal area of El Salvador, Nat. Hazards Earth Syst. Sci. 14:1223–1244, doi:10.5194/nhess-14-1223-2014, 2014.

Greiving, S., Fleischhauer, M., and Lückenkötter, J.: A methodology for an integrated risk assessment of spatially relevant hazards, J. Environ. Plann. Man., 49, 1–19, doi:10.1080/09640560500372800, 2006.

IDB, I.-A.D.B., (2011). Indicators for Disaster Risk and Risk Management: Programme for Latin-America and The Caribbean - Bahamas - IDB. Tech. Notes 1–48.

IDOM and Hydraulics Institute of Cantabria (2017). Consulting Engagement 2: Disaster Risk and Climate Change vulnerability Assessment for Belize City. Washington D.C: Inter American Development Bank.

IFRC, I.F. of R.C. and R.C.S., (2016). Hurricane Earl, Situation Report.

IH Cantabria-MARN: Instituto de Hidráulica Ambiental IH Cantabria, Ministerio de Medio Ambiente y Recursos Naturales de El Salvador MARN: Catálogo de Peligrosidad debida a la inundación por Tsunami en la costa de El Salvador, Spanish Agency for International Development Cooperation (AECID), available at:

http://www.ihcantabria.com/es/proyectos-id/item/839-tsunami-hazard-el-salvador (last access: 1 December 2014), 2010 (in Spanish).

IH Cantabria-MARN: Instituto de Hidráulica Ambiental IH Cantabria, Ministerio de Medio Ambiente y Recursos Naturales de El Salvador MARN: Catálogo de Vulnerabilidad y Riesgo debido a la inundación por Tsunami en la costa de El Salvador, Spanish Agency for International Development Cooperation (AECID), available at: http://www.ihcantabria.com/es/proyectos-id/item/843-tsunami-vulnerability-risk-el-salvador (last access: 1 December 2014), 2012 (in Spanish).

IPCC, (2014). Climate Change 2014: Synthesis Report. Contribution of Working Groups I, II and III to the Fifth Assessment Report of the Intergovernmental Panel on Climate Change [Core Writing Team, R.K. Pachauri and L.A. Meyer (eds.)]. IPCC, Geneva, Switzerland. https://doi.org/10.1046/j.1365-2559.2002.1340a.x

IPCC, (2007). Climate Change 2007: impacts, adaptation and vulnerability: contribution of Working Group II to the fourth assessment report of the Intergovernmental Panel, Geneve, Swiezerland. https://doi.org/10.1256/004316502320517344

IPCC (2013). Climate Change 2013: The Physical Science Basis. Contribution of Working Group I to the Fifth Assessment Report of the Intergovernmental Panel on Climate Change, T.F. StockerD. QinG.-K. PlattnerM. TignorS.K. AllenJ. BoschungA. NauelsY. XiaV. BexP.M. Midgley (eds.), Cambridge, United Kingdom and New York.

IPCC (2019). Summary for Policymakers. In: IPCC Special Report on the Ocean and Cryosphere in a Changing Climate [H.-O. Pörtner, D.C. Roberts, V. Masson-Delmotte, P. Zhai, M. Tignor, E. Poloczanska, K. Mintenbeck, M. Nicolai, A. Okem,J. Petzold, B. Rama, N. Weyer (eds.)]. In press.

Izaguirre, C., Losada, I.J., Espejo, A., Diez-Sierra, J. and Diaz-Simal, P. (2017). Coastal flooding risk associated to tropical cyclones in a changing climate. Application to Port of Spain (Trinidad and Tobago). Nat. Hazards Earth Syst. Sci. Discuss. doi:10.5194/nhess-2017-150.

Jelínek, R., Eckert, S., Zeug, G., and Krausmann, E.: Tsunami Vulnerability and Risk Analysis Applied to the City of Alexandria, Egypt, Tsunami Risk ANd Strategies For the European Region (TRANSFER Project), 2009.

Jenks, G. F.: The data model concept in statistical mapping, Int. Yearbook Cartogr., 7, 186–190, 1967.

Jonkman, S. N., Vrijling, J. K., and Vrouwenvelder, A. C. W. M.: Methods for the estimation of loss of life due to floods: a literature review and a proposal for a new method, Nat. Hazards, 46, 353–389, 2008

Knaff, J. A., R. M. Zehr ,R. T. DeMaria, and D. A. Molenar (2015). Improved tropical cyclone flight-level wind estimates using routine infrared satellite reconnaissance. J. Appl. Meteor. Climatol., 54, 463–478, doi:10.1175/JAMC-D-14-0112.1

Kopp, R. E., DeConto, R. M., Bader, D. A., Hay, C. C., Horton, R. M., Kulp, S., Oppenheimer, M., Pollard, D. and Strauss, B. H. (2017). Evolving Understanding of Antarctic Ice-Sheet Physics and Ambiguity in Probabilistic Sea-Level Projections. Earth's Future. doi:10.1002/2017EF000663

Kopp, R. E., R. M. Horton, C. M. Little, J. X. Mitrovica, M. Oppenheimer, D. J. Rasmussen, B. H. Strauss, and C. Tebaldi (2014). Probabilistic 21st and 22nd century sea-level projections at a global network of tide-gauge sites, Earth's Future, 2, 383–406, doi:10.1002/2014EF000239.

Hagen, S.C., Westerink, J.J., and Kolar, R.L. (2001). One dimensional finite element grids based on a localized truncation error analysis, International Journal for Numerical Methods In Fluids, 32 (2): 241-261.

Holland, G. J. (1980). An analytic model of the wind and pressure profiles in hurricanes. Mon. Wea. Rev. 108, 1212-1218.

Lin, N., and Chavas, D. (2012). On hurricane parametric wind and applications in storm surge modeling. Journal of Geophysical Research, vol. 117, D09120, doi: 10.1029/2011JD017126.

Luettich, R. A., and J. J. Westerink (2004). Formulation and numerical implementation of the 2D/3D ADCIRC finite element model version 44.XX.

Menéndez, P., Losada, I. J., Beck, M. W., Torres-Ortega, S., Espejo, A., Narayan, S., … Lange, G.-M. (2018). Valuing the protection services of mangroves at national scale: The Philippines. Ecosystem Services, 34. https://doi.org/10.1016/j.ecoser.2018.09.005

Menéndez, Pelayo, Losada, I. J., Torres-Ortega, S., Toimil, A., & Beck, M. W. (2019). Assessing the effects of using high-quality data and high-resolution models in valuing flood protection services of mangroves. Plos One, 14(8), e0220941. https://doi.org/10.1371/journal.pone.0220941

Nakajo S., N. Mori, T. Yasuda, and H. Mase (2014). Global Stochastic Tropical Cyclone Model Based on Principal Component. Journal of Applied Meteorology and Climatology, 53, 1547-1577.

National Emergency Management Organization (NEMO) (2010). Initial Damage Assessment Report. Hurricane Richard.

National Emergency Management Organization (NEMO) (2016). Initial Damage Assessment Report. Hurricane Earl.

OECD (Organization for Economic Co-operation and Development)/EC-JRC (European Commission Joint Research Centre): Handbook on Constructing Composite Indicators, Methodology and Users Guide, OECD Publications, Paris, 2008.

Passeri, D., Hagen, S., Smar, D., Alimohammadi, N., Risner, A., White, R. (2011). Sensitivity of an ADCIRC tide and storm surge model to Manning's n. Estuar. Coast. Model.

Roelvink, D., Reniers, A., van Dongeren, A., van Thiel de Vries, J., McCall,R., Lescinski, J. (2009). Modelling storm impacts on beaches, dunes and barrier islands. Coast. Eng., 56 (11–12) (November-December 2009), pp. 1133-1152.

Slangen A.B.A., M. Carson, C.A. Katsman, R.S.W. van de Wal, A. Köhl, L.L.A. Vermeersen, and D. Stammer, (2014). Projecting twenty-first century regional sea-level changes. Climatic Change, doi: 10.1007/s10584-014-1080-9.

Smith Warner International (2001). Hurricane Rehabilitation and Disaster Preparedness Project: IADB Regional Shelter-Site Location Analysis Component Report. Submitted to Ministry of Economic Development, Government of Belize.

Stephenson, T.S. and Jones, J.J. (2017). Impacts of Climate Change on Extreme Events in the Coastal and Marine Environments of Caribbean Small Island Developing States (SIDS), Caribbean Marine Climate Change Report Card: Science Review 2017, pp. 10 -22.

Stewart, S.R., (2017). National Hurricane Center Tropical Cyclone Report. Hurricane Earl.

Trigg, M., Smith, A. and Sampson, C. (2016). CHaRIM Project: Belize National Flood Hazard Mapping Methodology and Validation Report. ACP-EU Natural Disaster Risk Reduction Program.

UNDRR (United Nations Office for Disaster Risk Reduction). Hyogo Framework for Action 2005-2015: building the resilience of nations and communities for disasters. Geneva: UNISDR, 2005. https://www.unisdr.org/we/inform/publications/1037 (accessed 03 June 2020).

UNDRR (United Nations Office for Disaster Risk Reduction). Sendai Framework for Disaster Risk Reduction 2015-2030. UNDRR, 2015. https://www.undrr.org/publication/sendai-framework-disaster-risk-reduction-2015-2030 (accessed 03 June 2020).

UNDRR (United Nations Office for Disaster Risk Reduction). Report of the open-ended intergovernmental expert working group on indicators and terminology relating to disaster risk reduction. United Nations General Assembly A/71/644.1 December 2016, New York, USA, 2016.

UNDRR (United Nations Office for Disaster Risk Reduction). Terminology. https://www.undrr.org/terminology (accessed 03 June 2020).

United Nations Development Program (UNDP) (2017). Consultancy for Development and Design of an integrated National Adaptation Plans (NAP) for the agriculture and water sectors in Belize. Inception Report, supported by The Japan-Caribbean Climate Change Partnership (J-CCCP).

Zijlema, M.; Van Vledder, G.P.; Holthuijsen, L.H. (2012). Bottom friction and wind drag for wave models. Coast.Eng., 65, 19–26

Appendix 1. Proposal of Risk Reduction Measures in Priority Hotspots

Disaster Risk Profile for Belize

Inter - American Development Bank

CONTENTS

LIST OF FIGURES

LIST OF TABLES

1. INTRODUCTION

Belize is highly susceptible to natural disasters, such as hurricanes and tropical storms. These events cause recurrent floods and severe damages.

In addition, the United Nations Framework Convention on Climate Change identifies Belize as one of the most vulnerable countries to climate change, since Belize's population and economic activity are largely concentrated in low-lying coastal zones. Sea level rise is expected to worsen damages derived from tropical cyclones in Belize.

This report aims to present a **final proposal of Risk Reduction Measures** (RRM) at selected Priority Hotspots (PHS), validated with local stakeholders. This report is structured into four chapters, plus the foreword (background of the project) and three annexes:

1. **Introduction.**
2. **Catalogue of RRM.**
3. **Identification of key issues and selection of RRM at PHS.**
4. **Conclusions.**

Following this final proposal of RRM, an on-line meeting (**Fourth Workshop**) was conducted in order to show final project results.

2. CATALOGUE OF RRM

2.1. Introduction

This section describes the catalogue of RRM measures developed for Belize addressing coastal flooding and erosion caused by tropical cyclones. The catalogue has been synthesized in a collection of **Risk Reduction Measures Technical Fact-Sheets** (see Annex 1) and it includes the feedback provided by local stakeholders by means of an on-line consultation (see Annex 3).

2.2. RRM included in the catalogue

After an intensive review of the state of the art of RRM related to coastal flooding and erosion due to tropical cyclones, a set of suitable RRM based in all pre and post-event phases of the risk management cycle (see 0) have been identified addressing diverse **strategies** and **approaches**.

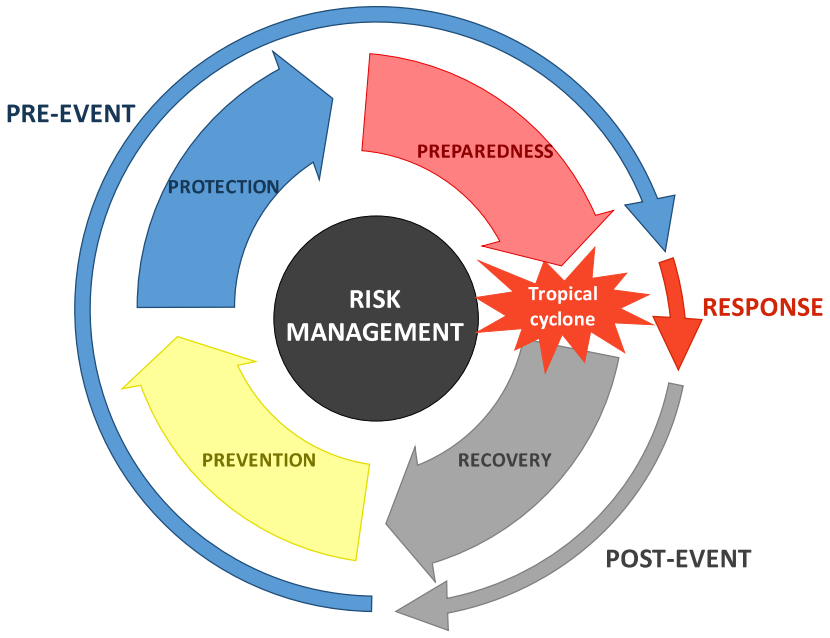

Figure 1. Phases of the risk management cycle and risk reduction strategies.

The RRM included in the catalogue can be related to four pre and post-event risk management **strategies**:

- **Prevention**: To protect from the hazard through action taken in advance reducing the hazard itself, the exposure to the hazard or the vulnerability of the exposed goods or people.
- **Protection**: To shield from the direct impacts of the hazard by mitigating the hazard itself.
- **Preparedness:** Knowledge and skills developed to anticipate and respond to the impacts of a coastal flooding event.
- **Recovery:** Actions taken after an emergency to restore and resume normal operations.

As for the diverse **approaches** to tackle risk reduction, the **prevention strategy** includes the following:

- **Receptors adaptation**: Regulations and good practices targeted to reduce the vulnerability mainly related to the infrastructure dimension to coastal flooding and erosion.
- **Exposure reduction**: To prevent the location of receptors in hazardous areas or relocate receptors.
- **Modelling and assessments to enhance prevention**: Information system that helps to enhance our understanding and awareness of coastal risk to reduce the impact of coastal flooding and erosion.
- **Maintenance of the coastal system**: To ensure optimal levels of serviceability and safety of coastal structures, land features and ecosystems in order to minimize costs and environmental impacts.

Within the **protection strategy** there are the following approaches to address the problem of coastal flooding and erosion risk reduction:

- **Nature-based** measures: The use of ecological principles and practices targeted to reduce the coastal flooding and erosion, to enhance coastal areas safety, while enhancing habitat, improving aesthetics, and saving money.

- **Hard Engineering**: Controlled disruption of natural processes by using long term man-made structures targeted to reduce the coastal flooding and erosion hazard.
- **Soft Engineering:** Controlled disruption of natural processes by using engineering technics that restore the natural processes to reduce the coastal flooding and erosion hazard.

As for the **preparedness strategy** the identified approaches are:

- **Forecasting and warning:** Targeted to alert the public and enable evacuation of people and certain goods (i.e. vessels) at risk to safety areas or shelters when a tropical cyclone is detected or forecasted.
- **Emergency response**: Targeted to prepare measures that will be implemented during the event.
- **Enhance public awareness**: Targeted to reduce risk by enhancing the knowledge and capacities developed by communities and individuals to effectively anticipate and respond to the impacts of likely, imminent or current hazard events.

Finally, the **recovery strategy** covers the following approaches:

- **Individual and environmental recovery**: Clean-up and restoration activities to recover the coastal zones and avoid new impacts (health issues, aggravated poverty…) following a disastrous event.
- **Societal recovery**: Actions taken to assure prompt assistance to people affected by a disastrous event by means of the cooperation between institutions (e.g. government, NGO, international cooperation agency…) and individuals in order to streamline recovery.
- **Risk transfer**: To limit the financial impact to affected people by a disastrous event by quickly providing liquidity when an insurance policy is triggered.

Finally, all considered strategies, approaches and measures in the catalogue of RRM are listed in the following table:

Table 1.Strategies, approaches and RRM in the catalogue.

Strategy	Approach	RRM
Prevention	Receptors adaptation	Building codes and regulations
		Flood-proofing
	Exposure reduction	Land use regulations and urban planning
	Modelling and assessments to enhance prevention	Hazard, exposure, vulnerability and risk assessments under coastal flooding and erosion
	Maintenance and conservation of the coastal system	Maintenance of coastal structures, beach width, coastal ecosystems and habitats
Protection	Nature-based	Beach restoration
		Wetland restoration
		Coral reef conservation
	Hard Engineering	Seawalls
		Breakwaters and groins
		Land claim
	Soft Engineering	Managed retreat
		Sand re-nourishment
Preparedness	Forecasting and warning	Early warning systems
	Emergency response	Emergency and contingency plans
	Enhance Public awareness	Education programs
		Raising awareness campaigns
Recovery	Individual and environmental recovery	Clean-up and restoration activities
	Societal recovery	Disaster assistance
	Risk transfer	Insurance policies

Description of the RRM Technical Fact-Sheets

The main characteristics of every RRM included in the catalogue are summarized in the corresponding **Technical Fact-Sheets** which includes: Heading, goal, description, relevant stakeholders, suitability (SWOT analysis) and bibliographic references.

The description of the RRM includes the rationale, a list of preliminary requirements for the implementation of the measure, a list of supplementary measures, some considerations regarding the expected efficiency, durability and cost, a graphical scheme of the measure and some examples of application in Belize, if available, or abroad.

The structure of the RRM technical factsheets is schematized in the following figure.

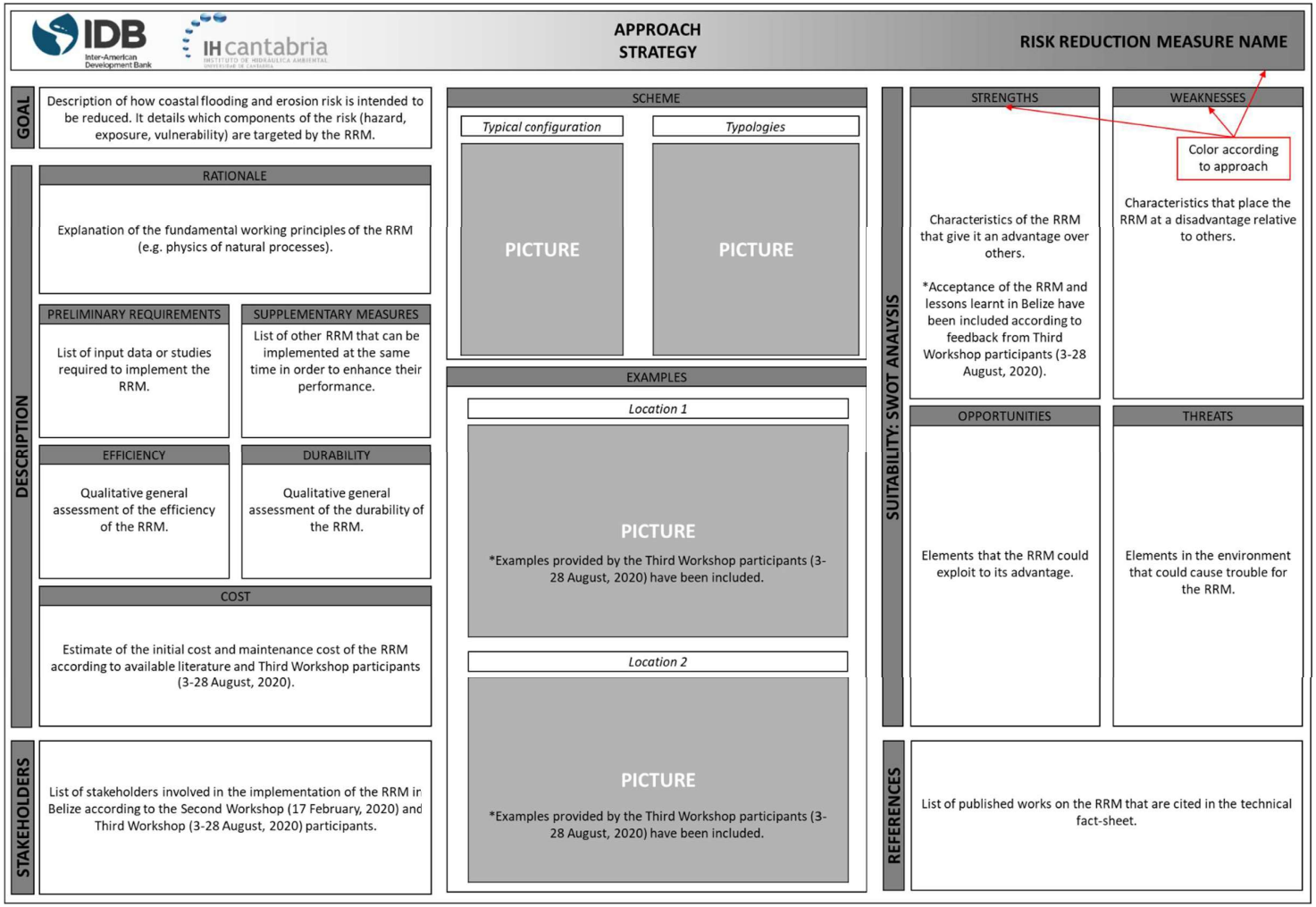

Figure 2. Description of the RRM Technical Fact-Sheets.

3. IDENTIFICATION OF KEY ISSUES AND SELECTION OF RRM AT PHS

3.1. Introduction

The following ten sites were selected as PHS (see 0) in agreement with local stakeholders during the Second Workshop, held in Belize City on the 17th of February, 2020 (see Annex 2):

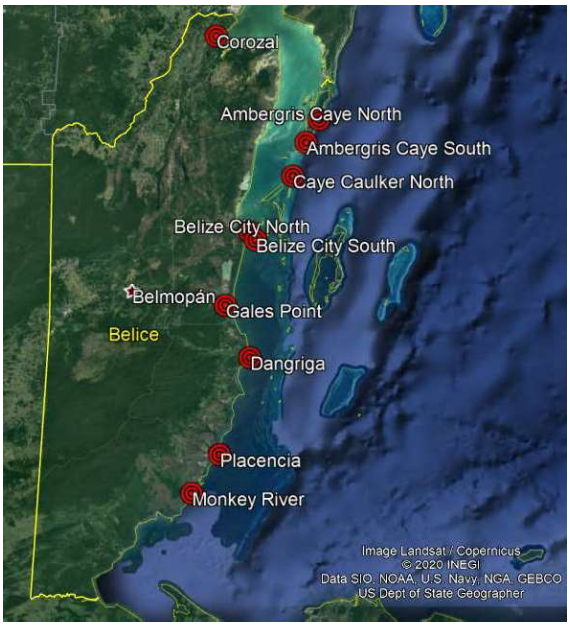

Figure 3. Location of the ten selected PHS.

The following sections include a brief description of each site, with the focus on the key issues regarding coastal flooding and erosion along with a proposal of RRM per site. Both, diagnosis and recommended RRM, have been validated with local stakeholders by means of an on-line consultation (Third Workshop), conducted between the 3rd and 28th August, 2020 (see Annex 3).

The ten PHS are listed from north to south:

1. Corozal
2. Ambergris Caye North
3. Ambergris Caye South
4. Caye Caulker North
5. Belize City North

6. Belize City South
7. Gales Point
8. Dangriga
9. Placencia
10. Monkey River

3.2. Corozal

3.2.1. Site description and key issues

Corozal PHS is located along 0.8 Km of Corozal town seafront (see Figure 3). Corozal town is the capital of Corozal District, its population is estimated in 10,287 people and 2,699 households[1].

[1] SIB, census 2010.

Figure 4. Coastal stretch under study in Corozal.

A road (1st Avenue) stretches along this PHS and several piers and mooring docks have been built (see Figure 4 and Figure 5).

Figure 5. Northern half of Corozal PHS.

Figure 6. Mooring dock on the northern end of Corozal PHS.

The northern half of this PHS is covered with vertical seawalls (see Figure 7) whereas the southern half is mostly a rocky coast.

Figure 7. Seawall on the northern half of Corozal PHS.

Coastal erosion related to tropical cyclones in this area (Northern Region-North) has been found to be negligible[2] except for the erosion of mangroves. However, in this PHS, there are no mangroves along the coast. The existing seawall has limited coastal erosion and the only observed changes in the last 15 years on the shoreline position are related to small portions of reclaimed land (see Figure 8).

Figure 8. Reclaimed land on the western half of Corozal PHS (orange line: 2011 rocky shoreline).

As for coastal flooding related to tropical cyclones, in this area (Northern Region-North), it has been estimated to reach up to 1 m flood height for the 10 year return period, 2.5 m for 100 years

[2] See Risk Profile Report of this very same project: Coastal Disaster Risk Profile and Adaptation Recommendations considering Climate Change Scenarios for Belize.

and 4 m for 500 years in the current situation[3]. Under climate change scenario in the future horizon year 2050, flood height rises up to 2 m flood height for the 10 year return period and over 4 m for the 100 years return period. Therefore, flooding caused by tropical cyclones is the key issue in Corozal PHS. Particularly, in the future, under sea-level rise derived from climate change.

In fact, Hurricane Janet (27th of September, 1955) caused devastating winds and also produced massive flooding which destroyed completely Corozal Town[4] (see Figure 9).

Figure 9. Corozal town after Hurricane Janet (1955).

3.2.2. Recommended RRM

In this PHS, the existing seawall already provides protection against coastal flooding and, at the same time, it limits coastal erosion. Therefore **maintenance of coastal structures** is highly recommended, in order to maintain the protection level provided by the existing seawall regarding both coastal flooding and coastal erosion. This PHS is located in an urban area densely populated. So additionally, all preparedness measures are recommended regarding coastal flooding, such as **early warning systems** and **emergency plans** for the evacuation during tropical cyclones.

---

[3] See Risk Profile Report of this very same project: Coastal Disaster Risk Profile and Adaptation Recommendations considering Climate Change Scenarios for Belize.
[4] Consejo Belize. Hurricanes and Tropical Storms affecting Belize since 1930. http://consejo.bz/weather/storms.html

In view of the increase in flood height caused by climate change in the future, flood protection might become too costly and therefore other prevention measures are recommended. In the first place a complete **hazard, exposure, vulnerability and risk assessment under climate change** is recommended to estimate the expected damages related to coastal flooding caused by tropical cyclones in the future. Based on this assessment **other prevention measures** and **recovery measures** can be recommended, including nature-based solutions.

3.3. Ambergris Caye North

3.3.1. Site description and key issues

Ambergris Caye North PHS is located approximately 13 Km north-northeast of San Pedro Town and it spans for 1.2 Km along the eastern coast of Ambergris Caye (see Figure 9), which is the largest island of Belize (about 40 Km long from north to south, and about 1.6 Km wide), located northeast of the country's mainland, in the Caribbean Sea.

Figure 10. Coastal stretch under study in Ambergris Caye North.

Ambergris Caye North PHS is mostly covered with a narrow white sand beach backed by mangrove forests. The seafront is protected by the Belize Barrier Reef, which is a series of coral reefs located 1 Km east of this PHS (see Figure 10). The coastal stretch of this PHS is surrounded by the Hol Chan Marine Reserve (HCMR) (since 2015) which is composed of coral reefs, seagrass meadows and mangrove forest (see Figure 11).

Figure 11. The Hol Chan Marine Reserve (blue area) around Ambergris Caye North PHS.

There are two touristic resorts within this PHS: *La Beliza Resort* on the northern end and *Tuto Belize* on the southern end.

- Buildings on the northern end of this PHS are located on the shorefront, protected by means of a rip-rap seawall (see Figure 12) which has caused some erosion on the southern adjacent area (see Figure 13).

Figure 12. Rip-rap seawall on the northern end of Ambergris Caye North PHS.

Figure 13. Shoreline change along the northern area of Ambergris Caye North PHS.

- On the southern end of this PHS, buildings are located inland behind a sandy beach backed by a narrow strip of vegetation (see Figure 14) and no major changes have been observed on the shoreline (see Figure 15).

Figure 14. White sandy beach backed by vegetation on the southern end of Ambergris Caye North PHS.

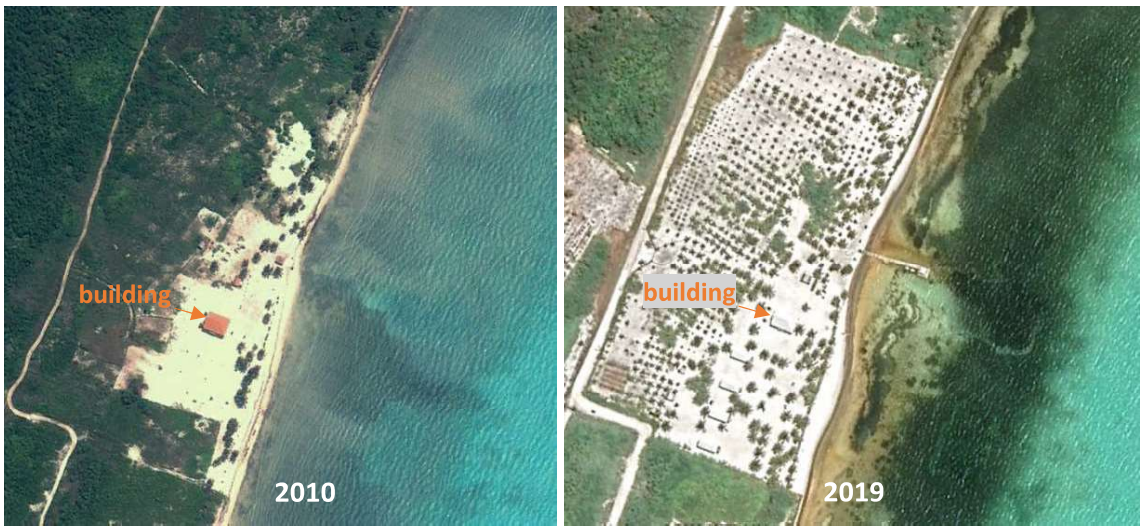

Figure 15. Shoreline change along the southern area of Ambergris Caye North PHS.

Impacts on beaches related to coastal erosion caused by tropical cyclones in this area (Ambergris Caye North) has been found to be second highest in the country (after Ambergris Caye South)[5]. Around 5 m of beach retreat is estimated for the 10 years return period hurricane and over 20 m (total beach width) is estimated for the 50 or higher return period.

The estimated erosion of mangroves in this area[6], although very limited, is also remarkable, reaching 0.15 m of erosion under a 100-year-return-period tropical cyclone and 0.3 m for the 500-year-return-period tropical cyclone. This erosion estimates remains steady under climate change scenario in the future horizon year 2050.

Nevertheless, aerial pictures of the area (see Figure 13 and Figure 15) do not show durable major changes on the shoreline and thus it is assumed that erosion recovery takes place rapidly after a hurricane hits this area.

[5] See Risk Profile Report of this very same project: Coastal Disaster Risk Profile and Adaptation Recommendations considering Climate Change Scenarios for Belize.
[6] See Risk Profile Report of this very same project: Coastal Disaster Risk Profile and Adaptation Recommendations considering Climate Change Scenarios for Belize.

Coastal flooding under tropical cyclones is the key issue in this PHS, since the storm surge can cover the entire island, with a return period of 100 years or higher in the current situation and aver 50 years return period under climate change scenario in the future horizon year 2050[7].

3.3.2. Recommended RRM

On the one hand, most of the shore of this PHS is covered with mangroves, which have been proven to provide an efficient protection against coastal erosion, and on the other, the Belize Barrier Reef provides additional protection against all hurricane-derived impacts. Therefore, **coral reef conservation** and **maintenance of coastal ecosystems and habitats** (particularly mangroves) are highly recommended in this PHS.

In view of the high flooding risk along with the already ongoing urban development in this PHS, **preparedness measures** are also highly recommended for the evacuation of people during a hurricane. Regarding the already existing resorts and developments, **risk transfer** measures are recommended to boost recovery following a hurricane, and in the areas that remain natural in this PHS, **land use regulations** are recommended to limit further development along the seafront by means of coastal setbacks.

3.4. Ambergris Caye South

3.4.1. Site description and key issues

Ambergris Caye South PHS spans for 1.1 Km along the eastern seashore of San Pedro Town (see Figure 15), which is the main town in Ambergris Caye (see section 3.3 for further details on Ambergris Caye).

[7] See Risk Profile Report of this very same project: Coastal Disaster Risk Profile and Adaptation Recommendations considering Climate Change Scenarios for Belize.

Figure 16. Coastal stretch under study in Ambergris Caye South.

San Pedro town is located on the southern part of the island of Ambergris Caye in the Belize District. The town has a population of 11,767[8] people in 3,784 households and it is the second-largest town in the Belize District after Belize City (see section 3.6).

Ambergris Caye South PHS is covered with seawalls alternated with narrow sandy beaches (see Figure 17). The seafront in this PHS is under severe urban pressure as beaches and seawalls are backed by buildings with no coastal setback (see Figure 18).

[8] SIB, census 2010.

Figure 17. Vertical seawall on the left of the pier and sandy beach on the right along the Ambergris Caye South PHS.

Figure 18. Aerial view of Ambergris Caye South PHS.

The following figures show the various coastal typologies, including several types of vertical seawalls that can be found in this PHS.

Figure 19.Narrow sandy beach backed by buildings on Ambergris Caye South PHS.

Figure 20. Various types of seawalls on Ambergris Caye South PHS.

Impacts on beaches related to coastal erosion caused by tropical cyclones in this area (Ambergris Caye South) has been found to be the highest in the country[9]. Around 10 m of beach retreat is estimated for the 10 years return period hurricane and over 20 m (total beach width) is estimated for the 50 or higher return period. This erosion estimates remains steady under climate change scenario in the future horizon year 2050. Nevertheless, the vertical seawalls in this PHS hold the shoreline and no major changes on the shoreline have been observed.

In fact, after Hurricane Earl (2016) piers and houses on the seafront were destroyed but the seawall and beaches withstood the impact (see Figure 21). From the 252 docks that line the coast of Ambergris Caye, 227 were affected, while 135 were totally destroyed[10]. The assessment also includes several dive shops which were partially or totally destroyed.

Figure 21. Seawall and beach in San Pedro right after Hurricane Earl (2016).

Coastal flooding under tropical cyclones is the key issue in this PHS, since the storm surge can cover the entire island, with a return period of 100 years or higher in the current situation and aver 50 years return period under climate change scenario in the future horizon year 2050[11]. In fact, the grand total damage caused by Hurricane Earl (2016) is estimated at $11 million along the eastern coast of Ambergris Caye due to the strong winds and surges.

[9] See Risk Profile Report of this very same project: Coastal Disaster Risk Profile and Adaptation Recommendations considering Climate Change Scenarios for Belize.
[10] Final Report Hurricane Earl 2016 by the National Emergency Management Organization.
[11] See Risk Profile Report of this very same project: Coastal Disaster Risk Profile and Adaptation Recommendations considering Climate Change Scenarios for Belize.

3.4.2. Recommended RRM

Most of the shore of this PHS is covered by seawalls that hold the shoreline and therefore, **maintenance of coastal structures** is highly recommended, in order to maintain the protection level provided by the existing seawall regarding coastal erosion. **Coral reef conservation** is also recommended in order to ensure that the protection provided by the Belize Barrier Reef is preserved. Regarding coastal flooding, this PHS is densely populated, so all preparedness measures are highly recommended for the evacuation during tropical cyclones, such as **early warning system** and **emergency plans**, along with **risk transfer** measures to boost recovery after a hurricane hits this PHS, in view of the large amount of resorts and developments along the seafront.

3.5. Caye Caulker North

3.5.1. Site description and key issues

Caye Caulker North PHS spans for 1.1 Km along the eastern shore of Caye Caulker, which is a small island off the coast of Belize in the Caribbean Sea, located approximately 30 km north-northeast of Belize City. This PHS is located north of *the Split*, which is a narrow waterway that divides the island in two (see Figure 22).

Figure 22. Caye Caulker and Belize Barrier Reef.

Caye Caulker is an 8 Km long (north to south) and 1.5 Km wide (east to west) limestone coral island, made up of a sand bar over a limestone shelf. East of the island there is a shallow lagoon (0.1-4 m) and the Belize Barrier Reef, with the reef exposed at the surface in front of Caye Caulker Village (south of *the Split*), while further north the reef is a deep reef that lies under 0.5 to 2.5 m of water (see Figure 22). The population of Caye Caulker is 1,763 people in 555 households[12].

[12] SIB, census 2010.

The Caye Caulker Marine and Forest Reserve (CCMFR) comprises 11.1 km in length, with the top portion crossing the Caye's north point and extending into lagoon waters to the west. It encompasses five habitats: mangroves and littoral forests, lagoon marsh-lands, sea-grass beds and coral reef. The use of the Marine Reserve is regulated based on a zoning scheme (see Figure 23).

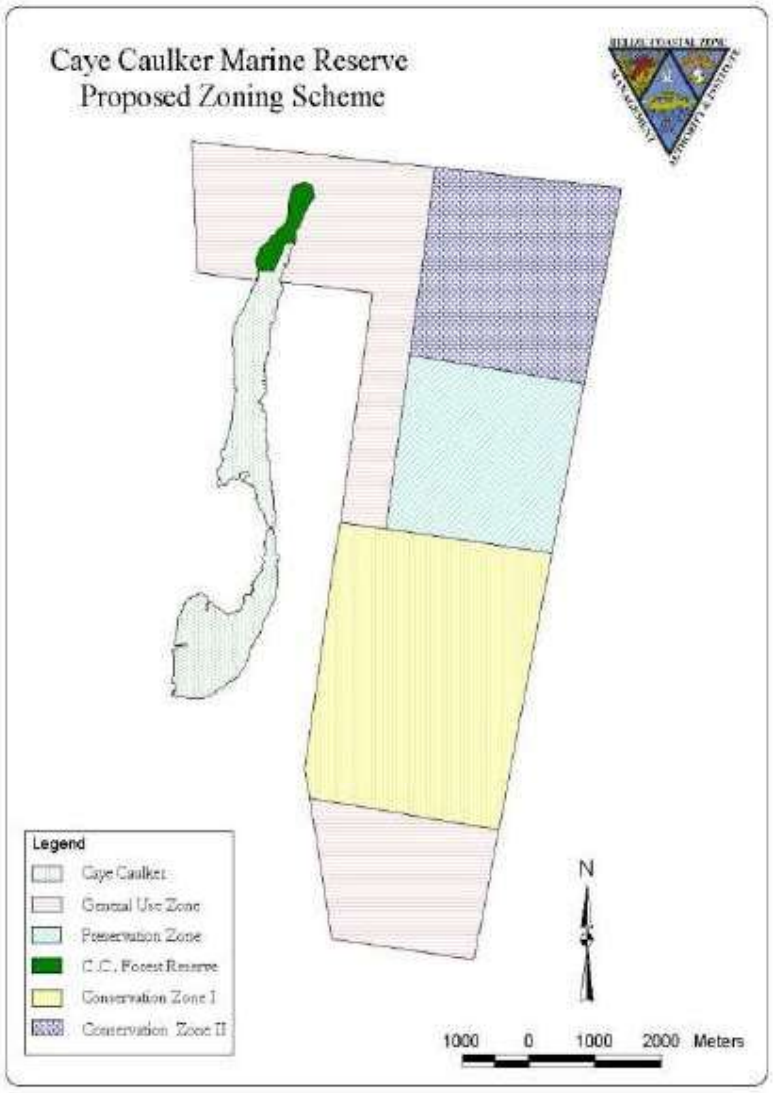

Figure 23. Caye Caulker Marine Reserve and Forest Reserve .

In 2012, approximately an area of 500 m (longshore) by 5 m (cross-shore) was replanted with mangroves on the northern tip of the island. The works took one year and over BZ$ 50,000.

Figure 24.Replanted mangroves in Caye Caulker.

Caye Caulker North PHS is located 1.5 Km south of the Caye Caulker Forest Reserve and it has experienced intense urban development in the last 15 years. In the central area of this PHS, mangroves have been replaced by artificial beaches (see Figure 25) and touristic resorts.

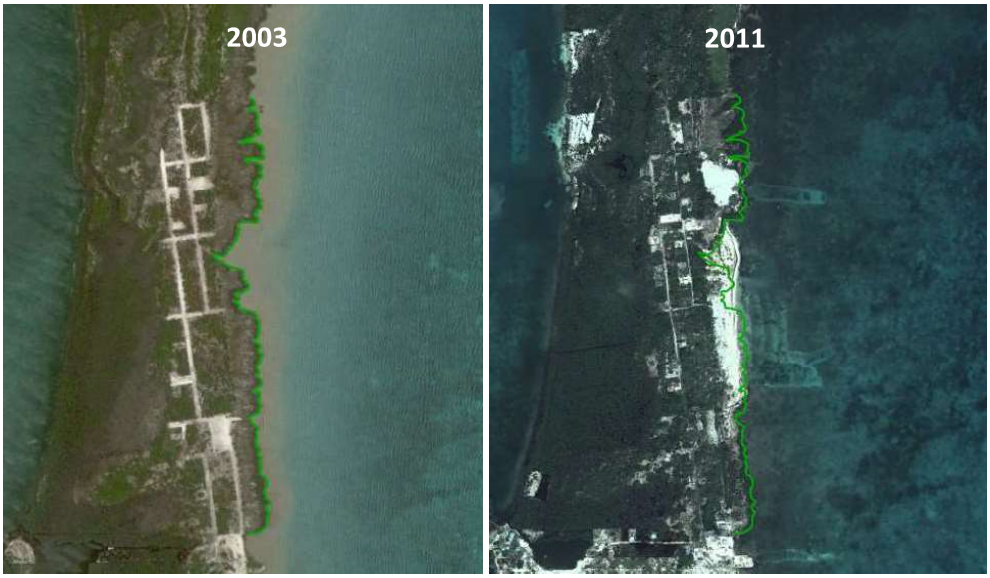

Figure 25. Removal of mangroves, beach nourishment and dredging of the seafloor on the central area of Caye Caulker North PHS (green line: 2003 shoreline covered with mangroves).

In the northern area of this PHS mangroves have been replaced by resorts and seawalls (see Figure 26).

Figure 26. Removal of mangroves and land claim based on a seawall protection on the northern area of Caye Caulker North PHS (green line: 2003 shoreline covered with mangroves).

Impacts on beaches and coastal structures related to coastal erosion caused by tropical cyclones in this area (Caye Caulker) has been found to be negligible[13]. Nevertheless, it is remarkable that the estimated erosion of mangroves in Caye Caulker, although very limited, is the highest in in the country, reaching 0.15 m of erosion under a 100-year-return-period tropical cyclone and 0.3 m for the 500-year-return-period tropical cyclone. Under climate change scenario in the future horizon year 2050, erosion of mangroves increases up to 0.3 m for the 100 year return period and 0.6 m for the 500 years return period. In Caye Caulker North PHS only remain only 450 m of shoreline are covered by mangroves: 150 m on the northern end and 300 m on the southern end.

Coastal flooding under tropical cyclones is the key issue in the whole island of Caye Caulker, since the island is only 2.5 m at its highest point and storm surge can cover the entire island, as occurred during Hurricanes Hattie (1961) and Keith (2000). Other major hurricanes have devastated the island such as Mitch (1998) and Earl (2016). This is also the key issue in Caye Caulker North PHS, especially after the removal of most mangroves in the area. This issue is expected to be exacerbated in the future due to sea-level rise caused by climate change.

[13] See Risk Profile Report of this very same project: Coastal Disaster Risk Profile and Adaptation Recommendations considering Climate Change Scenarios for Belize.

3.5.2. Recommended RRM

The Belize Barrier Reef provides protection against all hurricane-derived impacts along with the remaining mangroves in this PHS. Therefore, **coral reef conservation** and **maintenance of coastal ecosystems and habitats** (particularly mangroves) are highly recommended in this PHS. Given the number of visitors to Caye Caulker, **education programs** for residents and **raising awareness campaigns** for tourists can be linked to this activities.

In view of the already ongoing urban development in this PHS, **preparedness measures** are also highly recommended for the evacuation of people during a hurricane. Regarding the already existing resorts and developments, **risk transfer** measures are recommended to boost recovery following a hurricane, and in the small areas that remain natural in this PHS, **land use regulations** are recommended to limit further development along the seafront by means of coastal setbacks to preserve the remaining stretches of mangroves along the seafront and maintaining their valuable protection against coastal erosion and flooding.

3.6. Belize City North and South

3.6.1. Site description and key issues

Belize City is the largest city in Belize and was once the capital of the country until the government was moved to the new capital of Belmopan in 1970. It has a population of 57,164 people in 16,199 households[14].

In Belize City, two different PHS have been selected: Belize City-North and Belize City-South: Belize City North PHS stretches for 1.9 Km along the Philip Goldson Highway (Northern Hwy) and the western half of the Seashore Promenade (see Figure 27) whereas Belize City South PHS is located between the ESSO terminal in the Port of Belize City and Bird's Islet along 1.5 Km of shoreline (see Figure 28).

[14] SIB, census 2010.

Figure 27. Coastal stretch under study in Belize City North.

Figure 28. Coastal stretch under study in Belize City South.

Coastal erosion related to tropical cyclones in this area (Central Region-Central) has been found to be negligible[15]. The only observed changes in the last 15 years on the shoreline position are related to small portions of reclaimed land (see Figure 29 and Figure 30).

[15] See Risk Profile Report of this very same project: Coastal Disaster Risk Profile and Adaptation Recommendations considering Climate Change Scenarios for Belize.

Figure 29. Reclaimed land on the western end of Belize City North PHS (orange line: 2006 shoreline).

Figure 30. Reclaimed land on the eastern end of Belize City South PHS (orange line: 2006 shoreline).

As for the coastal flooding related to tropical cyclones in this area (Central Region-Central), around 2 m of flood height can be reached for the 100 years return period[16].

A detailed study for Belize City[17] estimated the coastal flooding caused by the storm surge but also by the river overtopping (fluvial flooding) and intense rainfall (pluvial flooding). Including all these different causes of flooding, Belize City North reaches 3-5 m of flood height and Belize City South 1-2 m for the 100 year return period (see Figure 31).

[16] See Risk Profile Report of this very same project: Coastal Disaster Risk Profile and Adaptation Recommendations considering Climate Change Scenarios for Belize.
[17] IDB, 2017. Baseline Study for Belize City. Disaster Risk and Climate Change Vulnerability Assessment for Belize City. Emerging and sustainable Cities Initiative (ESCI).

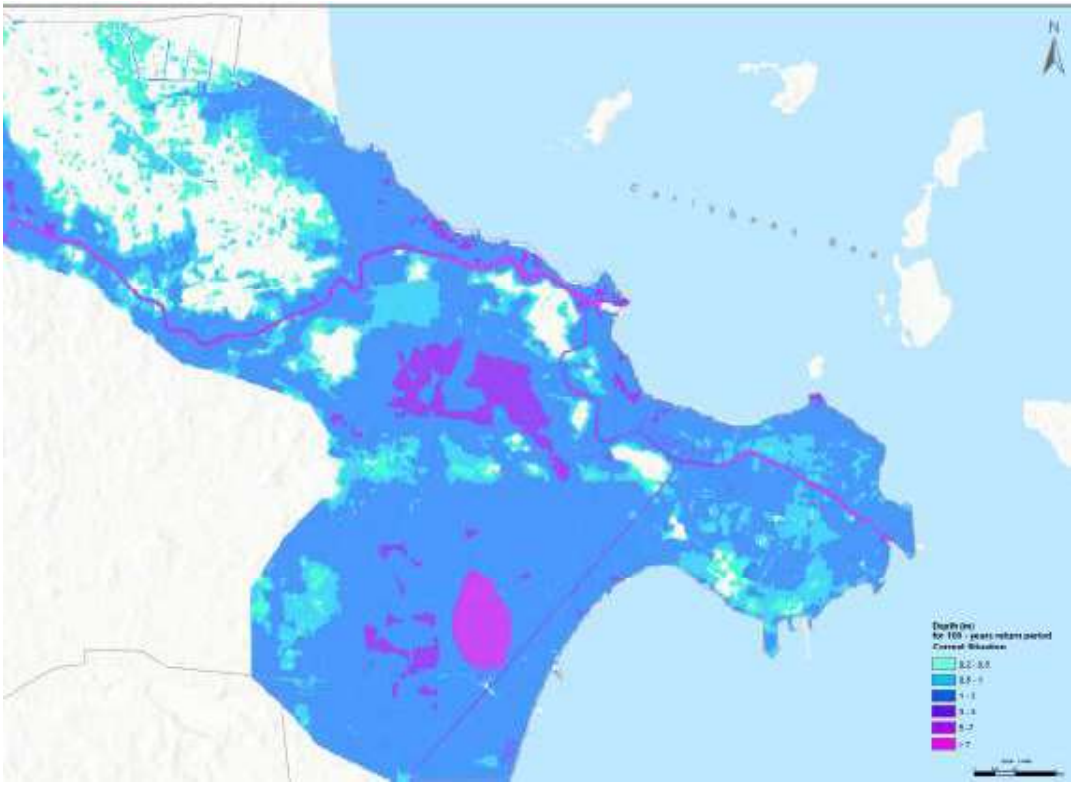

Figure 31. 100-year return period flood map.

According to the same detailed study, for small return periods (10 years), flood height in Belize City North PHS reaches up to 1-3 m, whereas Belize City South PHS is not flooded at all (see Figure 32).

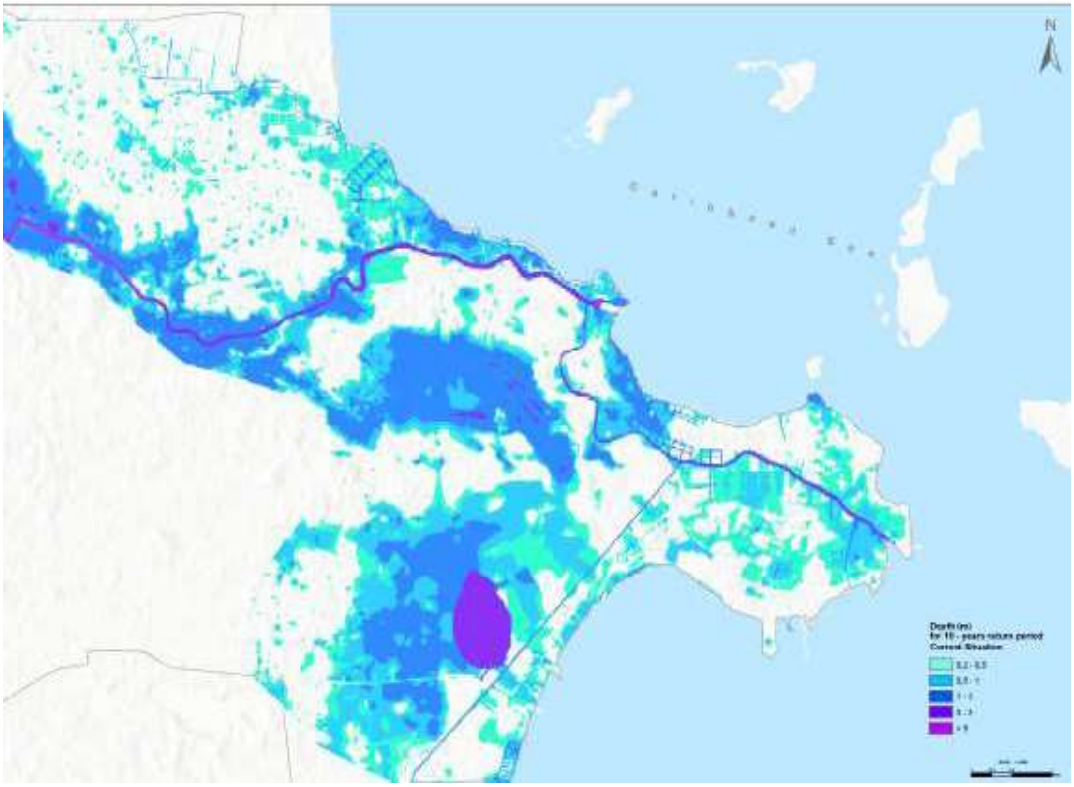

Figure 32. 10-year return period flood map.

Thus, the key issue in both Belize City North and South PHS is not only coastal flooding associated with tropical cyclones but the combination of pluvial, fluvial and coastal flooding. In fact, Hurricane Hattie destroyed almost half of the city in 1961 and Hurricane Keith in 2000 caused losses estimated to be over BZ$ 560 million[18]; both hurricanes were category 5 and presented a north-easterly track when making landfall (see Figure 33).

[18] IDB, 2017. Baseline Study for Belize City. Disaster Risk and Climate Change Vulnerability Assessment for Belize City. Emerging and sustainable Cities Initiative (ESCI).

Figure 33.Tracks of most destructive tropical cyclones for Belize City in the last 60 years.

It was Hurricane Hattie that motivated the relocation of the capital city from Belize City to the safer location of Belmopan. Besides the destruction of Belize City, the accompanying storm surge killed more than 400 people and left thousands homeless between Dangriga and Belize City[19] (see Figure 34).

Figure 34.Belize City after Hurricane Hattie (1961).

In the future, the current coastal flooding risk associated to tropical cyclones is expected to be exacerbated due to climate change effects, particularly sea-level rise.

3.6.2. Recommended RRM

Given the existing urban development and population density in this PHS, the implementation of **building codes and regulations** and **flood-proofing** are highly recommended regarding

[19] Consejo Belize. Hurricanes and Tropical Storms affecting Belize since 1930. http://consejo.bz/weather/storms.html

coastal flooding, particularly in Belize City North PHS. For the whole city and not only for the selected PHS, the recommended RRM against coastal flooding[20] is the construction of a coastal perimeter **seawall** and several sluices to prevent seawater getting into the urban area during flood events as well as all **preparedness measures** for the evacuation of people during a hurricane. Additional soft engineering or nature-based RRM can also be implemented in this PHS, in combination with the recommended hard-engineering RRM.

Additional RRM can be recommended regarding fluvial and pluvial flooding[21], that are out of the scope of this document.

3.7. Gales Point

3.7.1. Site description and key issues

Gales Point PHS is located in the Southern Lagoon which is a coastal lagoon of brackish waters and a manatee reserve. This PHS spans along 2 Km long but narrow peninsula mostly covered with mangroves (see Figure 35).

[20] IDB, 2017. Baseline Study for Belize City. Disaster Risk and Climate Change Vulnerability Assessment for Belize City. Emerging and sustainable Cities Initiative (ESCI).
[21] IDB, 2017. Baseline Study for Belize City. Disaster Risk and Climate Change Vulnerability Assessment for Belize City. Emerging and sustainable Cities Initiative (ESCI).

Figure 35. Coastal stretch under study in Gales Point.

Gales Point is a small village of Belize District, with 297 inhabitants[22] who are scattered throughout this peninsula with most of them in the southern area. A road stretches along the peninsula and several piers have been built (see Figure 36).

[22] SIB, census 2010.

Figure 36. The northern tip of the peninsula.

Shores along the peninsula are stable according to observations (see Figure 37) and therefore no erosion problems have been detected in this PHS.

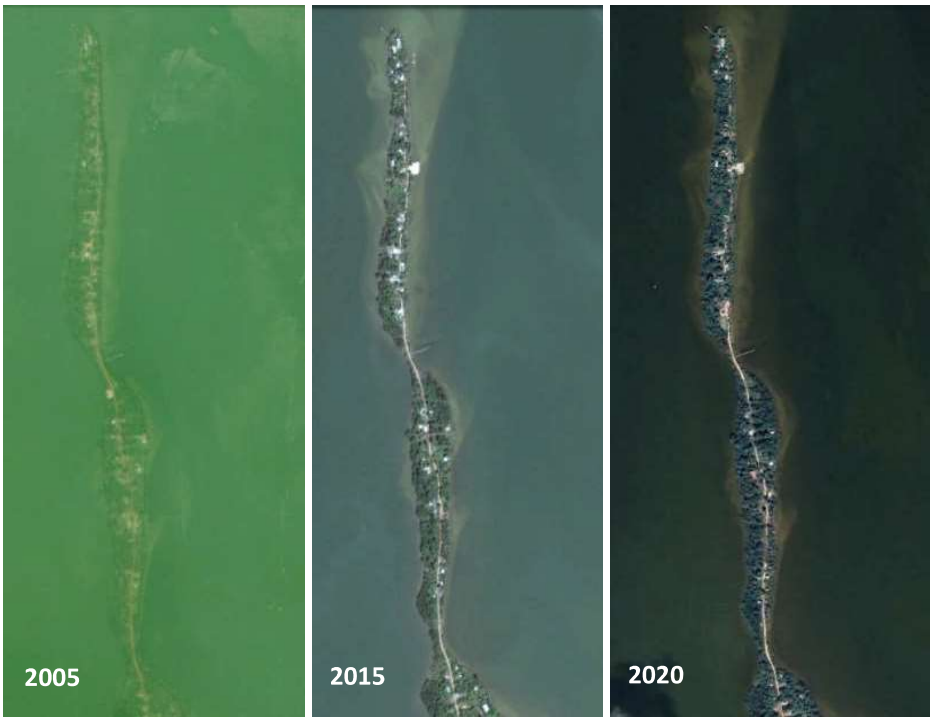

Figure 37.The shape of Gales Point along time.

As for flooding, the narrow shape of the peninsula makes it highly vulnerable to tropical cyclones. In this area (Central Region-South), coastal flooding related to tropical cyclones has been estimated to reach up to 2 m flood height for the 500 year return period but negligible for

shorter return periods[23]. Under climate change scenario in the future horizon year 2050, flood height rises up to 3.5 m. Therefore, flooding caused by tropical cyclones is the key issue in Gales Point. Particularly, in the future, under sea-level rise derived from climate change.

3.7.2. Recommended RRM

Due to the low probability of flooding due to tropical cyclones in this area, no immediate action is recommended. However, if there are signs of an increasing flooding hazard associated to tropical cyclones in the future due to climate change, **preparedness measures** for the evacuation of the peninsula during a hurricane might be recommended (preparedness measure) along with **building codes and regulations** (prevention measure) to encourage property owners to implement **flood proofing**. Building codes and regulations might be difficult to implement in such a small village, so **raising awareness campagins**, among all preparedness measures, are specially relevant in this PHS.

3.8. Dangriga

3.8.1. Site description and key issues

Dangriga PHS is located along a coastal stretch of 1.3 Km in Dangriga town, south of the mouth of the North Stann Creek River (see Figure 38). Dangriga town is the capital of Belize's Stann Creek District and the largest settlement in southern Belize with a population of around 9.500 people[24].

[23] See Risk Profile Report of this very same project: Coastal Disaster Risk Profile and Adaptation Recommendations considering Climate Change Scenarios for Belize.
[24] SIB, census 2010.

Figure 38. Coastal stretch under study in Dangriga.

Besides the mouth of North Stann Creek on the northern boundary of Dangriga PHS, Havana Creek mouth is located in the middle point of this PHS. Both river mouths are clogged for long periods, cutting off river flow and retaining river sediment yield, until heavy rains open-up the river mouths, particularly at Havana Creek (see Figure 39).

Figure 39. Mouth of North Stann Creek (left) and Havana Creek (right).

Between North Stann Creek mouth and Havana Creek mouth, the urban area is densely populated with several properties located on the seafront, whereas south of Havana Creek the seafront is mainly covered with parks and recreation areas. There are sandy beaches along the whole study area.

In this area (South Norther Region-North) coastal flooding related to tropical cyclones has been found to be negligible[25]. In fact, Hurricane Greta (1978) made landfall in Dangriga town and there was minimal flooding on the mainland despite a high storm surge. Storm tides in Dangriga were 1.8 to 2.1 m above normal, which did not cause much flooding[26]. Beach erosion related to tropical cyclones has been estimated in around 6 m of shoreline retreat for the 500 year return period and over 8 m including the effect of climate change.

The key issue in Dangriga PHS is shoreline erosion. Shoreline change has been observed mainly between North Stann Creek mouth and Havana Creek mouth, where there has been some level of intervention taking place to minimize the amount of damage that is being done to the beach. Residents have taken it upon themselves to begin to throw old car tires at the point of erosion in an effort to prevent any more from taking place (see Figure 40).

[25] See Risk Profile Report of this very same project: Coastal Disaster Risk Profile and Adaptation Recommendations considering Climate Change Scenarios for Belize.
[26] Hurricane Greta and Hurricane Olivia Preliminary Report (JPG) (Report). National Hurricane Center. p. 3. Retrieved 2013-12-20.

Figure 40. Car tires north of Havana Creek river mouth.

Nevertheless, this erosion has been observed to be partially related to annual oscillations caused by changing prevailing waves and the sporadic sediment yield from the rivers (see Figure 41). Northward prevailing marine climate washes away sediments from beaches in this PHS, whereas southward prevailing marine climate distributes the river sediment along this PHS preventing erosion.

Figure 41. Southward prevailing marine climate in 2011 (left) and in 2019 (right). Northward prevailing marine climate in 2014 (center).

Southward of Havana Creek mouth no major shoreline changes have been observed. At the southern boundary of this PHS a rigid structure partially retains sediments, although a sediment by-pass southward of Dangriga PHS is evident (see Figure 42).

Figure 42. Shoreline position in 2006 (left), 2017 (center) and 2020 (right). Note evidences of sand by-pass southward in 2017.

3.8.2. Recommended RRM

Although coastal erosion has been observed in this PHS, many uncertainties remain regarding the processes that cause this erosion. Therefore, in the first place, a complete **coastal morphodynamic modelling and assessment** (prevention measure) including a **hydrological assessment** to determine the river sediment yield and the effects of climate change is recommended in order to understand the causes of erosion, sediment sources and sinks and estimate shoreline position changes. This hazard assessment is recommended to be completed with a **vulnerability and risk erosion assessment** in order to estimate the expected damages in the mid-long term.

Following this assessment, a combination of prevention and protection measures are recommended for different areas of this PHS. These RRM include: hard engineering (**seawall**) and soft engineering (**sand re-nourishment** for **beach restoration**) measures to limit or completely avoid erosion and the definition of coastal setbacks (**land use regulations and urban planning**), where erosion cannot be avoided. Note that the construction of seawalls is the least preferred option of all proposed RRM in this PHS.

3.9. Placencia

3.9.1. Site description and key issues

Placencia PHS is located on the eastern side of the Placencia Peninsula, along a coastal stretch of 2.4 Km close to Placencia Airport (see Figure 43), at around 4 Km of the southern tip of the 29 Km long peninsula.

Figure 43.Coastal stretch under study in Placencia.

The eastern side of the Placencia Peninsula is covered with white sand beaches and heavy mangrove in some areas. The western side is bounded by a long narrow north-south trending bay. Southward of the Placencia PHS is the southern-most village on the peninsula, Placencia Village, home to 1,752 people[27].

In 2001 Hurricane Iris, a Category 4 hurricane with a storm surge of 3 – 5 m destroyed 80% of houses, 90% of the tourist accommodation facilities and nearly all bridges and piers in Placencia Peninsula[28]. However, in this area (South Central Region-North) this kind of coastal flooding event is related to a return period higher than 500 years[29] and beach erosion related to tropical cyclones has been found to be negligible, with less than 5 m of shoreline retreat for the 500 year return period.

As for chronic erosion not directly relate to tropical cyclones, over 20 m of erosion since 2004 have been recorded at the Rum Point, the westernmost point of the Placencia Peninsula, northward of Placencia Airport. Southward of the airport no erosion has been observed in the last few years.

[27] SIB, 2010 census.
[28] The University of the West Indies. http://www.uwi.edu/ekacdm/node/75.
[29] See Risk Profile Report of this very same project: Coastal Disaster Risk Profile and Adaptation Recommendations considering Climate Change Scenarios for Belize.

Figure 44. Shoreline change at Serenity Beach Resort.

The Placencia Airport, located in the middle point of Placencia PHS, is surrounded by the Placencia Road, which is only a few meters from the shoreline (see Figure 44 and Figure 45).

Figure 45. Views from the North side (left) and south side (right) of Placencia Road next to Placencia Airport.

The Placencia Road is the only route by land than links Placencia Village and the mainland. So, it is a critical infrastructure. In this area, the shoreline has been stabilized by means of a vertical seawall (see Figure 46).

Figure 46. Air crash (2014) behind the vertical seawall next to Placencia Airport (left) and aerial view or Placencia Airport and Placencia Road (right).

Impacts of tropical cyclones on coastal structures are remarkable in this area[30], with the highest seawall scour rate in the country, reaching 0.3 m of estimated scour at the foot of vertical seawalls under a 100-year-return-period tropical cyclone and 0.5 m for the 500-year-return-period tropical cyclone.

Therefore, the key issue in Placencia is seawall stability along the Placencia Road, next to the Placencia Airport, keeping in mind that climate change is expected to exacerbate the impacts of tropical cyclones on coastal structures. Additionally, coastal erosion at Rum Point is also relevant.

3.9.2. Recommended RRM

Due to the high risk of collapse of coastal structures under tropical cyclones in this area[31] and the relevance of the road and airport located in this PHS, in the first place, the **maintenance of the existing seawall** (prevention measure) is recommended to avoid damages to the Placencia Road and Airport. Additionally, a complete **hazard, vulnerability and risk erosion assessment** (prevention measure) including the effects of climate change is recommended in order to estimate the shoreline position and expected impacts to the Placencia Road and Airport in the mid-long term. Following this assessment, **land claim** (hard engineering protection measure) for the relocation of the Placencia Road and/or Airport might be necessary.

[30] See Risk Profile Report of this very same project: Coastal Disaster Risk Profile and Adaptation Recommendations considering Climate Change Scenarios for Belize.
[31] See Risk Profile Report of this very same project: Coastal Disaster Risk Profile and Adaptation Recommendations considering Climate Change Scenarios for Belize.

Although coastal erosion has been observed at Rum Point, some uncertainties remain regarding the processes that cause this erosion. Therefore, a complete **coastal morphodynamic modelling and assessment** (prevention measure) including the effects of climate change is recommended in order to understand the causes of erosion and estimate the shoreline position and expected damages in the mid-long term. Following this assessment, prevention and/or protection measures might be recommended to prevent damages to properties and infrastructures and to limit or completely avoid erosion.

3.10. Monkey River

3.10.1. Site description and key issues

Monkey River PHS stretches along the coast for 1.4 Km on both sides of the mouth of Monkey River (see Figure 47) in the north of the Toledo District. The population in Monkey River Village is estimated in 196 people and 37 households[32].

[32] SIB, 2010 Census.

Figure 47. Coastal stretch under study in Monkey River.

In 2001, Hurricane Iris, a Category 4 hurricane with a storm surge of 3 – 5 m, destroyed Monkey River Village[33]. However, in this area (border between South Central Region-South and South Region-North) this kind of event is related to a return period higher than 500 years[34] and coastal erosion related to tropical cyclones has been found to be negligible, with less than 5 m of shoreline retreat for the 500 year return period.

[33] Vulnerability Assessment of the Belize Coastal Zone, 2007. UNDP/GEF Climate Change Project, prepared by Dwight Neal, Eugene Ariola, and William Muschamp.
[34] See Risk Profile Report of this very same project: Coastal Disaster Risk Profile and Adaptation Recommendations considering Climate Change Scenarios for Belize.

Therefore, the key issue in Monkey River is coastal erosion caused by a reduction in the river sediment yield attributed to sand mining along the river banks, the diversion of river waters for irrigation and the construction of an upstream river dam.

Erosion is not uniform along this PHS, which can be split into 4 different sections:

- The northern area
- The river mouth
- The main village
- The southern area

On the northern area, there are no major changes in shoreline position (see 08).

Figure 48. Shoreline changes along the northern area of Monkey River PHS.

In this area, the shoreline has been locally stabilized by means of a seawall. However, on the left bank of the river mouth, 15 m of erosion have been recorded since 2005, southward of the existing seawall (see Figure 49).

Figure 49.Shoreline changes along the left bank of the river mouth.

The river mouth itself is highly dynamic and shows seasonal features that change rapidly (see Figure 50).

Figure 50. Various features on the river mouth throughout the last 15 years.

Along the Monkey River Village, on the southern shore of the river mouth, 15 m of erosion has been recorded since 2005 (see Figure 51); two rows of streets and more than ten homes have been lost.

Figure 51.Shoreline change along the village.

Consequently, several RRM have been implemented in this area. In May 2015, 200 students and villagers planted trees, cleaned the beach and placed sandbags and, since 2018, a number of geo-tubes have been installed (see Figure 52).

Figure 52.Examples of RRM implemented in Monkey River PHS.

The geo-tubes have effectively limited erosion along the village. However, in the southern area, erosion has been exacerbated, reaching 50 m of shoreline retreat since 2005.

Figure 53.Shoreline change in the southern area.

3.10.2. Recommended RRM

A complete hazard, vulnerability and risk erosion assessment has been completed in this PHS. Nevertheless, some uncertainities remain regarding the causes of observed erosion in this PHS. Therefore, further **hazard, vulnerability and risk erosion assessments** including the effects of climate change are recommended in order to estimate shoreline position and expected damages in the mid-long term.

Following this assessment, a combination of prevention and protection measures are recommended for different areas of this PHS. These RRM include: hard engineering (**seawall**) and soft engineering (**sand re-nourishment** for **beach restoration**) measures to limit or completely avoid erosion and the definition of coastal setbacks (**land use regulations and urban planning**), where erosion cannot be avoided. In fact, land use regulation is also recommended upstream where sand mining is done. Note that the construction of seawalls is the least preferred option of all proposed RRM in this PHS for it is a relatively expensive RRM.

4. CONCLUSIONS

A wide variety of coastal typologies and key issues have been detected in the selected PHS, based on a desktop analysis. Accordingly, different sets of risk reduction measures (RRM) have been recommended for each PHS (see Table 2).

Table 2.Summary of recommended RRM in PHS.

		Corozal	Ambergris Caye North	Ambergris Caye South	Caye Caulker North	Belize City North &	Gales Point	Dangriga	Placencia	Monkey River
Key issues	Coastal erosion	✖	✓	✓	✓	✖	✖	✓	✓	✓
	Coastal flooding	✓	✓	✓	✓	✓	✓	✖	✖	✖
	Impacts of climate change	✓	✓	✓	✓	✓	✓	✖	✓	✖
Recommended RRM	Building codes and regulations	✓	✖	✖	✖	✓	✓	✖	✖	✖
	Flood-proofing	✓	✖	✖	✖	✓	✓	✖	✖	✖
	Land use regulations and urban planning	✓	✓	✖	✓	✖		✓	✖	✓
	Hazard, exposure, vulnerability and risk assessments under coastal flooding and erosion	✓	✖	✖	✖	✖	✖	✓	✓	✓
	Maintenance of coastal	✓	✓	✓	✓	✖	✖	✖	✓	✖

	structures, beach width, coastal ecosystems and habitats									
	Beach restoration	✖	✖	✖	✖	✖	✖	✓	✖	✓
	Wetland restoration	✖	✖	✖	✖	✖	✖	✖	✖	✖
	Coral reef conservation	✖	✓	✓	✓	✖	✖	✖	✖	✖
	Seawalls	✖	✖	✖	✖	✓	✖	✓	✖	✓
	Breakwaters and groins	✖	✖	✖	✖	✖	✖	✖	✖	✖
	Land claim	✖	✖	✖	✖	✖	✖	✖	✓	✖
	Managed retreat	✖	✖	✖	✖	✖	✖	✖	✖	✖
	Sand re-nourishment	✖	✖	✖	✖	✖	✖	✓	✖	✓
	Early warning systems	✓	✓	✓	✓	✓	✓	✖	✖	✖
	Emergency and contingency plans	✓	✓	✓	✓	✓	✓	✖	✖	✖
	Education programs	✖	✓	✖	✓	✓	✓	✖	✖	✖
	Raising awareness campaigns	✖	✓	✖	✓	✓	✓	✖	✖	✖
	Clean-up and restoration activities	✓	✖	✖	✖	✖	✖	✖	✖	✖
	Disaster assistance	✓	✖	✖	✖	✖	✖	✖	✖	✖

	Insurance policies	✓	✓	✓	✓	✖	✖	✖	✖	✖

The remote analysis of key issues at the ten selected PHS, has some limitations and therefore consultation to local stakeholders is indispensable in order to validate the preliminary diagnosis, along with the preliminary proposed recommendations (see Deliverable 5. Preliminary Proposal of RRM in PHS), based on a risk assessment (see Deliverable 4. Risk Profile Report) and expert criteria. Thus, an on-line consultation has been performed (see Annex 3) in order to gather local insight, which has been integrated in this final report.